

MASTER THESIS

Investigation of the applicability of Discrete Elements on the backfill of Segments

Untersuchung der Anwendung der Diskreten Elemente Methode an der
Hinterfüllung von Tübbing-Elementen

Christoph Sinkovec, BSc

Institute of Rock Mechanics and Tunnelling
Graz University of Technology

Supervisors:

O.Univ.-Prof. Dipl.-Ing. Dr.mont. Wulf Schubert

Institute for Rock Mechanics and Tunnelling
Graz University of Technology

Dipl.-Ing. Michael Henzinger

Institute for Rock Mechanics and Tunnelling
Graz University of Technology

Graz, January 2015

Eidesstattliche Erklärung

Ich erkläre an Eides statt, dass ich die vorliegende Arbeit selbstständig verfasst, andere als die angegebenen Quellen/Hilfsmittel nicht benutzt und die den benutzten Quellen wörtlich und inhaltlich entnommene Stellen als solche kenntlich gemacht habe.

Graz, Jänner 2015

Christoph Sinkovec

Affidavit

I declare that I have authored this thesis independently, that I have not used other than the declared sources / resources, and that I have explicitly marked all material which has been quoted either literally or by content from the used sources.

Graz, January 2015

Christoph Sinkovec

Danksagung

An dieser Stelle möchte ich allen Personen danken, die mir während meiner Studienzeit zur Seite standen.

Besonders möchte ich mich für die kompetente Betreuung am Institut für Felsmechanik und Tunnelbau bei Herrn O.Univ.-Prof. Dipl.-Ing. Dr. mont. Wulf Schubert sowie Herrn Dipl.-Ing. Michael Henzinger bedanken. Durch die Möglichkeit, die Arbeit am Institut zu verfassen und jederzeit persönliche Betreuung zu erhalten, wurde ein Grundstein für eine erfolgreiche Zusammenarbeit gelegt.

Weiters möchte ich mich bei meinen Freunden in Graz, mit denen ich eine tolle Studienzeit verbrachte, bedanken. Insbesondere möchte ich hier die Supergruppe erwähnen, es war eine schöne Zeit. Danke Jungs!

Bedanken möchte ich mich auch bei meiner Freundin Rosi, die mich immer unterstützte und mir dabei immer die nötige Motivation gab.

Danken möchte ich auch meiner Familie. Besonderer Dank gebührt dabei meinen Eltern, die mich durch die gesamte Ausbildungszeit hindurch immer unterstützten und mir diese Ausbildung ermöglichten.

Vielen Dank!

Abstract

Mechanized driven tunnels due to high drill performance and less ventilation demand in many cases are an economic method for excavating a tunnel. When shield machines are used, precast concrete segments form the outer lining. The erector installs the segments within the protection of the shield.

The backfilling process starts as soon as possible after the shield tail passes the lining. Due to the operational procedure within the working area of a TBM, a fully backfilled annular gap might not be established after every ring closure. This leads to an unfavorable distribution of the pea gravel leaving the segmental lining only partially bedded.

For approaching this problem, we used a numerical method, which represents the natural behavior of a grained material. The discrete element considering the deformational behaviour of pea gravel is a CPU-intensive method.

The software Abaqus/Explicit implemented the particle method based on „*Discrete Element Method*“ (Cundall, 1971) on their latest update to version 6.13 (2013). The main advantage of the Software Abaqus compared to other DEM solutions, is the possibility of a combination of discrete and finite elements in one model. Using this advantage for that problem, it is possible to model the spatial system. Therefore, finite elements are used for the lining segments and discrete elements for the pea gravel within the annular gap.

Prior to these calculations, it is necessary to perform validations on laboratory tests. Main part of this thesis is the verification of the numerical rock parameters of pea gravel. Based on laboratory shear and oedometer tests, the input parameters for the numerical simulation of pea gravel were determined. The results show comparability, though the implementation of the discrete elements within Abaqus contains shortcomings compared to other particle codes.

The work shows the application of this numerical method for an overall outer lining situation. A major point for further research is the determination of the deformations in the annular gap after the refilling process and during the “regripping process”.

Kurzfassung

Maschinelle Vortriebe stellen auf Grund der hohen Vortriebsleistungen und des geringen Bewetterungsbedarfs oftmals eine sehr wirtschaftliche Lösung für die Herstellung von Tunnelbauwerken dar. Der Ausbau mittels Stahlbetontübbingem kommt bei Schildmaschinen zum Einsatz. Die Tübbinge werden hierbei mittels Erektor im Schutze des Schildmantels, welcher eine vorläufige Sicherung des Gebirges darstellt, eingebaut.

Um die notwendige Bettung des Tübbingausbaus und eine gleichmäßige Verteilung der Spannungen aus dem Gebirgsdruck zu gewährleisten, wird der Ringspalt zwischen Gebirge und Tübbingring möglichst frühzeitig nach Ringschluss mit einem feinkörnigen, enggestuften Kies (Perlkies) oder mit Mörtel verfüllt. Nach dem Verlassen des Schildmantels und vor dem Verfüllen mit Perlkies steht der Ring jedoch ohne Bettung frei. Lediglich an der Sohle steht er in Kontakt mit dem Gebirge.

Aus dieser Problemstellung entwickelte sich die Idee, das Verhalten der Bettung bzw. von Perlkies numerisch abzubilden. Eine besonders realitätstreue, jedoch rechenintensive Methode für solche Problemstellungen ist die Diskrete Elemente Methode, kurz DEM.

Die Software Abaqus/Explicit beinhaltet ab Version 6.13 (2013) die Partikel Methode auf Basis der „*Discrete Element Method*“ (Cundall, 1971). Ein wesentlicher Vorteil von Abaqus gegenüber anderen Softwarelösungen im Bereich der DEM ist die Möglichkeit, Diskrete Elemente mit Finiten Elementen in einem Modell zu kombinieren. Im Hinblick auf die Bettung der Stahlbetontübbinge (FEM) in Perlkies (DEM), ist eine Modellierung des gesamten Systems im dreidimensionalen Raum möglich.

Um diese numerischen Berechnungen durchführen zu können sind im Vorfeld Validierungen an Laborversuchen notwendig.

Hauptaugenmerk dieser Arbeit ist die Verifizierung der numerischen Gesteinseigenschaften von Perlkies. Hierfür werden Parameterstudien an numerischen Scher- sowie Ödometerversuchen durchgeführt und an Laborversuchen validiert. Die Resultate zeigen Vergleichbarkeit, jedoch wurden durch die Anwendung von Abaqus Defizite in der Implementierung des Partikel Codes im Vergleich zu anderen Softwarelösungen festgestellt.

In weiterer Folge wird die Anwendung dieser Methode im Bereich der Tübbingbettung an numerischen Modellen gezeigt. Die Ermittlung der Verformungen im Ringspalt nach Verfüllung während eines „Regripping-Vorgangs“ und die damit resultierende Auswirkung auf die Tübbinge sind dabei von besonderem Interesse.

Contents

| | | |
|----------|--|-----------|
| 1 | Introduction | 1 |
| 1.1 | State of the art..... | 2 |
| 1.1.1 | Bedded frame model..... | 2 |
| 1.1.2 | Double shield machine | 5 |
| 1.2 | Definition of objectives | 6 |
| 2 | Applicability of FLAC3D | 7 |
| 3 | Discrete Element Method | 10 |
| 3.1 | Discrete Element Method in Abaqus | 11 |
| 3.2 | Contact Law | 12 |
| 3.2.1 | Hertz Contact Formulation..... | 14 |
| 3.3 | Particle packing / Initial Placing | 16 |
| 3.4 | Incrementation | 17 |
| 3.5 | Calculation procedures..... | 18 |
| 3.6 | Software for discrete element problems | 19 |
| 4 | Calibration | 20 |
| 4.1 | Input Parameters..... | 20 |
| 4.1.1 | Particle Diameter..... | 21 |
| 4.1.2 | Particle shape | 22 |
| 4.1.3 | Friction coefficient | 22 |
| 4.1.4 | Elastic modulus / poisson ratio of the intact rock | 22 |
| 4.1.5 | Density | 23 |
| 4.1.6 | Damping Factor..... | 23 |
| 4.2 | Numerical Tests | 24 |
| 4.2.1 | Shear test Calculation | 25 |
| 4.2.1.1 | <i>Geometry</i> | 25 |
| 4.2.1.2 | <i>Definition of the Sets</i> | 26 |
| 4.2.1.3 | <i>Steps</i> | 27 |
| 4.2.1.4 | <i>Parameter Variation</i> | 28 |
| 4.2.1.5 | <i>Evaluation</i> | 29 |
| 4.2.2 | Oedometer test | 30 |
| 4.2.2.1 | <i>Geometry and definition of the sets</i> | 30 |

| | | |
|----------|---|-----------|
| 4.2.2.2 | Steps | 31 |
| 4.2.2.3 | Parameter Variation | 33 |
| 4.2.2.4 | Evaluation | 34 |
| 4.3 | Laboratory tests | 37 |
| 4.3.1 | Shear test results | 38 |
| 4.3.2 | Oedometer test results | 39 |
| 4.4 | Results and conclusions of the numerical calculations | 40 |
| 4.4.1 | Shear test results | 40 |
| 4.4.1.1 | Comparison of representative results | 42 |
| 4.4.1.2 | Impact of the incrementation | 43 |
| 4.4.2 | Oedometer Test | 44 |
| 5 | Numerical Models implementing the DEM | 47 |
| 5.1 | Annular Gap Model | 47 |
| 5.1.1 | Geometry | 48 |
| 5.1.1 | Calculation steps | 50 |
| 5.2 | Segment Bedding Model | 51 |
| 5.2.1 | Geometry | 51 |
| 5.2.2 | Calculation steps | 53 |
| 6 | Conclusion and Outlook | 55 |
| | Bibliography | 56 |
| | Annex A | 58 |
| | Annex B | 59 |
| | Annex C | 61 |
| | Annex D | 66 |
| | Annex E | 72 |
| | Annex F | 76 |
| | Annex G | 83 |
| | Annex H | 88 |

List of Figures

| | |
|--|----|
| Figure 1: Approach for the radial bedding | 3 |
| Figure 2: Calculation methods of the beam spring model for tunnels in soft ground..... | 4 |
| Figure 3: Double shield TBM..... | 5 |
| Figure 4: Calculation process and descriptions in FLAC3D (1) | 7 |
| Figure 5: Calculation process and descriptions in FLAC3D (2) | 8 |
| Figure 6: Mesh design for the FLAC3D model | 8 |
| Figure 7: Definition of the interactions in the FLAC3D model | 9 |
| Figure 8: Number of publications related to discrete particle simulations | 10 |
| Figure 9: General form of the contact law | 12 |
| Figure 10: Interactions between ball shaped particles..... | 13 |
| Figure 11: Comparison of linear and nonlinear contact laws | 13 |
| Figure 12: “Softened” scale factor pressure-overclosure relationship..... | 14 |
| Figure 13: Process of particle placing | 16 |
| Figure 14: Calculation procedure of a DEM calculation..... | 18 |
| Figure 15: Grain size distribution of pea gravel | 21 |
| Figure 16: Discretization of the pea gravel..... | 22 |
| Figure 17: Geometry of the shear box..... | 25 |
| Figure 18: Initial particle positions..... | 26 |
| Figure 19: Definition of the sets | 26 |
| Figure 20: States of the 3D numerical shear test using the software Abaqus..... | 29 |
| Figure 21: Definition of the sets | 30 |
| Figure 22: Initial placing of the particles - oedometer test | 31 |
| Figure 23: Oedometer test on pea gravel..... | 37 |
| Figure 24: Shear test results of the laboratory test..... | 38 |
| Figure 25: σ/τ plot for determining cohesion and friction angle | 38 |

| | |
|---|----|
| Figure 26: Friction angle depending on the elastic modulus of the intact rock..... | 41 |
| Figure 27: Comparison of the laboratory tests with the numerical "3" variation (1) | 42 |
| Figure 28: Comparison of the laboratory tests with the numerical "1a" variation (2) | 42 |
| Figure 29: results of the "1b" variation (1) | 43 |
| Figure 30: results of the "1b" variation (2) | 43 |
| Figure 31: Summarization of the numerical and laboratory results of the oedometer test. | 45 |
| Figure 32: Summary of the numerical and laboratory tests (more detailed plot)..... | 45 |
| Figure 33: Strain time development of the first loading stage | 46 |
| Figure 34: Compressibility of discrete elements due to different intact rock elastic moduli | 46 |
| Figure 35: numerical annular gap model..... | 48 |
| Figure 36: Definition of the sets | 49 |
| Figure 37: Geometry of the segments model | 51 |
| Figure 38: Position of the segments and the interaction surfaces | 52 |

List of Tables

| | |
|--|----|
| Table 1: History of the development in the calculation method for tunnel segments..... | 2 |
| Table 2: Bedding approach of the EBT | 4 |
| Table 3: Variable definition of the Hertz contact solution..... | 15 |
| Table 4: Variable Definition | 17 |
| Table 5: Time incrementations depending on the particle stiffness | 18 |
| Table 6: Software solutions for DEM problems | 19 |
| Table 7: Units declaration | 20 |
| Table 8: Initial Input Parameters | 21 |
| Table 9: Friction coefficient | 22 |
| Table 10: Definition of the steps (1) | 27 |
| Table 11: Definition of the steps (2) | 28 |
| Table 12: Parameter variation of the shear test calculation (1)..... | 28 |
| Table 13: Parameter variation of the shear test calculation (2)..... | 28 |
| Table 14: Definition of the steps..... | 32 |
| Table 15: Parameter variation of the oedometer tests..... | 33 |
| Table 16: Variable Definition | 34 |
| Table 17: Export data of the Abaqus result file..... | 36 |
| Table 18: Oedometer laboratory results (1)..... | 39 |
| Table 19: Axial Strain / normal stress plot of the laboratory oedometer test..... | 39 |
| Table 20: Results of the shear test variations (1) | 40 |
| Table 21: Results of the shear test variations (2) | 40 |
| Table 22: Results of the numerical and laboratory oedometer test variations..... | 44 |
| Table 23: Calculation steps for the annular gap model..... | 50 |
| Table 24: Definition of the sets..... | 52 |
| Table 25: Calculation steps of the annular gap model (1) | 53 |

| | |
|--|----|
| Table 26: Calculation steps of the annular gap model (2) | 54 |
|--|----|

Defined symbols

| | | |
|---------------------|----------------------|---|
| A_{shear} | [mm ²] | shear area |
| A_{oed} | [mm ²] | area of the oedometer box |
| c | [N/mm ²] | cohesion |
| $CFORCE_x$ | [N] | contact force in x-direction |
| $CFORCE_z$ | [N] | contact force in z-direction |
| $CSHEAR_z$ | [N] | shearing contact force in z-direction |
| C_n | [-] | normal damping |
| C_t | [-] | tangential damping |
| d | [mm] | particle diameter |
| D_{50} | [mm] | midpoint of the grain size distribution |
| δ | [mm] | overclosure |
| $E_{s,i}$ | [N/mm ²] | elastic modulus of the particles |
| E_{oed} | [N/mm ²] | oedometer modulus / constraint secant modulus |
| $\varepsilon_{a,i}$ | [-] | axial strain of a load stage |
| f | [-] | calculation factor |
| F | [N] | force |
| h_0 | [mm] | initial specimen height of the oedometer grains |
| k | [N/mm ²] | contact stiffness |
| k_R | [N/mm ³] | radial spring stiffness |
| K_n | [N/mm ²] | normal stiffness |
| K_t | [N/mm ²] | tangential stiffness |
| m | [kg] | particle mass |
| μ | [-] | friction ratio |
| ν_i | [-] | poisson ratio |
| R_i, r_i | [mm] | particle radii |
| R_T, r_i | [mm] | tunnel radius |
| s_i | [mm] | compression / displacement in z-direction |
| σ_n | [N/mm ²] | normal stress |
| $\sigma_{n,i}$ | [N/mm ²] | normal stress of a load stage |
| σ_R | [N/mm ²] | radial stress |
| τ | [N/mm ²] | shear stress |
| u | [mm] | shear distance |

| | | |
|------------|---------|--------------------|
| u_R | [mm] | radial deformation |
| ω_i | [rad/s] | angle velocity |
| φ | [°] | friction angle |

Shortcuts

DEMDiscrete Element Method / Distinct Element Method

FEM.....Finite Element Method

PFCParticle Flow Code (Itasca)

TBM.....Tunnel boring machine

EBT(german) Empfehlung zur Berechnung von Tunneln im Lockergestein

1 Introduction

For tunnels driven by shield machines, the outer lining usually consists of reinforced concrete segments. Tunnel linings can only reach a stable and low deformation structural behavior, if the deflection forces within the segments are stabilised sufficiently. Due to the reason, that the segment is produced and applied in very high quantities, the different construction stages have to be investigated as detailed as possible. Therefore, the exact deformation behavior of pea gravel within the annular gap is essential.

This thesis is organized in three main parts. The first part (Chapter 3) represents the theoretical background of the discrete element method. Further details of this method applied in this research are given. Chapter 4 contains the calibration part, all numerical input parameters and validations on laboratory tests. The main task of this part is to elucidate all input parameters and clarify all assumptions of this thesis. Chapter 5 shows the application of this method on numerical models. Based on two models, the applicability of the discrete element method for the deformation behaviour for pea gravel is given. A brief conclusion and a final outlook are summarizing some ideas and information for further research. All elaborated Abaqus codes are attached.

1.1 State of the art

1.1.1 Bedded frame model

The bedded frame model method is currently the state of the art in the German-speaking area for designing segments. A clear description of this model and the important literature is stated.

Table 1 shows the development of different calculation methods for segmental linings in tunnel constructions since 1944. The bedded frame model was developed by Anders Bull in 1944 and is still, in an adapted form, a frequently used method. The theory of second order was hereinafter developed and applied. Some additional details were investigated in the following years. From 1990 to 2000 the design of the longitudinal and radial joints was further developed.

Table 1: History of the development in the calculation method for tunnel segments
(Girmscheid, 2013)

| | author | topic / problem definition | year |
|---|---|--|---|
| 1 | Bull A. | elastic embedded circular ring, earth pressure approach | 1944 |
| 2 | Duddeck H., Schulze H. | elastic embedded circular ring, new earth pressure approach | 1964 |
| 3 | Windels R., Hain H. | second order theory of the elastic embedded circular ring | 1966/68 |
| 4 | Hain H., Falter B. | second order theory of the elastic embedded circular ring taking into account the pin-joint moments | 1975 |
| 5 | Melder V. | approach of coupling for offset rings - stiffness of the longitudinal joints - elastic ring-joint-coupling using the approach of Kaubits (because of the creeping visco-elastic material is the approach of the temporary elastic behaviour insufficient) | 1975 |
| 6 | Duddeck H. Ahrens H., Lux K. H., Lindner E. | recommondations for the dimensionation of tunnels respectively shield driven tunnel in soft ground - action - spare footbed approach k_r, k_t - bedding development for $h < 2d, 2d < h < 3d$ - loads, earth pressure approach, pre-displacements - evidences | 1982-86 |
| 7 | Baumann T. | constructive design of the longitudinal joint (see Leonhard/Reimann) | 1992 |
| 8 | field tests: Wayss + Freitag / material testing institute for civil engineering, Munich Dywidag / Underground - Nuremberg / Dywidag material testing institute munich Wesertunnel / IBMB - TU Braunschweig ARGE 4. Tube Elbtunnel / STUVA Cologne | clarification of the load bearing behaviour: - longitudinal joints - longitudinal joints - longitudinal and ring joints - Längsfugen und Ringfugen, behaviour of the combination, shearing, behaviour of the whole ring | 1972 1989 1992 1996-97 |

The outer lining of a tunnel is a thin curved layer. This layer can be modelled as several connected 2D beams bedded with springs. Using Equations 1 and 2, the spring stiffness is calculated.

$$\sigma_R = u_R k_R \quad (1)$$

$$k_R = f \frac{E_S}{RT} \quad (2)$$

Equation 1 defines the radial stress by the product of the radial displacement and the radial spring stiffness. A factor f represents the spring stiffness, which is usually assumed with 1.0 multiplied with the stiffness modulus of the bedding divided by the tunnel radius.

In Figure 1 the approach for the radial bedding discretization is shown. The deformations of the segments are calculated under the use of springs around the tunnel. The spring stiffness should be equal to the extension of the region r around the tunnel. (Thienert, et al., 2011).

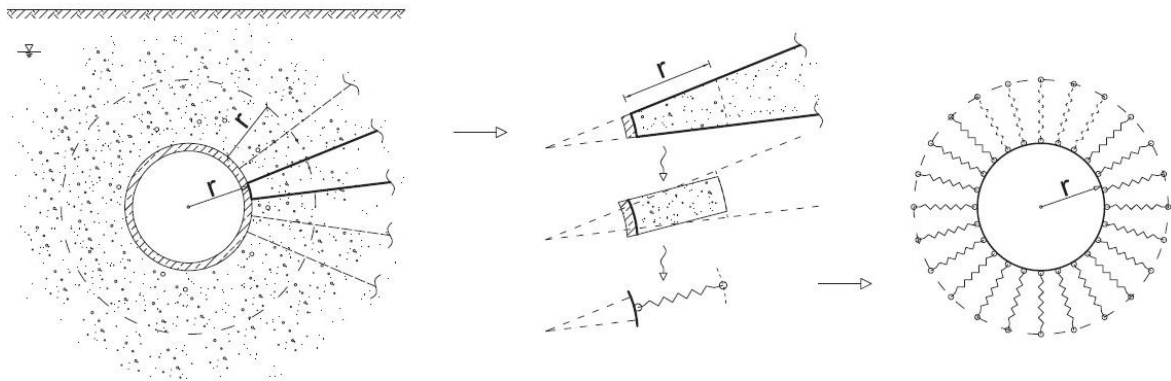


Figure 1: Approach for the radial bedding (Duddeck, 1972)

In case the pea gravel filled annular gap, the spring stiffness is evaluated using Equation 3. To obtain the radial spring stiffness, the stiffness of the pea gravel is divided by the thickness of the annular gap (Behnen, et al., 2013).

$$k_R = \frac{E_{S1}}{d_1} \quad (3)$$

Figure 2 shows different bedding situations for tunnels in soft ground. Version (a) shows a fully bedded outer lining represented by radial springs. Situation (b) is partially bedded neglecting the crown with additional bedding in tangential direction of the excavation boundary. In (c) the bedding situation equals version (b) without any tangential springs. The fourth bedding situation (d) removes the springs in the bench and in the crown. In this situation, the springs are tension free.

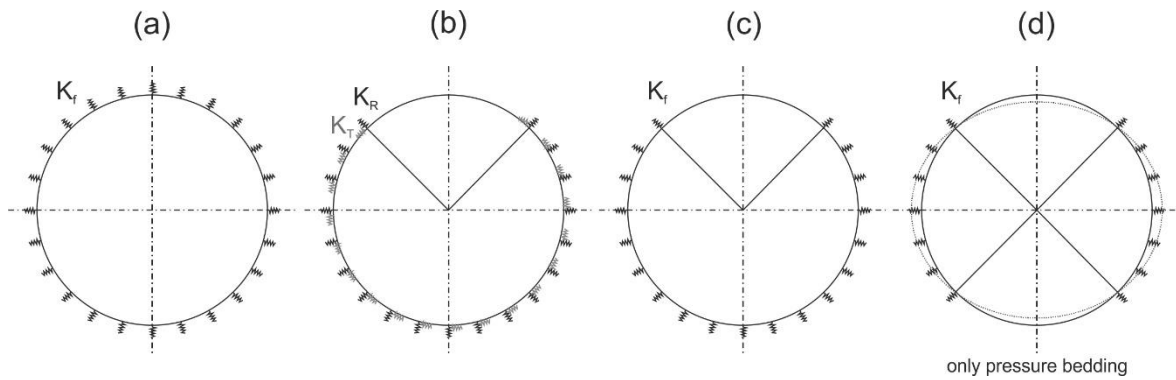


Figure 2: Calculation methods of the beam spring model for tunnels in soft ground
(Behnen, et al., 2013)

The bedding approach was summarized in the EBT (German for: recommendations for calculations of tunnels in soft ground) which is listed in Table 2.

Table 2: Bedding approach of the EBT

| Variable | overburden | Spring stiffness formulation |
|----------------|------------|------------------------------|
| Shallow tunnel | $< 2 D$ | $k_R = \frac{E_S}{R}$ |
| Deep tunnel | $\geq 3 D$ | $k_R = 0,50 \frac{E_S}{R}$ |

Considering calculating the deformations in the longitudinal and radial gaps or openings in cross passages, restrictions of this calculation method are reached. Therefore, 3D finite element models are useful to model these problems obtaining proper results.

1.1.2 Double shield machine

For a proper design of the numerical models a background of the double shield machine is given.

Figure 3 shows a double shield TBM. Basically the machine consists of two shields connected by the front thrust cylinders. The front shield containing the main bearing, the cutter head and the front thrust cylinders. The gripper shield contains the grippers, the rear thrust cylinders and the gripper shield sealing.

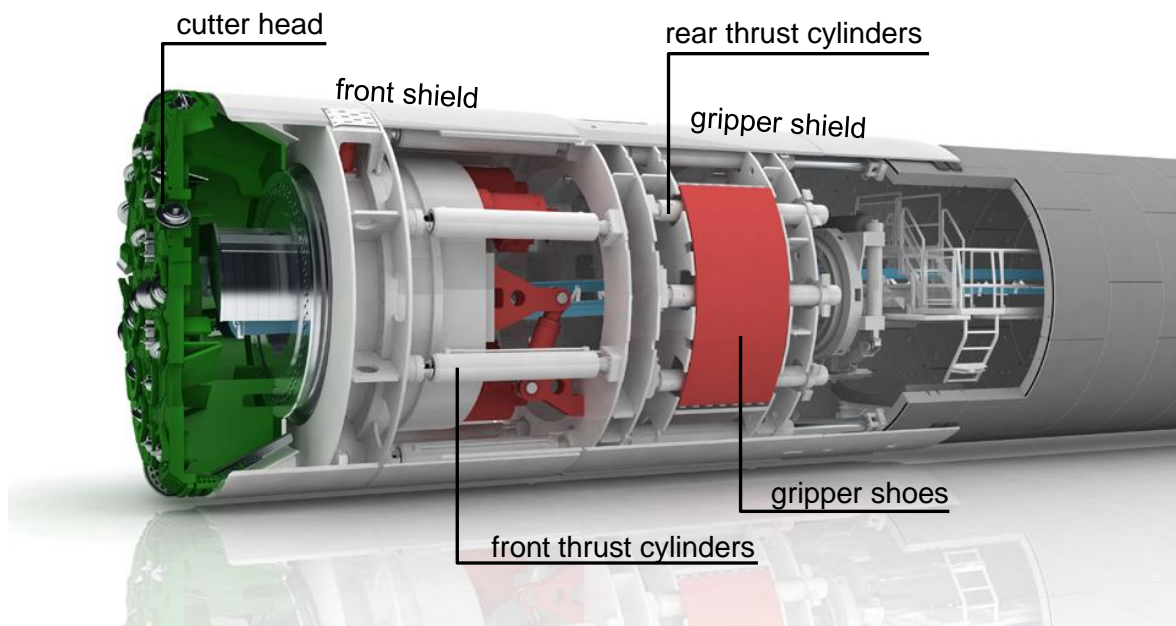


Figure 3: Double shield TBM (Herrenknecht)

While installing the support, which is represented by reinforced concrete segments, the DSM presses the cutter head against the tunnel face using the grippers and the front thrust cylinders. The rear thrust cylinders support the last ring of lining segments. The main advantage of this machine type is that the advance is not interrupted by the installation of the support.

The contact between the surrounding rock and the lining segments is provided by the backfilling. The backfilling consists of mortar, pea gravel or a combination of both.

At every excavation step the machine and the whole gantry is advanced by one width of the segments in the direction of the excavation. The rapid advance of the rear shield of a DSM after a boring stroke has been completed, increases the unbedded area by removing the abutment of the backfilled material in the annular gap. This leads to shear failure of the pea gravel and to relocation within the annular gap. Therefore, the position of the backfill within the annular gap is unknown and can be estimated only.

1.2 Definition of objectives

After a definition of the state of the art, all objectives for this thesis are defined:

1. **Applicability of FLAC3D**

FLAC3D is common software for solving numerical problems of tunnels and general excavation problems. An application of this software for different bedding situations and furthermore the implementation of the interfaces should be carried out.

2. **Applicability of the software Abaqus using the discrete element method**

Abaqus implemented in its newest update 6.13 (2013) the discrete element method. This research verifies the application of this method for this problem.

3. **Validation of the discrete element method**

Using DEM, a validation of the numerical particles is necessary. A comparison of numerical and laboratory tests determines the material parameters for further computational calculations.

4. **Application of the DEM on the annular gap problem**

Due to its similarity, discrete spheres model the pea gravel. This research elaborates the applicability for the annular gap.

5. **Design of a numerical model for future developments**

A numerical model for future research should be provided. As soon as the computational capacity and the simulation time are available, these calculations can be executed.

6. **Outlook of this method for further research**

An application on prospective problems of this method is shown and its pros and cons are discussed.

2 Applicability of FLAC3D

The initial problem definition of this thesis was to determine the influence of the segment bedding on the outer lining of the tunnel.

To elaborate the influence of the bedding, it is necessary to know the actual behavior of the bedding structure. Therefore, we started using the software FLAC3D (Itasca) to design a numerical model, which represents the conditions on the construction site.

Figure 4 and Figure 5 show the excavation and installation steps of the FLAC3D calculation.

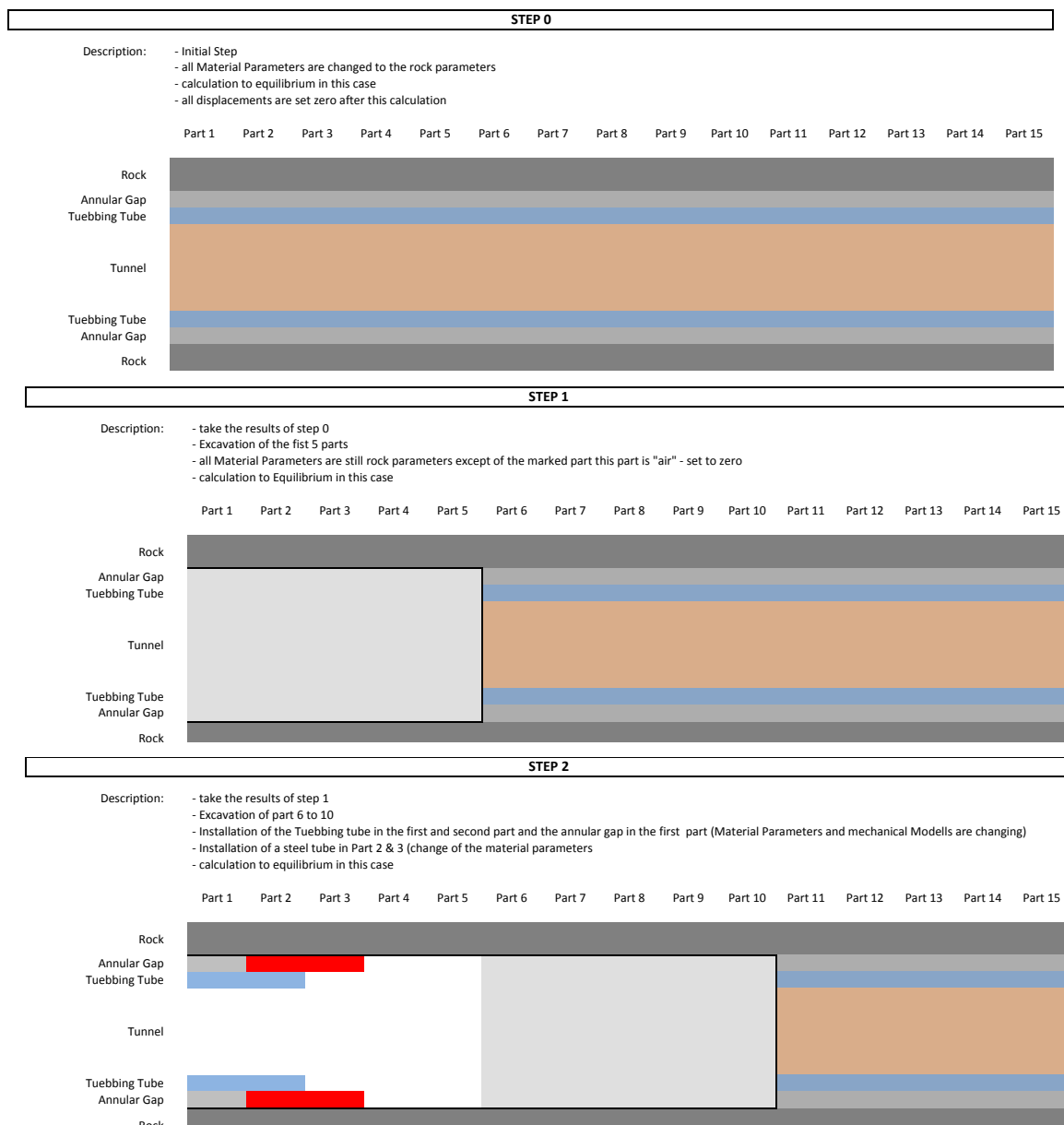


Figure 4: Calculation process and descriptions in FLAC3D (1)

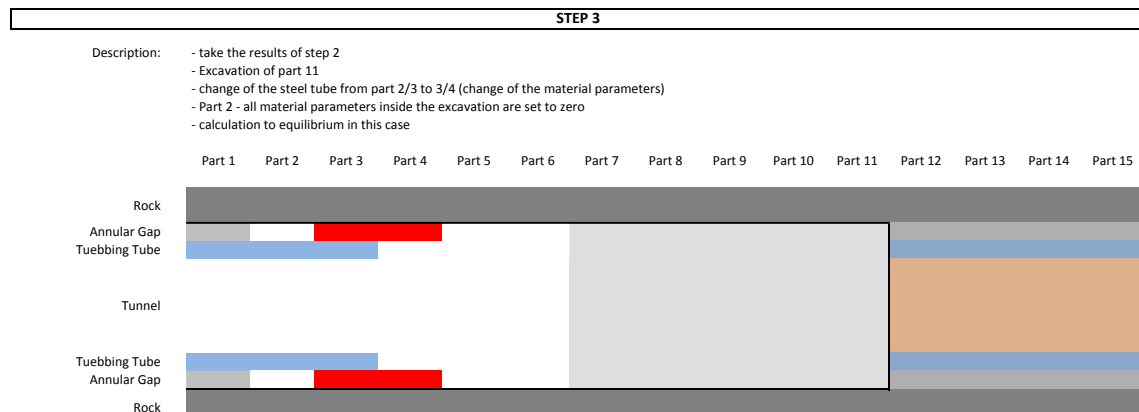


Figure 5: Calculation process and descriptions in FLAC3D (2)

A proper mesh design was essential for a calculation process shown in Figure 4 and Figure 5. All parts should be able to activate and deactivate which leads to the mesh shown in Figure 6.

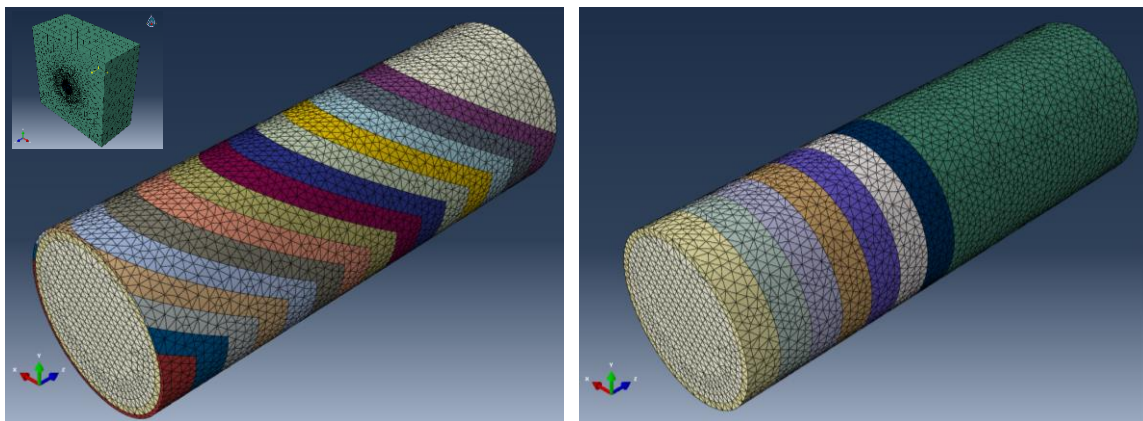


Figure 6: Mesh design for the FLAC3D model (the small picture in the left corner shows the full model)

Figure 6 shows the export mesh of the software Abaqus and the input mesh for FLAC3D, respectively. This mesh includes all the segments and different annular gap situations of the predefined steps. The left plot shows the inclined annular gap, which was assumed after the regripping process. The interaction properties and their position within the model had to be assumed based on existing literature.

Figure 7 shows the defined interactions fixed on the nodes. Pictures (a) and (b) show the interaction grid between the annular gap and the rock (cyan) as well as the annular gap and the segments (red). Additionally the interaction grid between the segments itself in longitudinal (green) and radial (blue) direction are shown in (c) and (d).

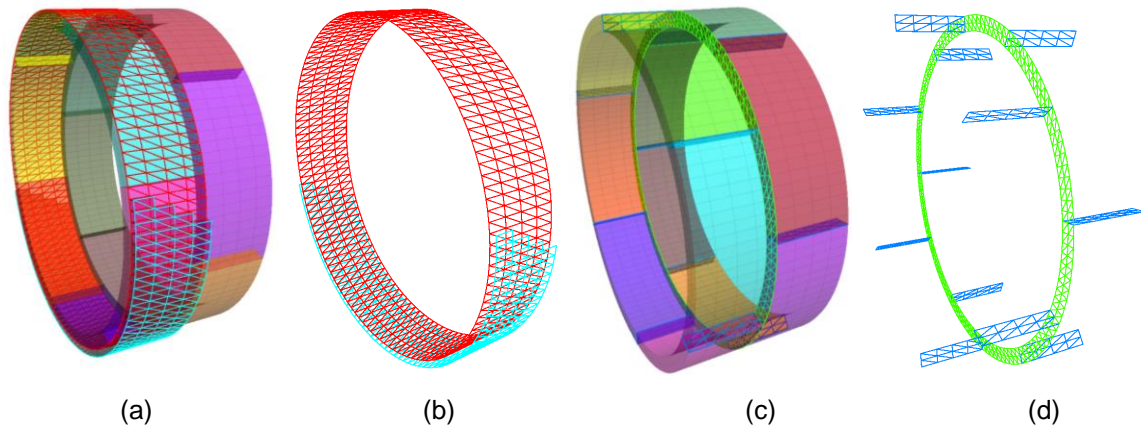


Figure 7: Definition of the interactions in the FLAC3D model

Due to the large deformations in the annular gap, a finite element/difference method is hardly implementable and the results may not be representative. A proper way for a design of a numerical model for this problem is the discrete element method. Using Abaqus 6.13 (2013) the model can be discretized combining finite and discrete elements.

3 Discrete Element Method

In general, the discrete element method (DEM) is a numerical method for the calculation of movements of a large number of particles in every size. Based on Newton's second law of motion this method uses simple contact mechanics. Cundall first introduced DEM in 1971 for the simulation of jointed rock. Since then the progress in this method was significant. Cleary & Campbell (1993) did further developments for simulations of landslides and Hopkins (1991) for a simulation of ice flows. To model the behavior of pharmaceutical powder (Johnson 2005, Yang 2002) as well as excavation and mixing problems (Cleary 2000) was the next step. Cundall's idea was first applied on 2D disks, later 3D spheres were implemented. Today it is possible to model any shape of particles. In every single time increment, the contacts are detected and equilibrium iteratively established. Due to this fact, this method needs high performance computers and the development became popular since computers are able to calculate millions of numbers of particles on a single processor.

Figure 8 shows the actuality of this computational method. The number of publications in the past 28 years were rising rapidly. The first publication was found in 1986. In 2013, 285 papers with keywords addressing discrete element, distinct element or discrete particle simulation have been published.

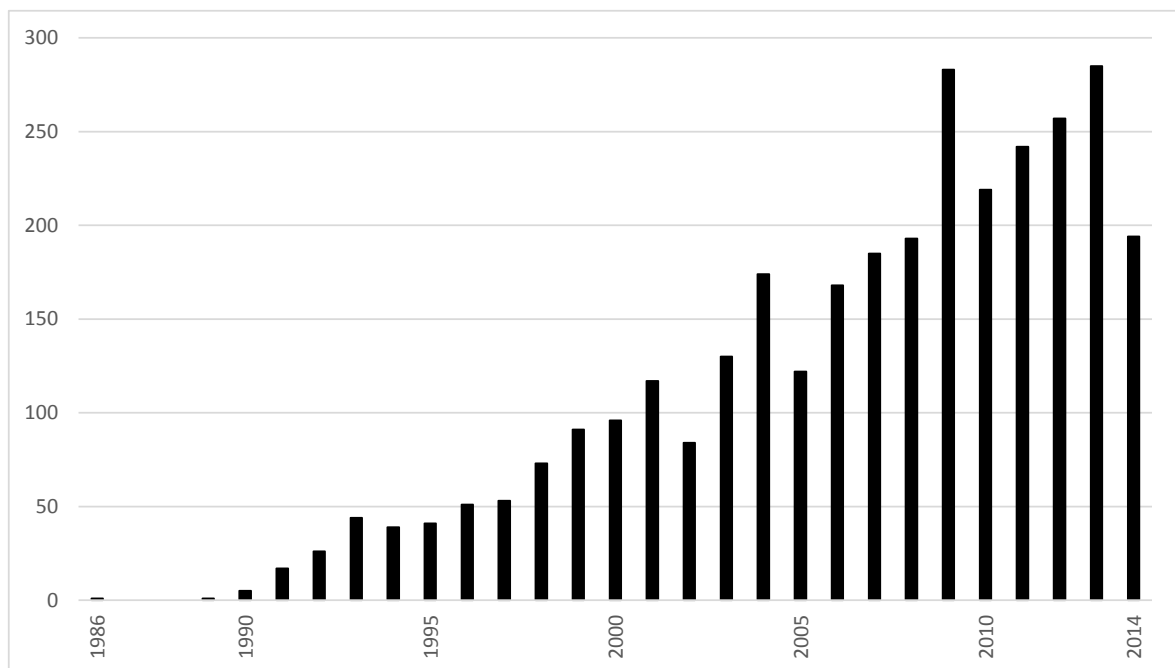


Figure 8: Number of publications related to discrete particle simulation in the recent 28 years (status as of 29th of September 2014), obtained from Web of Science

3.1 Discrete Element Method in Abaqus

With version 6.13 (2013) Abaqus provides the particle code based on the theory of Cundall (1971). It allows modelling individual particles with a rigid ball shape. The particles consisting of one node are implemented as linear elastic elements and have a uniform radius and density.

This method is typically used in calculations with a large number of discrete particle elements interacting with each other and other bodies. Furthermore, the DEM can be used in combination with finite elements for modeling discrete particles interacting with deformable continua or other rigid bodies. The calculation method has to be an explicit dynamic analysis.

Limitations of this method in the current Abaqus 6.13 Version:

(Extract from: ABAQUS 6.13 Documentation , 2013)

- In a multidomain analysis all PD3D elements will be forced to be in one of the domains.
- Volume average output for stress, strain, and other similar continuum element output is not available for DEM analysis.
- Only a ball shape is supported for PD3D elements.
- It is not possible to specify cohesive or thermal contact between PD3D elements or between PD3D elements and other elements.
- Rolling friction is ignored for contact between PD3D elements or between PD3D elements and other elements.
- Although supported in Abaqus/Viewer, the functionality is not supported in Abaqus/CAE. One can use the existing functionality in Abaqus/CAE to generate mass elements, write an input file, and then manually edit the input file to convert the mass elements to particles. Alternatively, one can create a mesh using C3D8R elements, write an input file, and then use a script to convert these elements to particles.

3.2 Contact Law

Figure 9 shows the general contact formulation in Abaqus with all its variable parameters. Between particle 1 and particle 2, the normal stiffness K_n and damping factor C_n are defined. The tangential contact properties tangential stiffness K_t , tangential damping C_t and the friction coefficient μ are acting perpendicular to that direction.

The particle itself is defined with the radius R_i , angular velocity ω_i and the coordinates u_i and v_i .

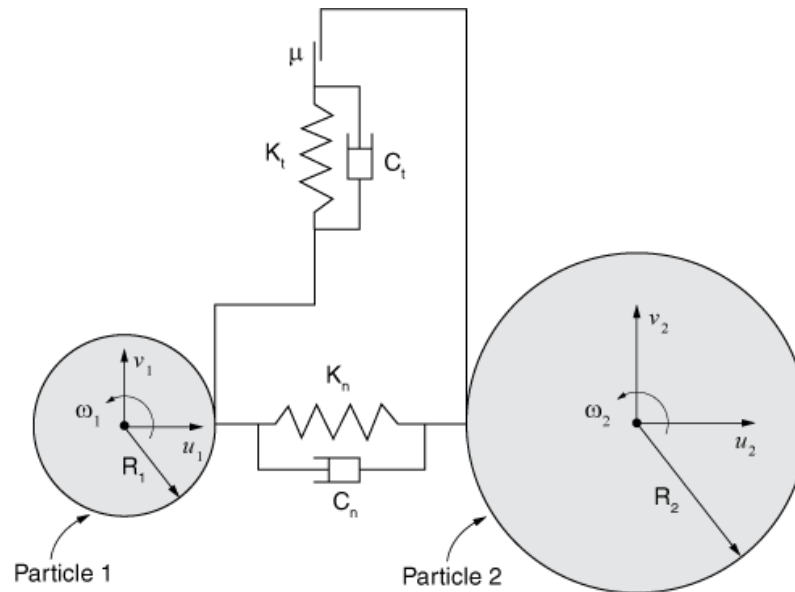


Figure 9: General form of the contact law (Abaqus 6.13 Documentation, 2013)

In discrete element calculations, the contact law describes the behaviour between two particles and between a surrounding rigid or deformable surface and the particle, respectively. In Abaqus this is implemented as a clearance/overclosure – contact force formulation. In general, the more overclosure the higher is the contact force.

$$\delta = r_1 + r_2 - d \quad (4)$$

Figure 10 shows three different states of particles. For this research, the particle itself is rigidly discretized with a linear elastic determination of the penetration due to the contact formulation.

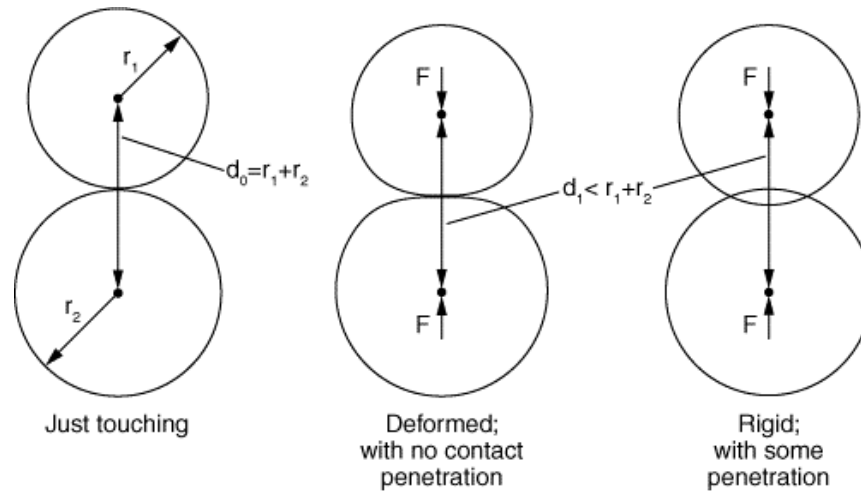


Figure 10: Interactions between ball shaped particles (Abaqus 6.13 Documentation, 2013)

Overclosure δ is zero if the spheres are just touching each other. With the definition of the overclosure, contact forces are only acting when δ becomes negative.

There are some technical problems existing where contact forces are acting if there is a clearance, which are neglected in this research due to the reason that these forces are very small.

Figure 11 and Figure 12 shows provided Contact laws in Abaqus. A linear and non-linear contact formulation is shown in Figure 11 while Figure 12 shows an incremental formulation based on the given equation.

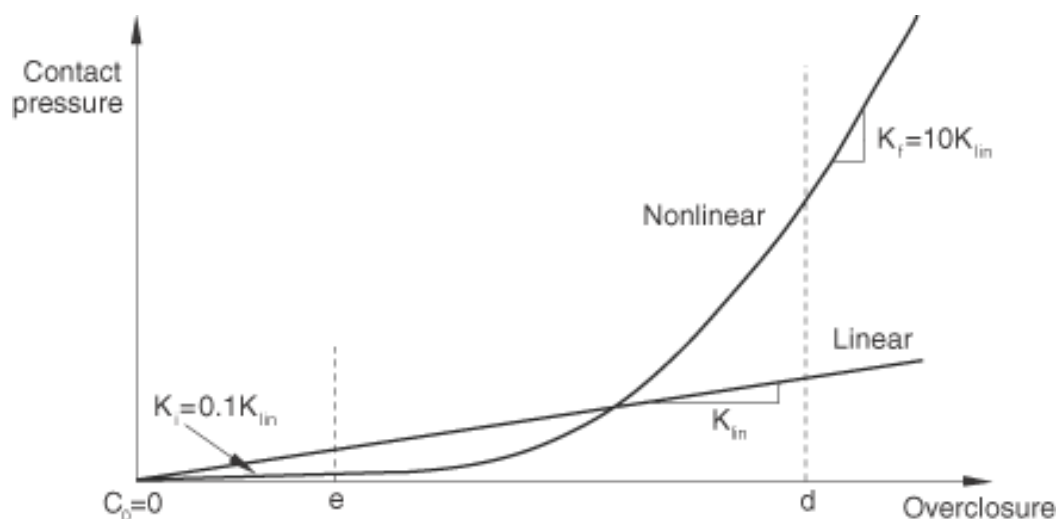


Figure 11: Comparison of linear and nonlinear contact laws

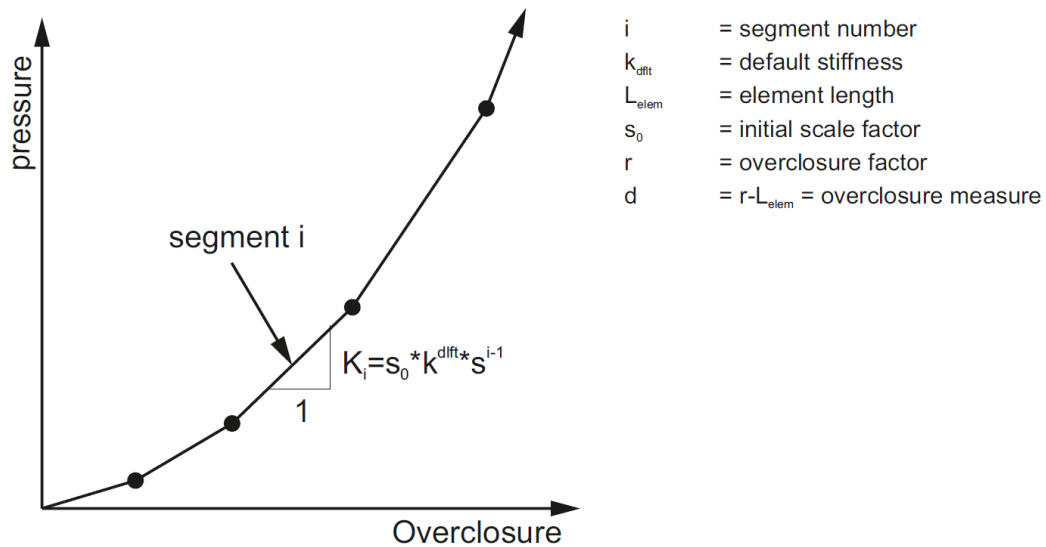


Figure 12: “Softened” scale factor pressure-overclosure relationship

For the problem if two spheres are getting in contact the overclosure – pressure relationship is not linear. The more overclosure the spheres have the more contact force is acting because the area of contact increases with the overclosure.

For this special problem, Heinrich Hertz provided an analytical approach in 1882. The deformation of an elastic Half-space being under the influence of surface forces is described in Chapter 3.2.1.

3.2.1 Hertz Contact Formulation

The Hertz Contact Formulation describes the contact interaction between two elastic bodies. It was solved by Hertz (1982) and is still a state of the art solution.

The contact stiffness is not linear because F is not linearly dependent on δ . Equation 5 defines the relationship for a given value of overclosure between two particles.

$$K = \frac{dF}{d\delta} = 2E^* \sqrt{R} \sqrt{\delta} \quad (5)$$

The Hertz contact solution (Equation 6) defines the contact force F , between two remote points using the approach distance, δ , the corresponding radius, R (Equation 7), and the modified elastic modulus, E^* (Equation 8).

$$F = \frac{4}{3} E^* \sqrt{R} \sqrt{\delta^3} \quad (6)$$

$$R = \frac{R_1 R_2}{R_1 + R_2} \quad (7)$$

$$\frac{1}{E^*} = \frac{1 - \nu_1^2}{E_1} + \frac{1 - \nu_2^2}{E_2} \quad (8)$$

The following variables are necessary to be defined:

(Chapter 4.2 contains a parametric study on the given variables)

Table 3: Variable definition of the Hertz contact solution

| Variable | Unit | Description |
|--------------|----------------------|---|
| F | [N] | contact force |
| E^* | [N/mm ²] | modified elastic modulus |
| R (case 1) | [mm] | modified radii (in case two spheres are in contact) |
| R (case 2) | [mm] | radius of a sphere which is in contact with an elastic half space |
| δ | [mm] | overclosure |
| R_i | [mm] | radii of the different spheres |
| E_i | [N/mm ²] | elastic modulus of the different spheres |
| ν_i | [-] | poisons ratio of the different spheres |

Contact Mechanics and Friction: Physical Principles and Applications p.55 ff. (Popov, 2010) provides detailed information on the Hertz contact solution.

The application of this contact formulation was done in an Excel file. This file represents the contact formulation for two particles with the same size and a planar surface respectively. It calculates the contact force associated to a special value of overclosure. The range between 0.005% and 20% of the particle radius defines the overclosure. Within this range, the Excel sheet generates 200 values. An Excel-macro converts these values into a text document, which is readable for the Software Abaqus. The source code of this macro is attached in the Annex A of this thesis.

3.3 Particle packing / Initial Placing

The initial process of particle placing is a complex procedure. Usually the particles are placed initially touching each other and settling during the first explicit dynamic step under gravitational influence.

The duration of this process/step depends on the number of particles and complexity of the geometry. Usually it is necessary to start a “test run” in order to obtain the time for the placing process.

Figure 13 shows the initial process. To the very left the initial state, every sphere is touching each other with no overclosure (in all three directions). The following steps show the settlement during the initial process leading to a randomly placed pack of particles in static condition.

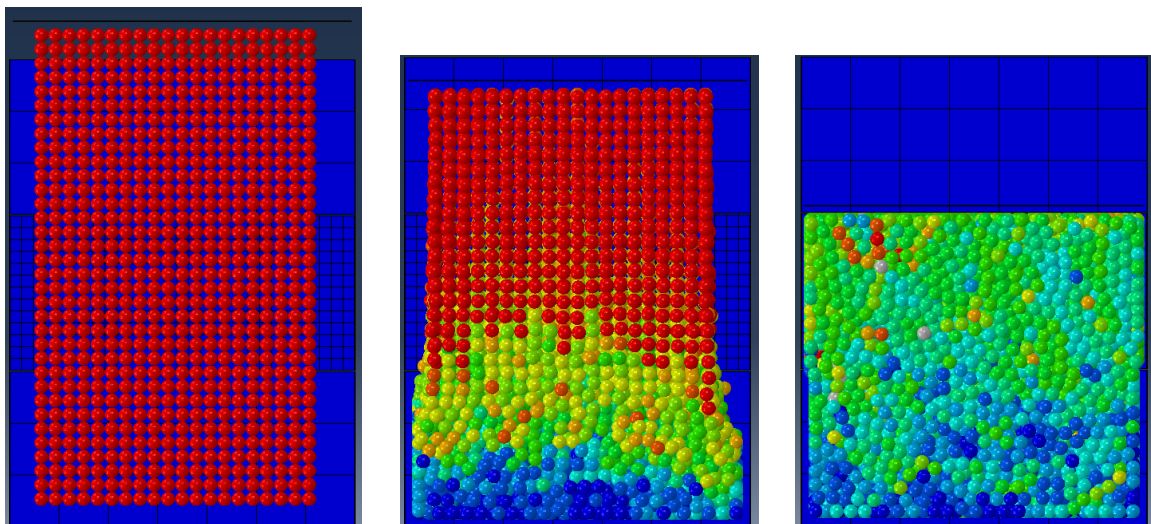


Figure 13: Process of particle placing

The model shown in Figure 13 has about 14.000 particles, the geometry is simple and it takes approximately 0.70 seconds in real-time for this initial step.

To create particle elements in Abaqus it is necessary to produce cubic elements first. After meshing them (C3D8) a particle element can be associated at every node by changing the mesh type (PD3D).

Equation 9 shows the space for this kind of initial particle placing:

$$\frac{\Sigma V_{shere}}{\Sigma V_{space}} = \frac{\Sigma \frac{1}{6} \pi D^3}{\Sigma D^3} = \frac{1}{6} \pi = 0.524 \triangleq 52.4\% \text{ of the full space} \quad (9)$$

3.4 Incrementation

“For dense three-dimensional packing of particles where each particle simultaneously contacts many particles, the numerical stability considerations are complex” (Abaqus 6.13 Documentation, 2013)

Concerning the reason that the particles are rigid the incrementation should be fixed and not like the most Abaqus Explicit problems with an automated control of the time incrementation. The incrementation bases on the stiffness and the mass properties of the model.

Abaqus suggests an incrementation range in order to avoid instabilities. Equation 10 is the maximum and Equation 11 is the minimum value of the incrementation.

$$0.4 \sqrt{\frac{m}{k}} \quad (10)$$

$$0.1 \sqrt{\frac{m}{k}} \quad (11)$$

Table 4: Variable Definition

| Variable | Unit | Description |
|----------|----------------------|-------------------|
| m | [t] | Particle mass |
| k | [N/mm ²] | Contact stiffness |

“If particle velocities become very large, the amount of incremental motion can influence the appropriate time increment size. Accurate resolution of particle motion sometimes requires specifying a smaller time increment than the maximum numerical stability time increment.” (Abaqus 6.13 Documentation, 2013)

Table 5 shows the used incrementations of this thesis, depending on the particle stiffness.

Table 5: Time incrementations depending on the particle stiffness

| particle stiffness | time increment |
|--------------------|-------------------|
| 20 GPa | $5 \cdot 10^{-5}$ |
| 50 GPa | $5 \cdot 10^{-6}$ |
| 100 GPa | $2 \cdot 10^{-6}$ |

Selecting a Suitable Time Step for Discrete Element Simulations that Use the Central Difference Time Integration Scheme (O'Sullivan, et al., 2004) provides more information about the determination of the incrementation.

3.5 Calculation procedures

Figure 14 shows the calculation procedure of a discrete element analysis.

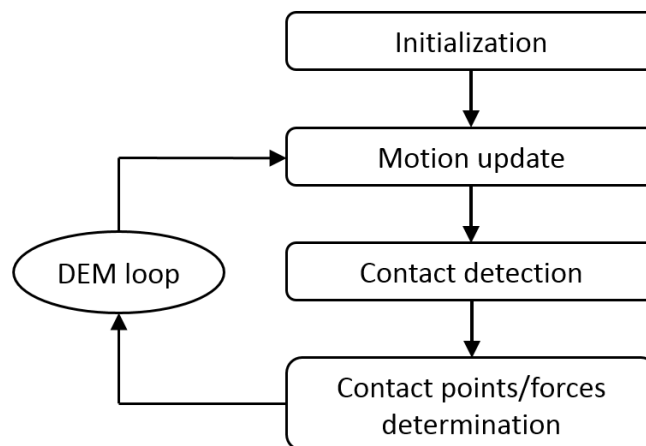


Figure 14: Calculation procedure of a DEM calculation (Lin, 2013)

After an initialization process, the software updates the motion of the particles, and exact positions for this incremental time step are determined. Contact detection follows. For this part, the distances between all particles in the model are determined. In case the distance is shorter or equals the sum of both radii specific contact forces can be evaluated. This loop continues until the explicit calculation is taking place. The user is defining the time for this process. The evaluation of this time should be carefully selected since a static state might not be reached.

3.6 Software for discrete element problems

Table 6 shows software solutions of the current products for DEM Simulations and gives a brief overview of the latest developments.

Table 6: Software solutions for DEM problems

| software | company | | first release | current version | |
|------------|-------------------|-------------|---------------|-----------------|----|
| Abaqus CAE | Dassault Systemes | commercial | 6.13 (2013) | 6.14 | 3D |
| PFC 2D | Itasca | commercial | PFC 1 (1994) | PFC 5 | 2D |
| PFC 3D | Itasca | commercial | PFC 1 (1994) | PFC 5 | 3D |
| EDEM | DEM solutions | commercial | 1.0 (2006) | 2.5 | 3D |
| YADE | - | open source | 0.20 (2009) | 1.11.0 | 3D |
| LIGGGHTS | - | open source | Beta 1 (2010) | 3.0.3 | 3D |

4 Calibration

First, it is necessary to calibrate all material parameters by simulating laboratory tests numerically. A description of assumed input parameters is given. Table 7 shows continuous units declaration.

Table 7: Units declaration

| parameter | used in this work | SI - Units |
|-------------|-------------------|------------|
| length | $[mm]$ | $[m]$ |
| density | $[t/mm^3]$ | $[kg/m^3]$ |
| force | $[N]$ | $[N]$ |
| stress | $[N/mm^2]$ | $[N/m^2]$ |
| gravitation | $[mm/s^2]$ | $[m/s^2]$ |

All calculations were done without scaling. The goal of this research was a numerical simulation of the laboratory tests.

X. Ding et al (2013) give a brief overview on the effect of particle size distribution on the simulated macroscopic mechanical properties, unconfined compressive strength (UCS), Young's modulus and Poisson's ratio.

4.1 Input Parameters

Table 8 shows the initial assumptions of the input parameters. Each parameter in the following Chapters is described in detail.

Table 8: Initial Input Parameters

| parameter | Initial value | unit |
|--|----------------------|-------------------|
| particle diameter | 10.0 | mm |
| shape | Sphere | |
| friction coefficient - $\tan(\varphi)$ | 0.70 | |
| elastic modulus | 20,000.0 | N/mm ² |
| Poisson ratio | 0.20 | mm/s ² |
| density | $2.60 \cdot 10^{-9}$ | t/mm ³ |
| mass proportional damping factor | 7.0 | % |
| shearing speed | 3.0 | mm/sec |

4.1.1 Particle Diameter

Figure 15 shows the grain size distribution of the pea gravel. This pea gravel is a closely graded material with a D_{50} of 9.2 mm. The variation of the grain size for the numerical studies was done between 8.0 mm and 10 mm. Due to the numerical limitation it is not possible to generate such a grain size distribution in the computational model. Initially the diameter was set to 10.0 mm.

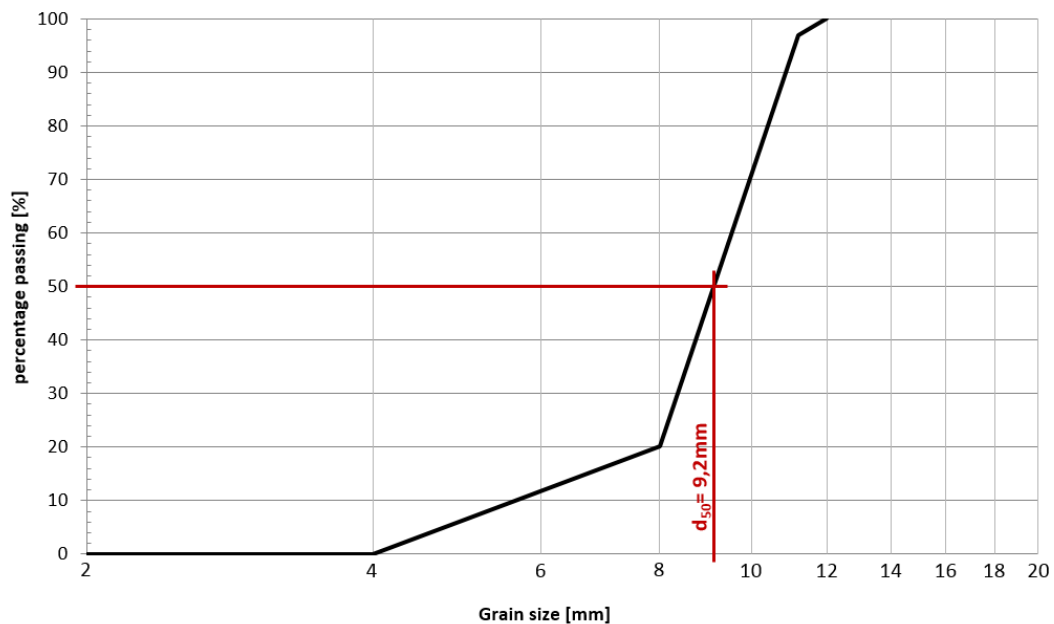


Figure 15: Grain size distribution of pea gravel

4.1.2 Particle shape

Using the DEM implementation of Abaqus, Abaqus 6.13 (2013) provides only ball shaped particles. Figure 16 compares circles with pea gravel in order to illustrate computational deviation of the numerical discretization.



Figure 16: Discretization of the pea gravel

4.1.3 Friction coefficient

Table 9 describes the friction behaviour between the discrete elements itself and between the discrete and the finite elements. The wall friction angle is $2/3$ times the inner friction angle between the particles, which is a common assumption for rough concrete walls.

Table 9: Friction coefficient

| friction between | $\tan(\varphi)$ | φ |
|------------------------------|-----------------|----------------------|
| discrete elements | 0.70 | 35° |
| discrete and finite elements | 0.43 | $\tan(2/3 \cdot 35)$ |

4.1.4 Elastic modulus / poisson ratio of the intact rock

To establish the elastic modulus of intact rock of the pea gravel grain is hardly possible. For this parameter, a parameter study was performed.

This pea gravel is a fluvial sediment out of the river Danube, therefore the elastic modulus can be assumed within a range of 20 and 100 GPa.

The Poisson ratio was set to 0.20, which is a reasonable value for rock in this category.

4.1.5 Density

To establish the density several immersion weighting tests were performed. The tests show a consistent value of $2.6 \cdot 10^{-9} \text{ t/mm}^3$ (2600 kg/m^3).

4.1.6 Damping Factor

To reduce the solution noise caused by several opening and closing procedures Abaqus suggests a mass proportional damping factor. A common value for rock applications is a mass proportional damping value of 7 %.

4.2 Numerical Tests

Chapters 4.2.1 and 4.2.2 show discussions on performed numerical tests for this research. To determine material parameters, it is necessary to execute numerical studies and compare the results with laboratory tests.

Explicit discrete analyses in Abaqus are done for two laboratory tests, in order to obtain the input parameters for further numerical studies.

In general, it is impossible to add parts during an ongoing calculation process. The below listed parameters are defined separately for each step:

- Duration of the step
- Incrementation
- Contact properties and contact inclusions for the interaction parameters
- Output parameters
- Output interval

If the duration of a calculation step changes, it is advisable to align the output interval of different calculations.

Before starting a calculation, it is necessary to define the needed information. Following listed output variables are defined in the input file. Each variable provides results in all three directions.

- Nodal Output:
 - U – translations and rotations
 - V – translational and rotational velocities
- Contact Output
 - $CFORCE$ – contact force
 - $CSTRESS$ – contact stress

A change of the particle stiffness or particle size leads to an adaption of the incrementation. Because of this discussion, we can state that the stiffer the particles are, the longer the calculation takes.

The execution of a shear test, specifying the shear strength of pea gravel and an oedometer test defining the loading and unloading deformation behavior under known stress conditions. For all numerical calculations, the surrounding surfaces were assumed rigid.

4.2.1 Shear test Calculation

For determining the numerical shear strength of pea gravel, a computational shear test model was designed. After an initial placing process, the particles are loaded with a specified vertical pressure and settle at this state until the horizontal shearing process starts. Due to the transferred horizontal forces from the upper to the lower part of the shear box, it is possible to recalculate the numerical shear stress of the continuum. Using the described assumptions in Chapter 4.1, a real sized shear box was discretized. To keep the numerical calculation time low, the shear velocity was set to 3 mm/sec.

4.2.1.1 Geometry

Figure 17 shows the geometry of the shear box. In the x-y plane, the shear box is a square of 225 mm with a height is 200 mm. On top of this box is the guiding-box, which is necessary to guide the particles during the initial placing process into the lower box. For an application of the vertical stress, a top plate was designed. Its position is on top of the particles, with a surrounding gap of 0.5 mm to the box.

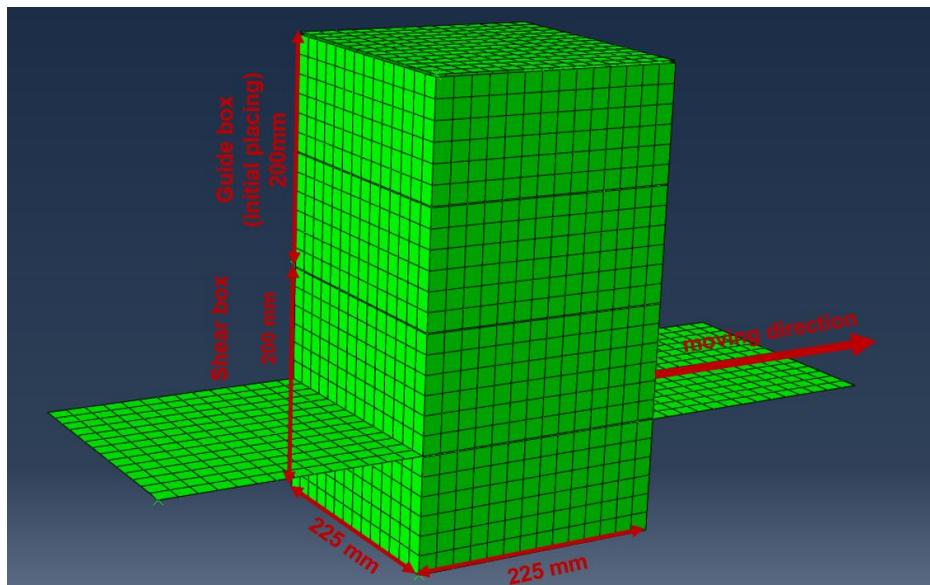


Figure 17: Geometry of the shear box

There are two “wings” placed on both sides of the shear box. These wings prevent the particles from falling out.

Figure 18 shows the initial placing of the particles in the shear box. The initial positions of the particles are just touching to each other. The lowest row of particles has an offset of half a diameter to the upper rows to avoid the straight elastic ball impact.

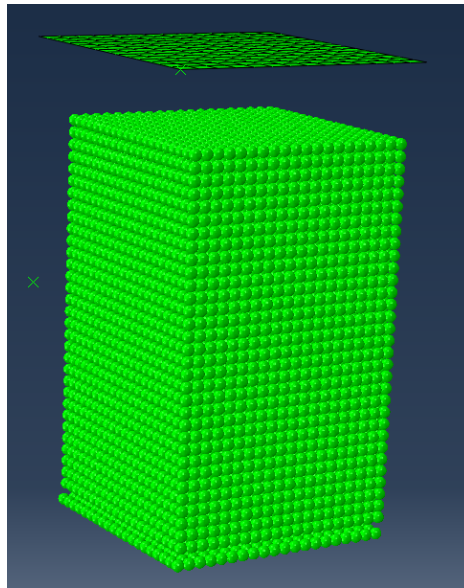


Figure 18: Initial particle positions

4.2.1.2 Definition of the Sets

Figure 19 shows the definition of the sets. Throughout the Abaqus code, it is necessary to access all nodes by the definition of these sets. All nodes with the same set-name have the same material parameters, boundary conditions and surface interactions.

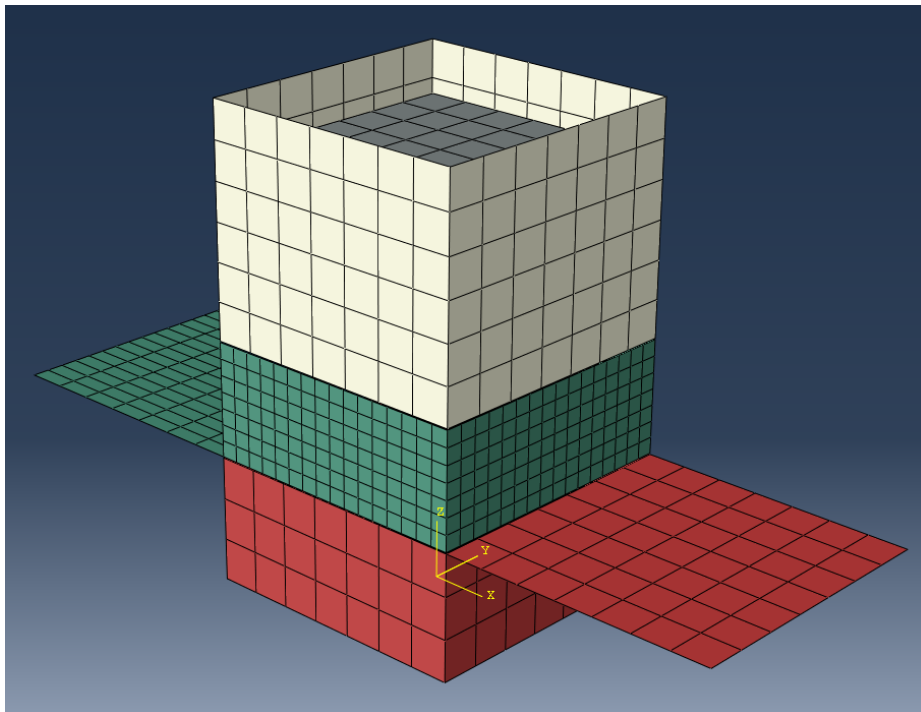


Figure 19: Definition of the sets (box_u – red; box_o1 – green; box_o2 – white; top plate – grey; dem1 – invisible, in the box)

Table 11: Definition of the steps (2)

Step 3 – shearing process

The upper part of the shear box (box_o1, box_o2 and top plate) is moving with a speed of 3mm/sec in x-direction. All other parts are still fixed.

| | Boundary conditions - velocity [mm/sec] | | | | | |
|----------|---|------|------|------|------|------|
| | x | y | z | x-r | y-r | z-r |
| box_u | - | - | - | - | - | - |
| box_o1 | 3.0 | - | - | - | - | - |
| box_o2 | 3.0 | - | - | - | - | - |
| topplate | 3.0 | - | free | - | - | - |
| dem1 | free | free | free | free | free | free |

4.2.1.4 Parameter Variation

Table 12 and Table 13 show the parameter variations of the numerical shear tests. In ascending order of the given test numbers, the plots in the attachment are shown.

Table 12: Parameter variation of the shear test calculation (1)

| | | | 1a | 1b | 2a | 2b | 3 | 4 | 5 | 6 |
|------------|------------------------------------|----------------------|-----------------------|-----------------------|----------|----------|-----------------------|------|-----------------------|------|
| PARAMETERS | | <i>standard</i> | | | | | | | | |
| | Particle Diameter | [mm] | 10.0 | 10.0 | 8.0 | 8.0 | 10.0 | 8.0 | 10.0 | 8.0 |
| | Friction ratio (tanφ) | [-] | 0.70 | 0.50 | 0.70 | 0.50 | 0.70 | 0.70 | 0.70 | 0.70 |
| | E-Modulus intact Rock | [N/mm ²] | 20,000.0 | 20,000.00 | | | 50,000.00 | | 100,000.00 | |
| | Poissons ratio | [-] | 0.20 | 0.20 | | | 0.20 | | 0.20 | |
| | density | [t/mm ³] | 2.60*10 ⁻⁹ | 2.60*10 ⁻⁹ | | | 2.60*10 ⁻⁹ | | 2.60*10 ⁻⁹ | |
| | Damping Factor (Particles) - ALPHA | [%] | 7.0 | 7.0 | | | 7.0 | | 7.0 | |
| | Damping Factor (everything else) | [-] | 0.07 | 0.07 | | | 0.07 | | 0.07 | |
| | Incrementation | [-] | 5.00E-07 | 5.00E-07 | 7.00E-07 | 5.00E-07 | 5.00E-07 | | 5.00E-07 | |
| | shearing speed | [mm/sec] | 3.0 | 3.0 | | | 3.0 | | 3.0 | |

Table 13: Parameter variation of the shear test calculation (2)

| | | | 7a | 7b | 8 | 9 | 10 | 11 | 12 | |
|------------|------------------------------------|----------------------|-----------------------|-----------------------|----------|----------|-----------------------|------|-----------------------|--|
| PARAMETERS | | <i>standard</i> | | | | | | | | |
| | Particle Diameter | [mm] | 10.0 | 10.0 | 8.0 | 10.0 | 8.0 | 10.0 | 8.0 | |
| | Friction ratio (tanφ) | [-] | 0.70 | 0.70 | | | 0.70 | | 0.70 | |
| | E-Modulus intact Rock | [N/mm ²] | 20,000.0 | 200,000.00 | | | 300,000.00 | | 500,000.00 | |
| | Poissons ratio | [-] | 0.20 | 0.20 | | | 0.20 | | 0.20 | |
| | density | [t/mm ³] | 2.60*10 ⁻⁹ | 2.60*10 ⁻⁹ | | | 2.60*10 ⁻⁹ | | 2.60*10 ⁻⁹ | |
| | Damping Factor (Particles) - ALPHA | [%] | 7.0 | 7.0 | | | 7.0 | | 7.0 | |
| | Damping Factor (everything else) | [-] | 0.07 | 0.07 | | | 0.07 | | 0.07 | |
| | Incrementation | [-] | 5.00E-07 | 5.00E-07 | 2.00E-07 | 5.00E-07 | 2.00E-07 | | 2.00E-07 | |
| | shearing speed | [mm/sec] | 3.0 | 3.0 | | | 3.0 | | 3.0 | |

The two mainly varied parameters are the elastic modulus of the intact rock and the particle diameter. In overall, twelve different tests with additional three minor variations on the incrementation were performed.

Four different load stages were performed in order to obtain the shear strength. For each numerical test run a final σ_n / τ plot was generated.

- Load stage 1: 100 kN/m²
- Load stage 2: 200 kN/m²
- Load stage 3: 300 kN/m²
- Load stage 4: 400 kN/m²

4.2.1.5 Evaluation

Due to the constant shearing speed the shearing distance is linearly time dependent. Equation 12 approach was used to evaluate the shear stress from the numerical calculation.

$$\tau = \frac{\sum CFORCE_x}{A_{shear}} \quad (12)$$

$\sum F_{cont}$Sum of all contact forces in shearing direction x at the surface of the set
box_u

A_{shear}Area of the shear plane

All contact forces acting on the set “box_u” (red part in Figure 19) in shearing direction x are summed up to an overall force and divided by the shearing area. The results arising from Equation 12 are calculated at each time step of the calculation.

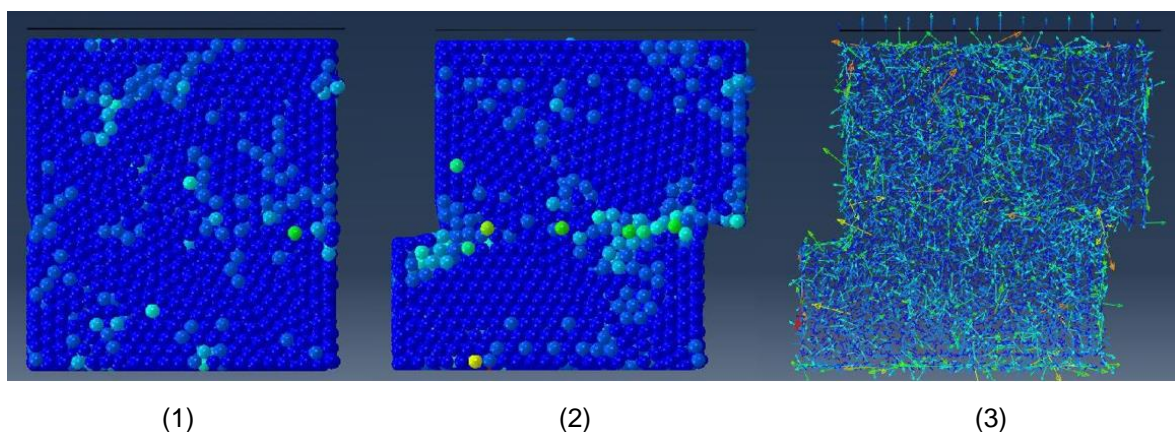


Figure 20: States of the 3D numerical shear test using the software Abaqus – (1) initial state prior to the shearing process; (2) velocities of the particles during the shearing process; (3) contact force vector plot

All plots of the results are summarised in Chapter 4.4.

4.2.2 Oedometer test

To develop the actual behaviour of one-dimensional deformation under incremental loading conditions, an oedometer test was performed. The surrounding cylindrical shaped box prevents the deformation in x-y direction.

A similar testing procedure and parameter variation as applied on the shear test was performed on the oedometer test.

4.2.2.1 Geometry and definition of the sets

The large oedometer test has a diameter of 300 mm. The green set at the bottom (box_u) has a height of 80 mm. Both white segments are used for the particle placing process. A common height-diameter ratio for designing an oedometer test is 3/1 or higher, which is implemented in that model.

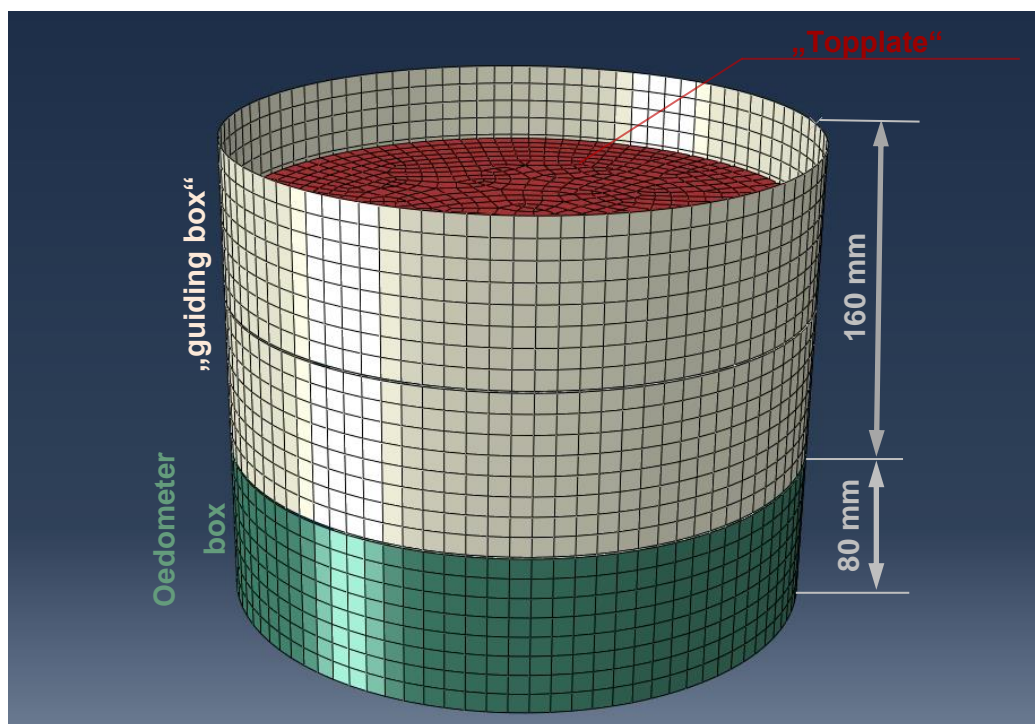


Figure 21: Definition of the sets (box_u – green; box_o – white; top plate – red; dem1 – invisible, in the box)

Figure 22 shows the initial placing of the particles in the oedometer box. The lowest row of particles has similar to the shear test, an offset of half a diameter to the upper rows to avoid the straight elastic ball impact.

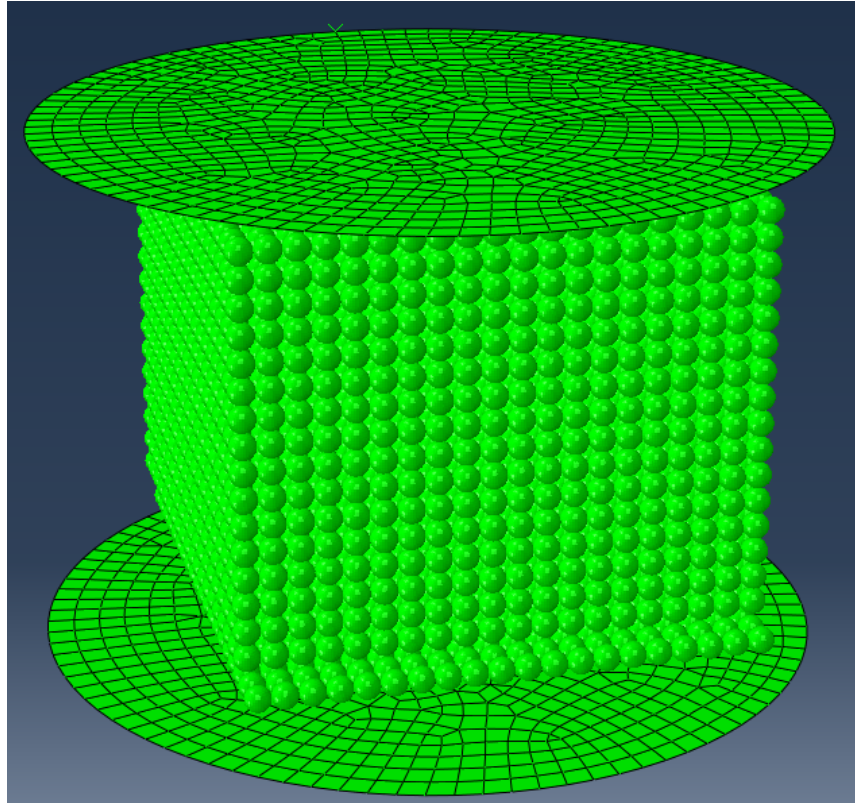


Figure 22: Initial placing of the particles - oedometer test

4.2.2.2 Steps

Table 14 shows a description of the numerical oedometer test steps. The first step represents the initial placing step. Beginning with step 2 different load steps for obtaining the oedometer stiffness is defined. While vertical pressure is applied on the set “topplate”, deformation and contact stiffness in all directions are recorded. The highest vertical stress level applied on the discrete elements was set to 12 N/mm². The stresses within the annular gap are supposed to be within this range. The highest stress level of the laboratory test was 20 N/mm², which led to an irreversible plastic deformation of the grains. DEM does not allow to reproduce this deformation behavior .

4.2.2.3 Parameter Variation

The numerical results of the shear tests have shown, that the diameter variation has minor influence on the results. According to this and due to the longer calculation time of the 8 mm particles for the oedometer test, only 10 mm particles were used. The variation of the elastic modulus of the intact rock was performed in the range between 20 and 200 GPa. Table 15 shows six parameter variations of the oedometer tests. The variations 05 to 08 only differ in the elastic modulus of the intact rock. The input parameters of the test series 09 and 10 vary the friction coefficient between the particles and the surrounding surface to determine the influence of the wall friction.

Table 15: Parameter variation of the oedometer tests

| | | | 05 | 06 | 07 | 08 | 09 | 10 | |
|------------|---------------------------------------|----------------------|-----------------------|-----------------------|-----------------------|-----------------------|-----------------------|-----------------------|-----------------------|
| PARAMETERS | | <i>standard</i> | | | | | | | |
| | Particle Diameter | [mm] | 10.0 | 10.0 | 10.0 | 10.0 | 10.0 | 10.0 | |
| | Shape | [-] | sphere | sphere | sphere | sphere | sphere | sphere | |
| | Friction ratio particle/particle | [-] | 0.50 | 0.70 | 0.70 | 0.70 | 0.70 | 0.70 | |
| | Friction ratio particle/surr. Surface | [-] | 0.70 | 0.50 | 0.50 | 0.50 | 0.00 | 0.20 | |
| | E-Modulus intact Rock | [N/mm ²] | 200,000.0 | 200,000.0 | 20,000.0 | 50,000.0 | 100,000.0 | 200,000.0 | 200,000.0 |
| | Poissons ratio | [-] | 0.20 | 0.20 | 0.20 | 0.20 | 0.20 | 0.20 | |
| | density | [t/mm ³] | 2.60*10 ⁻⁹ | 2.60*10 ⁻⁹ | 2.60*10 ⁻⁹ | 2.60*10 ⁻⁹ | 2.60*10 ⁻⁹ | 2.60*10 ⁻⁹ | 2.60*10 ⁻⁹ |
| | Damping Factor (Particles) - ALPHA | [%] | 7.0 | 7.0 | 7.0 | 7.0 | 7.0 | 7.0 | |
| | Damping Factor (everything else) | [-] | 0.07 | 0.07 | 0.07 | 0.07 | 0.07 | 0.07 | |

Considering the different interaction stiffnesses due to the change of the intact elastic modulus the incrementation of the calculation has to be adapted.

4.2.2.4 Evaluation

Using Equations 13, 14 and 15 the oedometer test is evaluated. Equation 15 shows the determination of the constraint secant modulus for one load stage. This calculation has to be done for each load stage.

$$\sigma_{N,i} = \frac{\sum CFORCE_z - \sum CSHEAR_z}{A_{oed}} \quad (13)$$

$$\varepsilon_{a,i} = \frac{s_i}{h_0} \quad (14)$$

$$E_{S,i} = \frac{\Delta\sigma_N}{\Delta\varepsilon_a} = \frac{\sigma_{N,i+1} - \sigma_{N,i}}{\varepsilon_{a,i+1} - \varepsilon_{a,i}} \quad (15)$$

Table 16: Variable Definition

| Variable | Unit | Description |
|---------------------|----------------------|---|
| $\sigma_{N,i}$ | [N/mm ²] | normal stress of a load stage |
| $CFORCE_z$ | [N] | contact force in z-direction |
| $CSHEAR_z$ | [N] | contact shear force in z-direction |
| A_{oed} | [mm ²] | area of the oedometer box |
| $\varepsilon_{a,i}$ | [-] | axial strain |
| s_i | [mm] | compression / displacement in z-direction |
| h_0 | [mm] | initial specimen height of the oedometer grains |
| $E_{S,i}$ | [N/mm ²] | elastic modulus of the particles |

Table 17 shows all exported parameters of the Abaqus output file. All parameters are tracked through the whole calculation procedure. For this reason, all export parameters are time depended.

Table 17: Export data of the Abaqus result file

| export variable | unit | description |
|-----------------|------|--|
| <i>time</i> | s | real-time of the calculation |
| $\sum CFORCE_z$ | N | sum of all contact forces in z-direction acting on the set top plate |
| $\sum CSHEAR_z$ | N | sum of all shear forces in z direction acting on the surrounding box due to friction |
| s_i | mm | Compression / displacement in z-direction of the top plate |

For determining the oedometer stiffness all parameters are exported in an Excel file. In order to get comparable results, the evaluation of the numerical calculation was done using the same Excel template as for the laboratory tests.

4.3 Laboratory tests

All laboratory tests were carried out at the laboratory for Rock Mechanics and Tunnelling at Graz University of Technology. The material for those tests was pea gravel provided by a tunnel construction project for scientific research.

Chapter 4.1.1 shows the performed grain size distribution. The shear test was performed with the same load stages as the numerical tests. For the laboratory tests, a shearing velocity of 0.3 mm/min was applied. In order to reach a reasonable calculation time the numerical tests were executed with a higher advance rate.

A large oedometer test device was developed in the laboratory for Rock Mechanics and Tunnelling at the Graz University of Technology (further information on the large oedometer test the master thesis: *Design of a Large Oedometer for the Determination of Stress Dependent Moduli on Fault Rocks* (Wieser, 2011) is recommended). Figure 23 shows the oedometer box filled with pea gravel.



Figure 23: Oedometer test on pea gravel

The Chapters 4.3.1 and 4.3.2 show the evaluation of the conducted laboratory test.

4.3.1 Shear test results

Figure 24 and Figure 25 show the results of the laboratory shear test. Attached to this research is a detailed laboratory report.

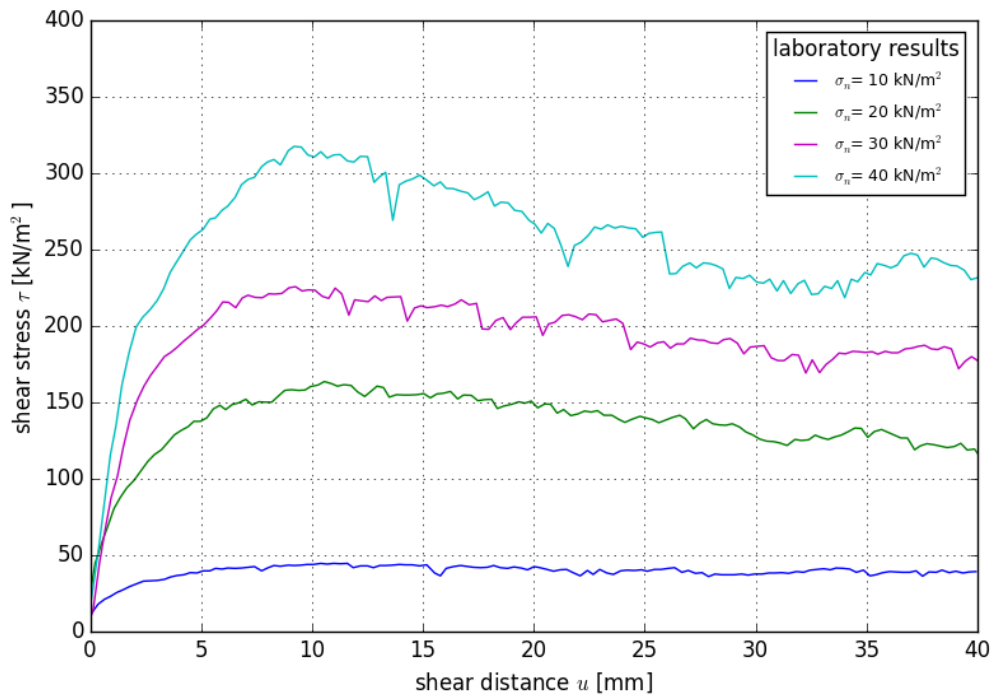


Figure 24: Shear test results of the laboratory test

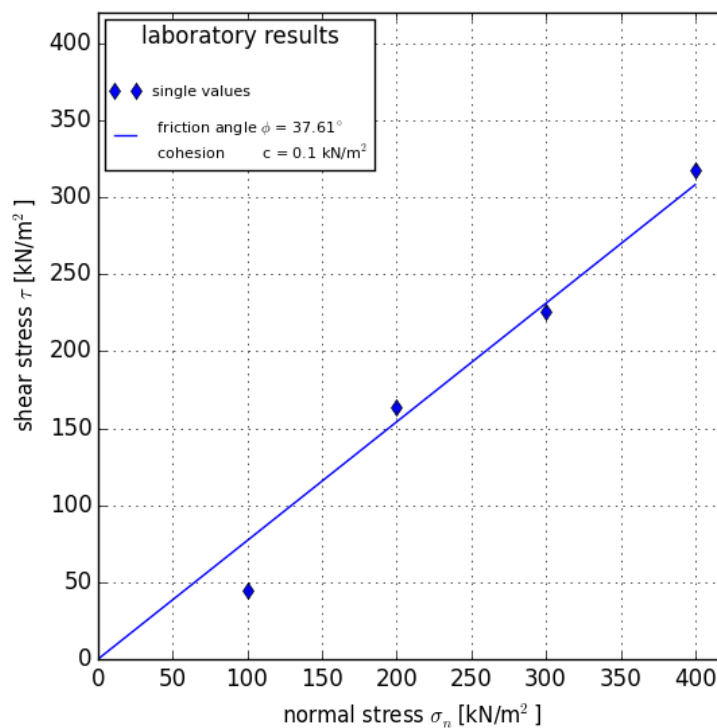


Figure 25: σ/τ plot for determining cohesion and friction angle

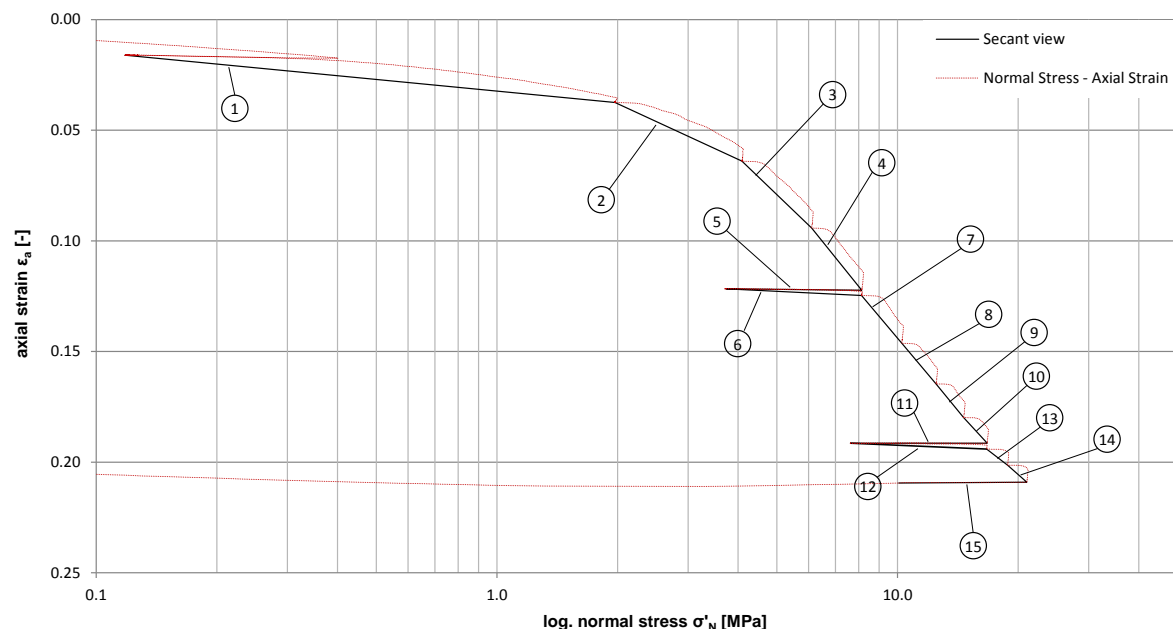
4.3.2 Oedometer test results

Table 18 and Table 19 show all results of the laboratory oedometer test.

Table 18: Oedometer laboratory results (1)

| | Situation | Normal Stress σ'_N [MPa] | Strain ϵ_a [-] | E_s [MPa] | Duration [hh:mm] |
|----|-------------|------------------------------------|----------------------------|----------------|---------------------|
| 1 | loading 1 | 0.12 | 0.0161 | 90 | 01:04 |
| | | 1.97 | 0.0374 | | |
| 2 | loading 2 | 1.97 | 0.0374 | 80 | 01:05 |
| | | 4.09 | 0.0640 | | |
| 3 | loading 3 | 4.09 | 0.0640 | 70 | 01:05 |
| | | 6.10 | 0.0942 | | |
| 4 | loading 4 | 6.10 | 0.0942 | 70 | 01:05 |
| | | 8.14 | 0.1223 | | |
| 5 | unloading 1 | 8.14 | 0.1223 | 6,860 | 01:10 |
| | | 3.73 | 0.1217 | | |
| 6 | reloading 1 | 3.73 | 0.1217 | 1,440 | 01:10 |
| | | 8.13 | 0.1247 | | |
| 7 | loading 5 | 8.13 | 0.1247 | 100 | 01:05 |
| | | 10.25 | 0.1463 | | |
| 8 | loading 6 | 10.25 | 0.1463 | 120 | 01:05 |
| | | 12.48 | 0.1647 | | |
| 9 | loading 7 | 12.48 | 0.1647 | 140 | 01:05 |
| | | 14.62 | 0.1799 | | |
| 10 | loading 8 | 14.62 | 0.1799 | 180 | 01:05 |
| | | 16.74 | 0.1915 | | |
| 11 | unloading 2 | 16.74 | 0.1915 | - | 01:21 |
| | | 7.63 | 0.1915 | | |
| 12 | reloading 2 | 7.63 | 0.1915 | 3,450 | 01:20 |
| | | 16.68 | 0.1941 | | |
| 13 | loading 9 | 16.68 | 0.1941 | 300 | 01:05 |
| | | 18.83 | 0.2014 | | |
| 14 | loading 10 | 18.83 | 0.2014 | 290 | 01:05 |
| | | 21.03 | 0.2090 | | |
| 15 | unloading 3 | 21.03 | 0.2090 | 25,730 | 00:00 |
| | | 10.07 | 0.2095 | | |

Table 19: Axial Strain / normal stress plot of the laboratory oedometer test



A detailed laboratory report is attached to this thesis in Annex C.

4.4 Results and conclusions of the numerical calculations

The following Chapters 4.4.1 and 4.4.2 provide all results including a comparison of the computational calculations and the laboratory tests. Only significant plots are used to discuss the results. All remaining plots are listed in ascending order of the given numbers in the Annex F.

4.4.1 Shear test results

Table 20 and Table 21 show results for the different parameter variations. Due to the long calculation time, some variations did not lead to results.

Table 20: Results of the shear test variations (1)

| | | | 1a | 1b | 2a | 2b | 3 | 4 | 5 | 6 |
|-----------------------|------------------------------------|----------------------|-----------------------|-----------------------|--------------|--------------|-----------------------|------|-----------------------|------|
| PARAMETERS | | <i>standard</i> | | | | | | | | |
| | Particle Diameter | [mm] | 10.0 | 10.0 | 8.0 | 8.0 | 10.0 | 8.0 | 10.0 | 8.0 |
| | Friction ratio (tanφ) | [-] | 0.70 | 0.50 | 0.70 | 0.50 | 0.70 | 0.70 | 0.70 | 0.70 |
| | E-Modulus intact Rock | [N/mm ²] | 20,000.0 | 20,000.00 | | | 50,000.00 | | 100,000.00 | |
| | Poissons ratio | [-] | 0.20 | 0.20 | | | 0.20 | | 0.20 | |
| | density | [t/mm ³] | 2.60*10 ⁻⁹ | 2.60*10 ⁻⁹ | | | 2.60*10 ⁻⁹ | | 2.60*10 ⁻⁹ | |
| | Damping Factor (Particles) - ALPHA | [%] | 7.0 | 7.0 | | | 7.0 | | 7.0 | |
| | Damping Factor (everything else) | [-] | 0.07 | 0.07 | | | 0.07 | | 0.07 | |
| | Incrementation | [-] | 5.00E-07 | 5.00E-07 | 7.00E-07 | 5.00E-07 | 5.00E-07 | | 5.00E-07 | |
| | shearing speed | [mm/sec] | 3.0 | 3.0 | | | 3.0 | | 3.0 | |
| Friction Angle | | | 12.33 | 20.58 | 14.74 | 12.08 | 18.94 | - | 18.70 | - |
| Cohesion | | | 0.00 | 0.00 | 0.00 | 0.00 | 0.00 | - | 0.00 | - |

Table 21: Results of the shear test variations (2)

| | | | 7a | 7b | 8 | 9 | 10 | 11 | 12 | |
|-----------------------|------------------------------------|----------------------|-----------------------|-----------------------|----------|--------------|-----------------------|------|-----------------------|--|
| PARAMETERS | | <i>standard</i> | | | | | | | | |
| | Particle Diameter | [mm] | 10.0 | 10.0 | 8.0 | 10.0 | 8.0 | 10.0 | 8.0 | |
| | Friction ratio (tanφ) | [-] | 0.70 | 0.70 | | | 0.70 | | 0.70 | |
| | E-Modulus intact Rock | [N/mm ²] | 20,000.0 | 200,000.00 | | | 300,000.00 | | 500,000.00 | |
| | Poissons ratio | [-] | 0.20 | 0.20 | | | 0.20 | | 0.20 | |
| | density | [t/mm ³] | 2.60*10 ⁻⁹ | 2.60*10 ⁻⁹ | | | 2.60*10 ⁻⁹ | | 2.60*10 ⁻⁹ | |
| | Damping Factor (Particles) - ALPHA | [%] | 7.0 | 7.0 | | | 7.0 | | 7.0 | |
| | Damping Factor (everything else) | [-] | 0.07 | 0.07 | | | 0.07 | | 0.07 | |
| | Incrementation | [-] | 5.00E-07 | 5.00E-07 | 2.00E-07 | 5.00E-07 | 2.00E-07 | | 2.00E-07 | |
| | shearing speed | [mm/sec] | 3.0 | 3.0 | | | 3.0 | | 3.0 | |
| Friction Angle | | | 16.34 | | - | 16.54 | - | - | - | |
| Cohesion | | | 0.00 | | - | 0.00 | - | - | - | |

Figure 26 shows the results of the friction angle depending on the elastic modulus of the intact rock. We assume that intact rock stiffness higher than 200 GPa has no consequence on the friction angle.

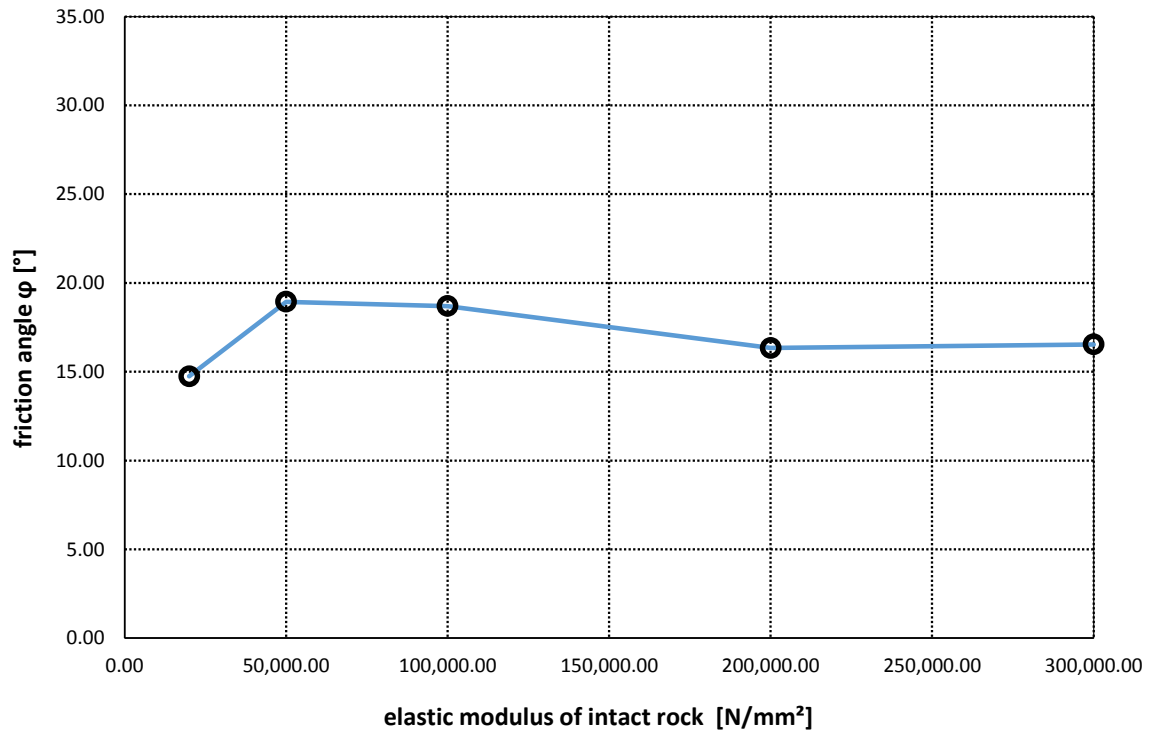


Figure 26: Friction angle depending on the elastic modulus of the intact rock

The numerical calculations result in a friction angle between 12 and 18 degrees. This value is not realistic for cohesion less gravel.

Following reasons were assumed to cause this friction angle:

- (1) no possibility of fracture simulation within the particles
- (2) deviation of the shape of simulated particles and pea gravel

Regarding fact (1): A failure criterion within the particle is not implemented in the actual Abaqus version. The laboratory test shows cracks in the grains along the shear plane, which may result in a higher shear stiffness.

Regarding fact (2): Due to the perfect circular shape of the particles and one continuous particle diameter, an interlocking can be expected. For pea gravel used on construction sites, we consider a discontinuous circular shape. This is traced back to the erosion and transport mechanism of fluvial sediments. This leads to smaller void volume and a higher friction angle.

4.4.1.1 Comparison of representative results

Figure 27 and Figure 28 compare the laboratory test and the numerical simulation with the parameter variation 3 (see Table 20). A shear stress / shear distance and a shear stress / normal stress diagram illustrates the deviation between the two tests.

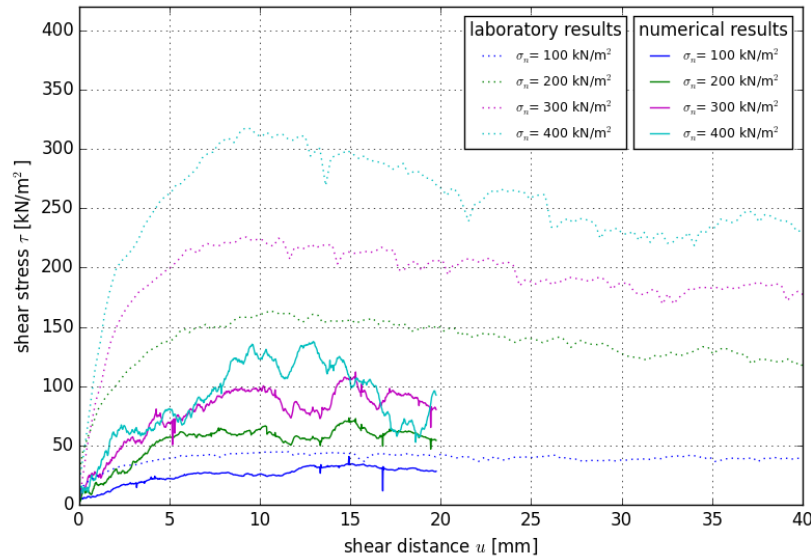


Figure 27: Comparison of the laboratory tests with the numerical "3" variation (1)

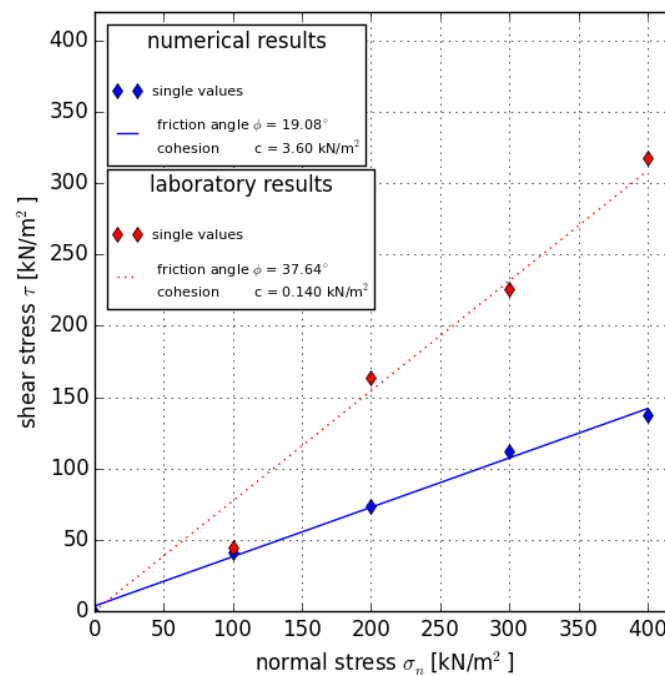


Figure 28: Comparison of the laboratory tests with the numerical "1a" variation (2)

A Python code, used for generating the two diagrams from the Abaqus output file is attached in Annex E.

4.4.1.2 Impact of the incrementation

In Figure 29 and Figure 30, the impact of the incrementation is shown. The solution noise of the numerical results increases with the vertical stress σ_n . The incrementation depends on the mass of the particles and their stiffness. An adaptation of the incrementation would reduce the numerical solution noise.

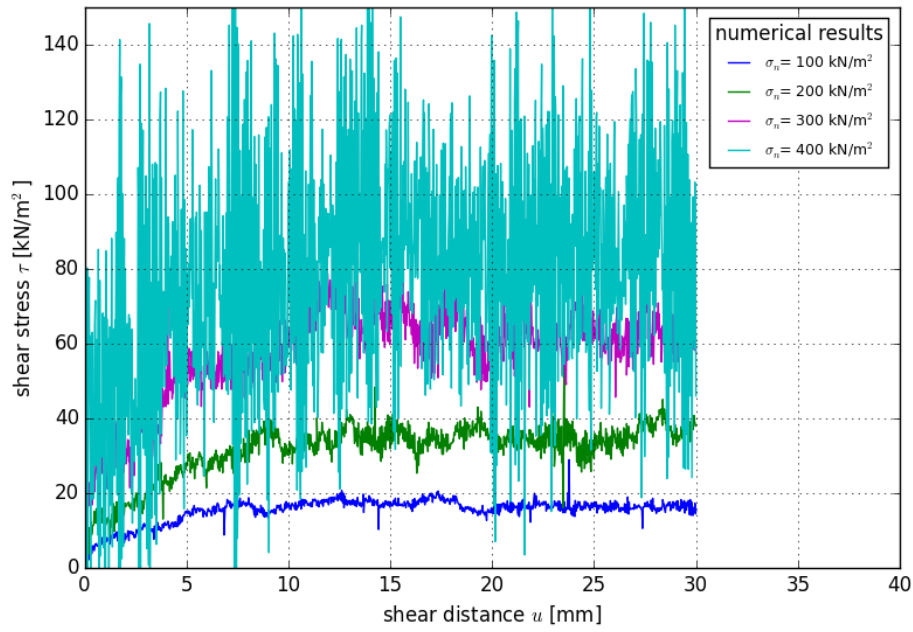


Figure 29: results of the “1b” variation (1)

The solution noise causes a higher friction angle as seen on load stage 4 with 400 kN/m² in Figure 30.

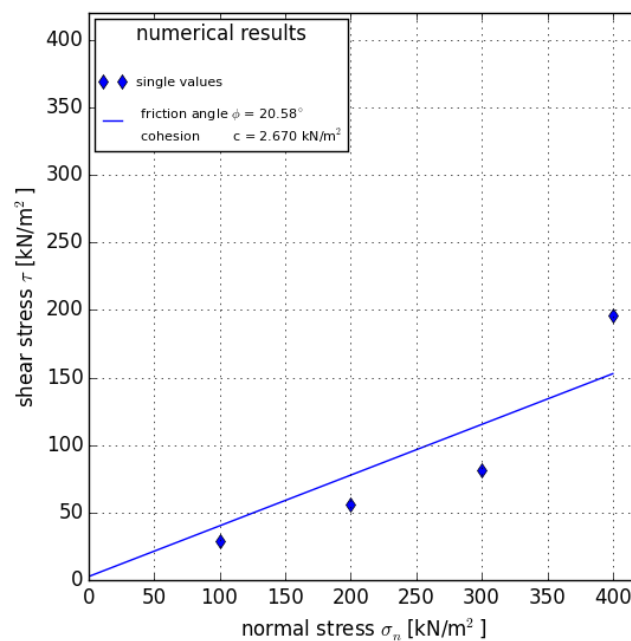


Figure 30: results of the “1b” variation (2)

4.4.2 Oedometer Test

Table 22 lists the numerical and laboratory results of the oedometer variations. Using Equations 13 to 15 in Chapter 4.2.2.4, the load dependent constraint secant moduli E_s are calculated.

Table 22: Results of the numerical and laboratory oedometer test variations

| # | Situation | 05 | | | 06 | | | 07 | | | 08 | | | 09 | | | 10 | | | lab | | |
|---|-------------|---------------------|----------------------------|----------------|---------------------|----------------------------|----------------|---------------------|----------------------------|----------------|---------------------|----------------------------|----------------|---------------------|----------------------------|----------------|---------------------|----------------------------|----------------|---------------------|----------------------------|----------------|
| | | σ_N [MPa] | Strain ϵ_a [-] | E_s [MPa] | σ_N [MPa] | Strain ϵ_a [-] | E_s [MPa] | σ_N [MPa] | Strain ϵ_a [-] | E_s [MPa] | σ_N [MPa] | Strain ϵ_a [-] | E_s [MPa] | σ_N [MPa] | Strain ϵ_a [-] | E_s [MPa] | σ_N [MPa] | Strain ϵ_a [-] | E_s [MPa] | σ_N [MPa] | Strain ϵ_a [-] | E_s [MPa] |
| 1 | loading 1 | 0.00 | 0.0000 | 10 | 0.00 | 0.0000 | 0 | 0.00 | 0.0000 | 0 | 0.00 | 0.0000 | 0 | 0.00 | 0.0000 | 0 | 0.00 | 0.0000 | 0 | | | |
| | | 0.08 | 0.0133 | | 0.08 | 0.1352 | | 0.09 | 0.0214 | | 0.09 | 0.0251 | | 0.08 | 0.0226 | | 0.08 | 0.0267 | | | | |
| 2 | loading 2 | 0.08 | 0.0133 | 300 | 0.08 | 0.1352 | 10 | 0.09 | 0.0214 | 80 | 0.09 | 0.0251 | 80 | 0.08 | 0.0226 | 90 | 0.08 | 0.0267 | 90 | 0.12 | 0.0161 | 90 |
| | | 1.99 | 0.0196 | | 1.88 | 0.4103 | | 1.95 | 0.0455 | | 1.86 | 0.0483 | | 1.96 | 0.0424 | | 1.93 | 0.0484 | | 1.97 | 0.0374 | |
| 3 | loading 3 | 1.82 | 0.0196 | 1080 | 1.88 | 0.4103 | 0 | 1.95 | 0.0455 | 420 | 1.86 | 0.0483 | 520 | 1.96 | 0.0424 | 480 | 1.93 | 0.0484 | 530 | 4.09 | 0.0640 | 80 |
| | | 3.86 | 0.0215 | | 0.00 | 0.0000 | | 3.99 | 0.0503 | | 3.96 | 0.0523 | | 3.93 | 0.0465 | | 3.87 | 0.0520 | | | | |
| 4 | loading 4 | 3.73 | 0.0215 | 1310 | 0.00 | 0.0000 | - | 3.99 | 0.0503 | 540 | 3.97 | 0.0523 | 850 | 3.93 | 0.0465 | 420 | 3.87 | 0.0520 | 1440 | 4.09 | 0.0640 | 70 |
| | | 5.96 | 0.0232 | | 0.00 | 0.0000 | | 5.78 | 0.0537 | | 6.07 | 0.0548 | | 5.90 | 0.0512 | | 5.85 | 0.0534 | | 6.10 | 0.0942 | |
| 5 | loading 5 | 5.55 | 0.0232 | 1880 | 0.00 | 0.0000 | - | 5.77 | 0.0537 | 1290 | 6.07 | 0.0548 | 1050 | 5.90 | 0.0512 | 390 | 5.85 | 0.0534 | 1440 | 6.10 | 0.0942 | 70 |
| | | 7.82 | 0.0244 | | 0.00 | 0.0000 | | 8.29 | 0.0556 | | 7.80 | 0.0565 | | 7.87 | 0.0563 | | 7.86 | 0.0548 | | 8.14 | 0.1223 | |
| 6 | unloading 1 | 7.65 | 0.0244 | 8720 | 0.00 | 0.0000 | - | 8.28 | 0.0556 | 1800 | 7.79 | 0.0565 | 2460 | 7.87 | 0.0563 | 7240 | 7.86 | 0.0548 | 4080 | 8.14 | 0.1223 | 6860 |
| | | 3.86 | 0.0240 | | 0.00 | 0.0000 | | 3.76 | 0.0531 | | 3.84 | 0.0549 | | 3.93 | 0.0557 | | 3.93 | 0.0538 | | 3.73 | 0.1217 | |
| 7 | reloading 1 | 3.85 | 0.0240 | 2990 | 0.00 | 0.0000 | - | 3.77 | 0.0531 | 1340 | 3.84 | 0.0549 | 2250 | 3.93 | 0.0557 | 1010 | 3.93 | 0.0538 | 3340 | 3.73 | 0.1217 | 1440 |
| | | 7.71 | 0.0253 | | 0.00 | 0.0000 | | 8.01 | 0.0563 | | 7.83 | 0.0566 | | 7.87 | 0.0596 | | 7.74 | 0.0549 | | 8.13 | 0.1247 | |
| 8 | loading 6 | 7.66 | 0.0253 | 3090 | 0.00 | 0.0000 | - | 8.00 | 0.0563 | 1000 | 7.82 | 0.0566 | 2550 | 7.87 | 0.0596 | 550 | 7.74 | 0.0549 | 140 | 8.13 | 0.1247 | 100 |
| | | 9.72 | 0.0259 | | 0.00 | 0.0000 | | 9.88 | 0.0581 | | 9.96 | 0.0575 | | 9.84 | 0.0632 | | 0.00 | 0.0000 | | 10.25 | 0.1463 | |
| 9 | loading 7 | 9.72 | 0.0259 | 30 | 0.00 | 0.0000 | - | 9.88 | 0.0581 | 170 | 9.96 | 0.0575 | 2650 | 9.84 | 0.0632 | 700 | 0.00 | 0.0000 | ##### | 10.25 | 0.1463 | 120 |
| | | 0.00 | ##### | | 0.00 | 0.0000 | | 0.00 | 0.0000 | | 11.98 | 0.0582 | | 11.82 | 0.0661 | | 0.00 | 0.0000 | | 12.48 | 0.1647 | |

Figure 31 shows a plot of the axial strain depending versus the logarithm of the normal stress. The parameter variation 06 with its intact elastic module of 20 GPa leads to a stiffness of 10 MPa in load stage 1. Due to this unrealistic assumption, this parameter variation was not considered in further discussions. Above the stress level of 2 MPa the laboratory test shows plastic deformation, which cannot be simulated with this numerical model.

The deformational behavior of this numerical calculation concurs with the laboratory test up to a normal stress of 2 MPa. The stress level within the annular gap is assumed to be within range of 2 MPa.

Figure 32 shows a more detailed plot of the variations. The unloading and reloading modulus of the computational simulations is also in the range of the laboratory test.

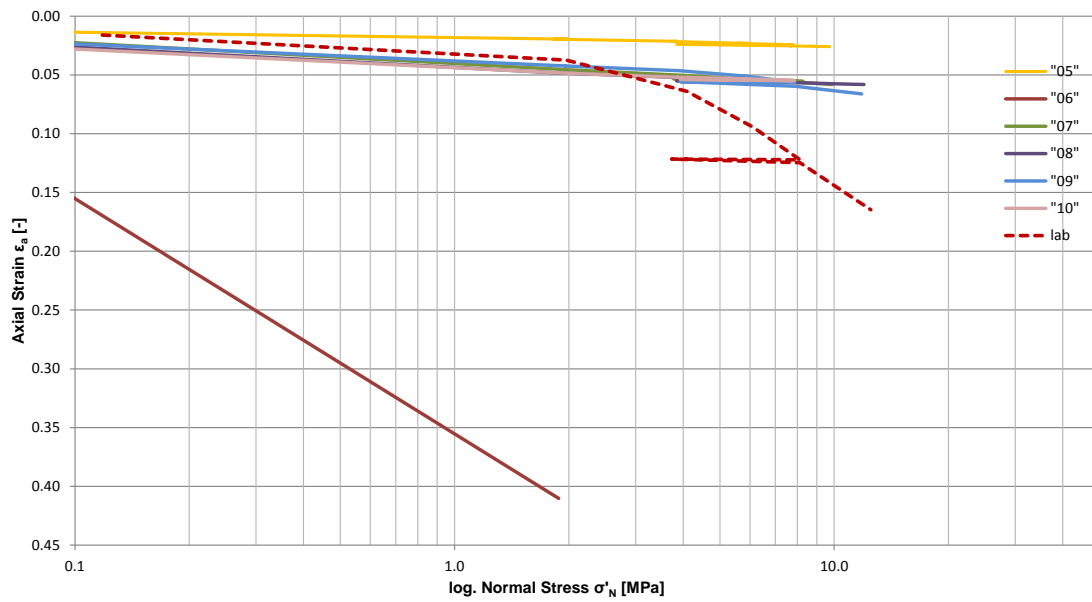


Figure 31: Summarization of the numerical and laboratory results of the oedometer test

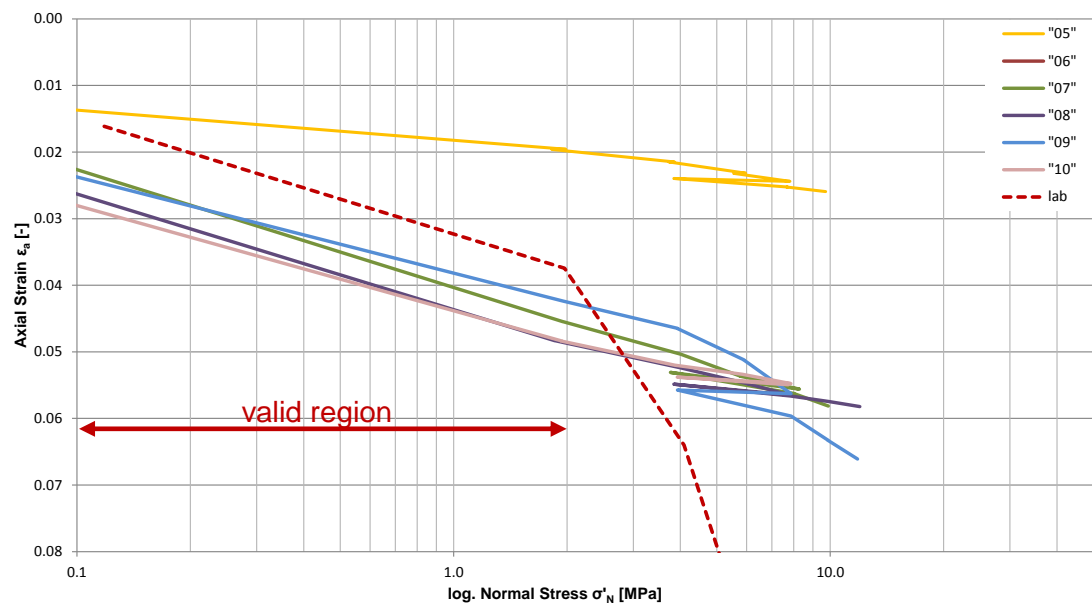


Figure 32: Summary of the numerical and laboratory tests (more detailed plot)

Figure 33 shows the comparison of the strain – time development of the numerical 05 variation and the laboratory test. For reason of comparability, the time of the numerical and laboratory test was normalized by a percentage value. Due to the drained material, excluding consolidation, these tests are comparable.

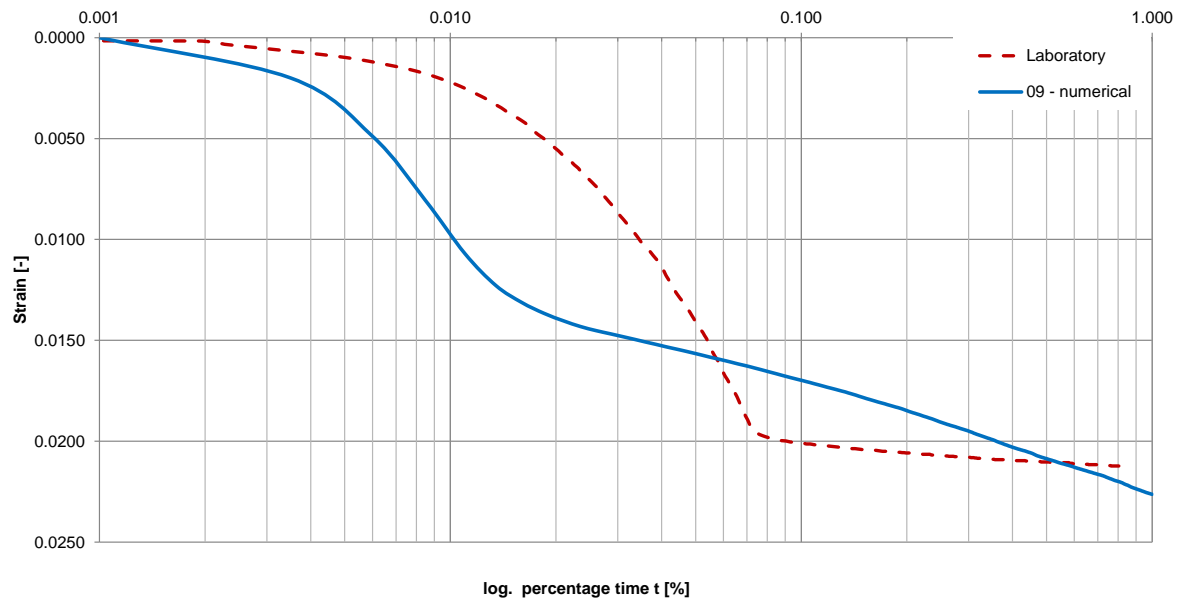


Figure 33: Strain time development of the first loading stage

Figure 34 shows the compressibility of discrete elements due to the different contact formulations. A full calculation for an intact elastic modulus of 20 GPa was not possible due to the high compressibility.

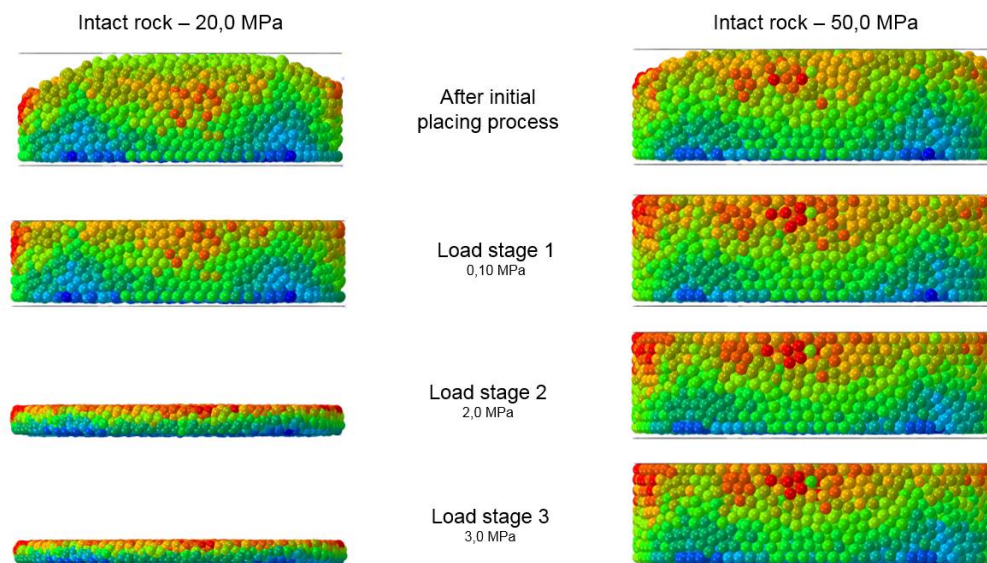


Figure 34: Compressibility of discrete elements due to different intact rock elastic moduli

5 Numerical Models implementing the DEM

Two models are discussed in this Chapter. These models should be realistic computational simulations for the bedding problem in the annular gap.

Due to the long calculation time, there are no results of this models listed in this thesis. The codes for those calculations are prepared and the input files tested under the use of some assumptions to keep the calculation time short in order to obtain a result.

In general, these models result out of the initial problem. Within this task, the distribution of the pea gravel after relocation in the annular gap and the influence on the segmental lining is investigated.

5.1 Annular Gap Model

For the determination of the actual behaviour of the pea gravel in the annular gap, the *annular gap model* was developed. This model is designed for a computational simulation of the grain movements in the annular gap due to the regripping process.

This annular gap, filled with pea gravel is the focus of this model. During the regripping process in the annular gap a slope failure occurs. This failure mechanism, the slope of this failure and the movements in the annular gap should be the main results of this numerical calculation.

Due to the operational procedure within the working area on a TBM, a fully backfilled annular gap might not be established after each ring closure. This leads to an unfavorable distribution of the pea gravel leaving the segmental lining only partially bedded. This fact was considered in the design of the numerical model length.

5.1.1 Geometry

Figure 35 shows the designed annular gap model. The model was designed respecting a full regripping process of a double shield machine.

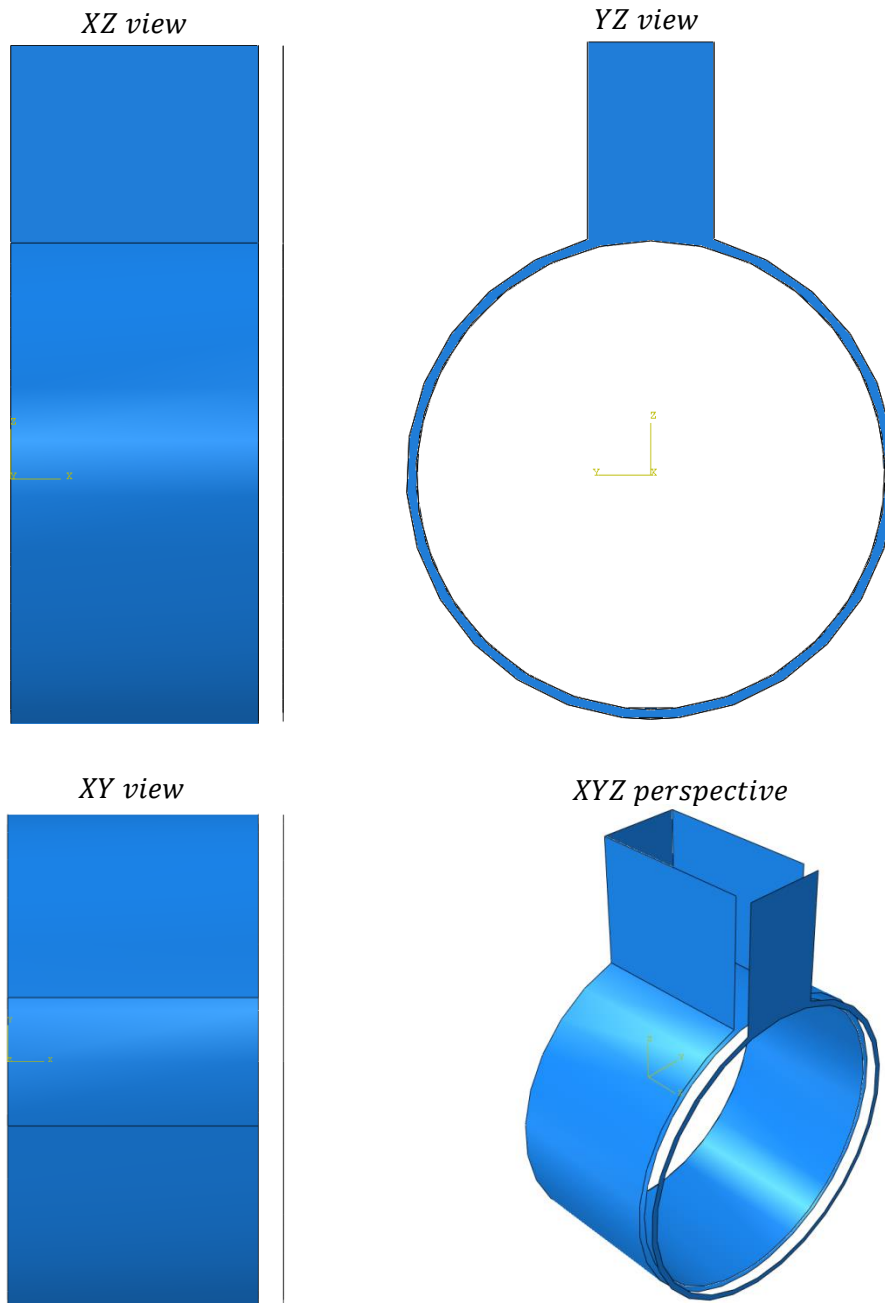


Figure 35: numerical annular gap model

For generating particles initially just touching, a box was designed on top of the annular gap.

Following dimensions are used for this model:

- Inner diameter: 9500 mm
- Outer diameter: 9900 mm
- Annular gap: 200 mm
- Model length: 5000 mm
- Box dimensions (top): $b/h/l = 2500 / 2700 / 5000$ mm

Figure 36 shows the set definitions of the annular gap model in detail.

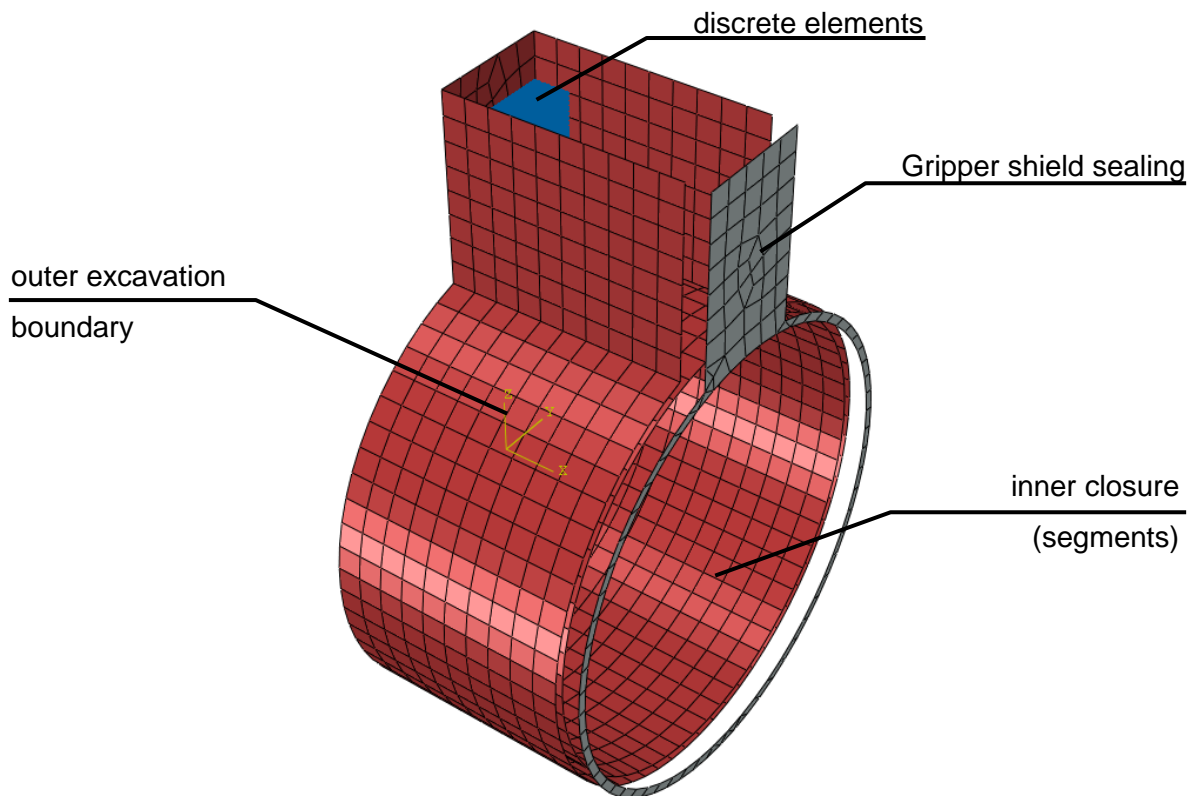


Figure 36: Definition of the sets (annular_gap – red; front – grey; dem1 – blue)

5.1.1 Calculation steps

Table 23 shows and describes the generated steps for the annular gap model.

Table 23: Calculation steps for the annular gap model

| Step 1 – movement back | | | | | | |
|--|--|----------|----------|------------|------------|------------|
| Duration: 0.10 sec | | | | | | |
| Movement back of the front to the actual place 4500 mm in 0,10 sec → 45,000.0 mm/sec | | | | | | |
| Everything else is locked in all directions | | | | | | |
| | Boundary conditions - velocity [mm/sec] | | | | | |
| | x | y | z | x-r | y-r | z-r |
| annular_gap | - | - | - | - | - | - |
| front | -45,000.0 | - | - | - | - | - |
| dem1 | - | - | - | - | - | - |
| Step 2 – settlement of the particles | | | | | | |
| Duration: 50 sec | | | | | | |
| Activation of the gravity for the set dem_1 (particles); | | | | | | |
| Stop the set front | | | | | | |
| | Boundary conditions - velocity [mm/sec] | | | | | |
| | x | y | z | x-r | y-r | z-r |
| annular_gap | - | - | - | - | - | - |
| front | - | - | - | - | - | - |
| dem1 | free | free | free | free | free | free |
| Step 3 – movement forward | | | | | | |
| Duration: 20 sec | | | | | | |
| Gravity is still active on the set dem_1 | | | | | | |
| Movement forward of the set front to generate a slope failure in the annular gap | | | | | | |
| | Boundary conditions - velocity [mm/sec] | | | | | |
| | x | y | z | x-r | y-r | z-r |
| annular_gap | - | - | - | - | - | - |
| front | 200 | - | - | - | - | - |
| dem1 | free | free | free | free | free | free |

Attached to this thesis is the full code of this calculation model.

5.2 Segment Bedding Model

Additional to the *annular gap model*, the *segment bedding model* includes the segments. After an initial placing process of the particles, the segments, modelled using finite elements, are bedded in discrete elements. Detailed information on the behavior of the segment gaps for longitudinal joints (Leonhardt, et al., 1966) and radial joints (Girmscheid, 1997) should be implemented. The interaction between discrete and finite elements is given as well.

5.2.1 Geometry

Figure 37 shows the geometry of the annular gap model and additional in Table 24 the set description is given. The green part represents the excavation boundary. The shield of the TBM is modeled by a moveable surface, representing the gripper shield sealing, which is initially placed in front of the whole model. Inside of this model, the segments modelled by finite elements and the pea gravel modelled by discrete elements are placed.

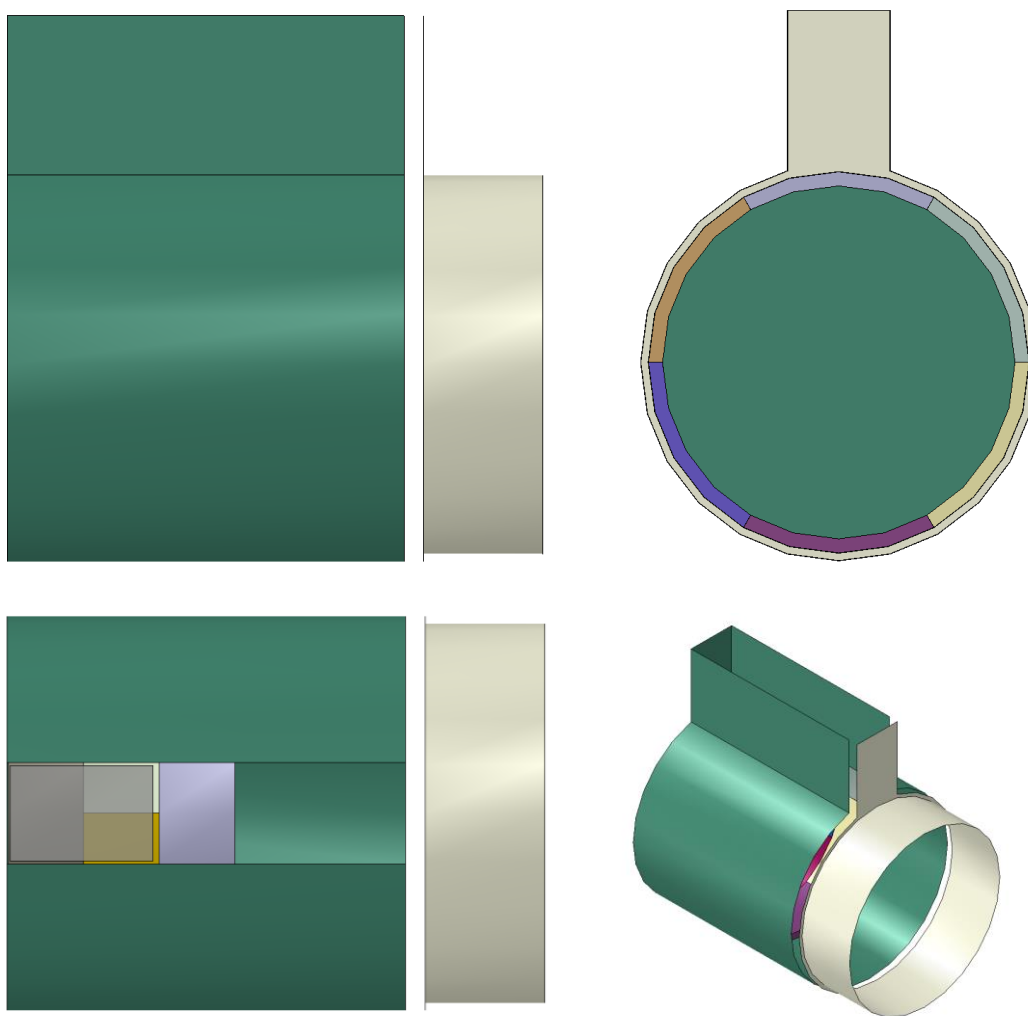


Figure 37: Geometry of the segments model

Table 24: Definition of the sets

| Set name | Colour in figure Figure 37 |
|---------------------------------|----------------------------|
| Annular_gap | green |
| front | grey |
| Segments (s_01,s_02, ..., s_ij) | diverse colours |
| dem1 (initially placed) | transparency box |

Figure 38 shows the segments and the interaction surfaces. The segments are 350 mm thick and 900 mm long. Six segments are placed radially. To avoid crossing joints, two adjacent rings are turned by half a segment length.

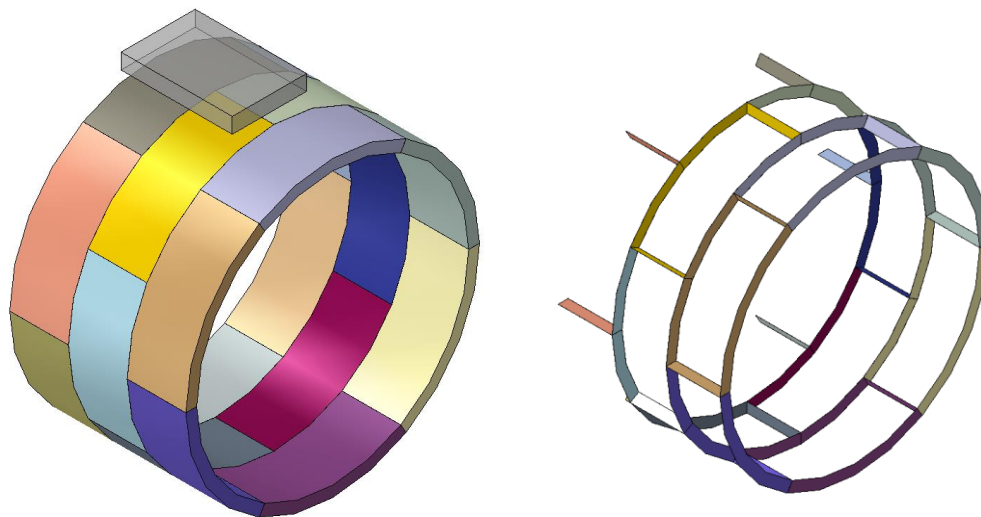


Figure 38: Position of the segments and the interaction surfaces

The interaction between the discrete elements and the segment surfaces are defined as general contact surfaces. For the interactions between the segments following interactions are activated:

- Tangential behavior: friction coefficient concrete/concrete
- Normal behavior: hard contact
- Cohesive behaviour: Spring stiffness in all 3 directions dependent on the connections between the segments in both directions

Initially the segments are placed with a fractional numerical gap allowing a general contact and a shearing deformation between the segments. As soon as the thrust pressure on the segments is activated, the gap is closed and a steady state of pressure in the segments is reached.

6 Conclusion and Outlook

The bedding situation of segments in general and their effect on the loading conditions in mechanised driven tunnels in literature is covered poorly. For modelling this problem several numerical software solutions are available. This thesis introduces the application of numerical methods for the bedding problem.

Due to the deformational behaviour of the pea gravel within the annular gap, the software FLAC3D is difficult to apply. If the behaviour of the pea gravel within the annular gap is established, the position and stiffness of the bedding springs have to be adapted. Therefore, a numerical calculation using FLAC3D can only be performed by assuming the spatial bedding conditions within the annular gap.

The explicit dynamic analysis is representing an applicable tool for a proper numerical design of the bedding situation in mechanized driven tunnels. Discrete elements are flexibly modelled in a rigid surrounding surface and represent the bedding of the segments.

Two laboratory tests have been numerically implemented. The oedometer test shows a good correspondence with the laboratory test. On the contrary, the numerical shear test divergences in the evaluated results. These deviations are attributed to the shape of the particles, the restriction in the failure behaviour and the friction coefficient. Due to the deficiency to model a realistic friction coefficient an investigation of the computational frictional behavior should be performed with a benchmark test.

Due to the high amount of particles in the real sized model (about 2.5 millions) and the restriction in Abaqus of using only one single processor for the calculation of the particle contact reactions, this method leads to long computational times. Complex calculations and comparisons due to this fact are hardly executable. Scientifically, this method is applicable for a demonstration of the partial bedding situation and the effect on the segments. The models discussed in Chapter 5 should be used for further developments. The numerically discretized models including discrete elements for pea gravel and finite elements for the lining segments are available. Further developments regarding different shaped particles and crack propagation models within the Abaqus code seem to be required. The influence of these extensions on the models should be evaluated.

In general, the application of the software Abaqus under the use of the discrete element method for civil engineering problems is possible. Numerical studies for scientific reasons are executable. Using this method solving on site problems, the calculation time is too extensive.

Bibliography

Abaqus 6.13 Documentation. 2013. RI, USA : Dassault Systèmes, 2013.

Baumann, T. 1992. Tunnelauskleidungen mit Stahlbetontübbing. *Die Bautechnik.* 1992, Vol. 69, 1, pp. 11-20.

Behnen, G., Nevrlly, T. and Fischer, O. 2013. *Bettung von Tunnelschalen.* s.l. : VGE Verlag, 2013.

C.S. Campbell, P.W. Cleary, M.A. Hopkins. 1995. Large scale landslide simulations: Global deformation, velocities and basal friction. *J. Geophys. Res.* s.l. : J. Geophys. Res., 1995, pp. 8267–8283.

Cundall, P. A. 1971. A computer model for simulating progressive large scale movements in blocky rock systems. *Proceedings Symposium Int. Soc. Rock Mech.* vol. 1, p. Paper II–8, 1971, Vol. Nancy Metz.

Duddeck, H. 1972. Zu den berechnungsmethoden und zur Sicherheit von Tunnelbauten. *Der Bauingenieur.* 1972, Vol. 47, 2, pp. 43-52.

Girmscheid, G. 1997. Schildvorgetriebener Tunnelbau in heterogenem Lockergestein, ausgekleidet mittels Stahlbetontübbing. *Die Bautechnik.* 1997, Vol. 74, 2, pp. 85-100.

—. **2013.** Tübbingauskleidung. *Bauprozesse und Bauverfahren des Tunnelbaus.* Weinheim, Germany : Wiley-VCH Verlag GmbH & Co. KGaA, 2013, pp. 569-586.

Hain, H. and Falter, B. 1975. Stabilität von biegesteifen oder durch Momentgelenke geschwächten und auf der Außenseite elastisch gebetteten Kreisringen unter konstanten Außendruck. *Straße Brücke Tunnel.* 1975, 4, pp. 98-105.

Herrenknecht. [Online] Herrenknecht. [Cited: 11 21, 2014.] <https://www.herrenknecht.com/en/products/core-products/tunnelling-pipelines/double-shield-tbm.html>.

Hertz, Heinrich. 1882. Ueber die Berührung fester elastischer Körper. *Journal für die reine und angewandte Mathematik.* 1882, 92, pp. 156-171.

Hibler, M. A. Hopkins & W. D. 1991. *CI International Glaciological Society. On the ridging of a thin sheet of lead ice.* s.l. : Annals of Glaciology 15, 1991. pp. 81-86. Vol. III.

Leonhardt, F. and Reimann, H. 1966. Betongelenke. *Der Bauingenieur.* 1966, Vol. 41, 2, pp. 49-52.

Lin, J. 2013. *Linking DEM with micropolar continuum.* Wien : Universität für Bodenkultur - Institut für Geotechnik, 2013.

Lin, Jia. 2013. *Linking DEM with micropolar continuum.* Wien : Universität für Bodenkultur - Institut für Geotechnik, 2013.

- Meldner, V. 1975.** Zur Statik der Tunnelauskleidungen mit Stahlbetontübbings. *100 Jahre Wayss & Freytag*. 1975, pp. 231-237.
- O'Sullivan, C and Bray, J. D. 2004.** Selecting a Suitable Time Step for Discrete Element Simulations that Use the Central Difference Time Integration Scheme. *Engineering Computations*. 2004, pp. 278–303.
- Popov, Valentin L. 2010.** *Contact Mechanics and Friction: Physical Principles and Applications*. Berlin, Heidelberg : Springer-Verlag, 2010.
- Thienert, Christian and Pulsfort, Matthias. 2011.** Segment design under consideration of the material used to fill the annular gap. *Geomechanics and Tunnelling*. 2011, Vol. 4, 6, pp. 665-680.
- Wieser, Paul. 2011.** *Design of a Large Oedometer for the Determination*. Graz : s.n., 2011.
- Windels, R. 1966.** Spannungstheorie zweiter Ordnung für den teilweise gebetteten Kreisring. *Die Bautechnik*. 1966, Vol. 43, 8, pp. 265-274.
- Xiaobin Ding, Lianyang Zhang, Hehua Zhu, Qi Zhang. 2013.** *Effect of Model Scale and Particle Size Distribution on PFC3D Simulation Results*. s.l. : Rock Mechanics and Rock Engineering, 2013.
- Zhu, H. P., Z. Y. Zhou, R. Y. Yang, and A. B. Yu. 2008.** Discrete Particle Simulation of Particulate Systems: A Review of Major Applications and Findings. s.l. : Chemical Engineering Science, vol. 63, 2008, pp. 5728–5770.
- Zhu, H. P., Z. Y. Zhou, R. Y. Yang, and A. B. Yu., 2007.** Discrete Particle Simulation of Particulate Systems: Theoretical Developments. *Chemical Engineering Science*, vol. 62. 2007, pp. 3378–3396.

Annex A

Excel Macro for exporting the interaction sheets into readable Abaqus input .csv file:

```

Sub ExportAsCsv()
Dim strFileToOpen As Variant
Dim i As Integer
Dim strSpeicherPfad As String
Dim strSpeicherDatei As String
Dim wkb As Workbook
Dim wks As Worksheet
Dim Regex As Object
Dim strTrennzeichen As String

strFileToOpen = Application.GetOpenFilename("Excel Dateien (*.xlsx), *.xlsx", , , , True)
If Not IsArray(strFileToOpen) Then Exit Sub

On Error GoTo ENDE
Application.ScreenUpdating = False
Application.EnableEvents = False
Application.DisplayAlerts = False

strSpeicherPfad = "C:\export\" 'Change in case!!



For i = 1 To UBound(strFileToOpen)
Set wkb = Workbooks.Open(strFileToOpen(i), 0)
For Each wks In wkb.Worksheets
strSpeicherDatei = Left$(wkb.Name, InStrRev(wkb.Name, ".") - 1) & "_" & wks.Name & ".csv"
wks.UsedRange.Copy
Open strSpeicherPfad & strSpeicherDatei For Output As #1
strTrennzeichen = " " '[Type here possible variables]
If strTrennzeichen = vbTab Then
Print #1, lesen
Else
Set Regex = CreateObject("Vbscript.Regexp")
With Regex
.Pattern = vbTab
.Global = True
Print #1, .Replace(lesen, strTrennzeichen)
End With
End If
Close #1
Next
wkb.Close False
Next
ENDE:
If Err Then
MsgBox Err.Description, , "Fehler: " & Err.Number
On Error Resume Next
Close #1
wkb.Close False
End If
Application.DisplayAlerts = True
Application.ScreenUpdating = True
Application.EnableEvents = True
End Sub

Private Function lesen() As String
Dim clp As New DataObject
With clp
.GetFromClipboard
lesen = .GetText
End With

```

Annex B

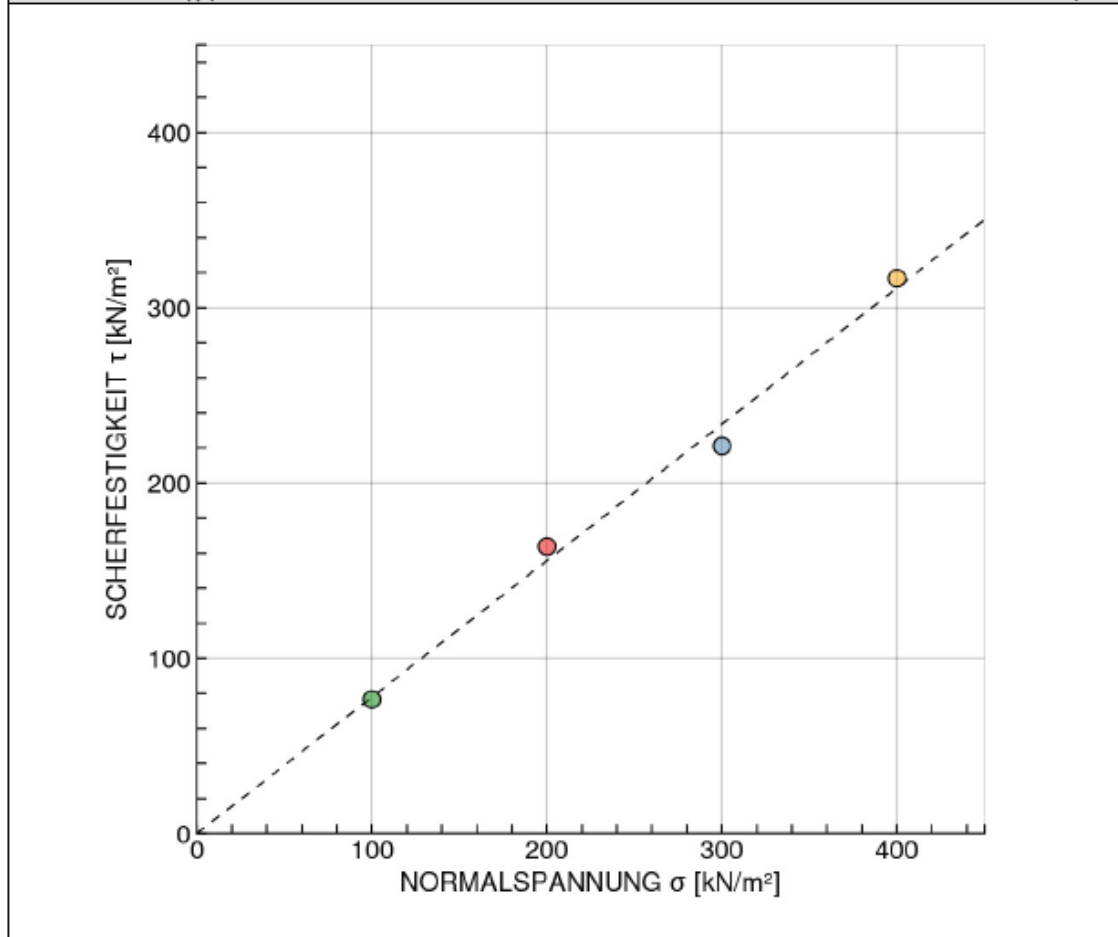
Results of the laboratory shear test

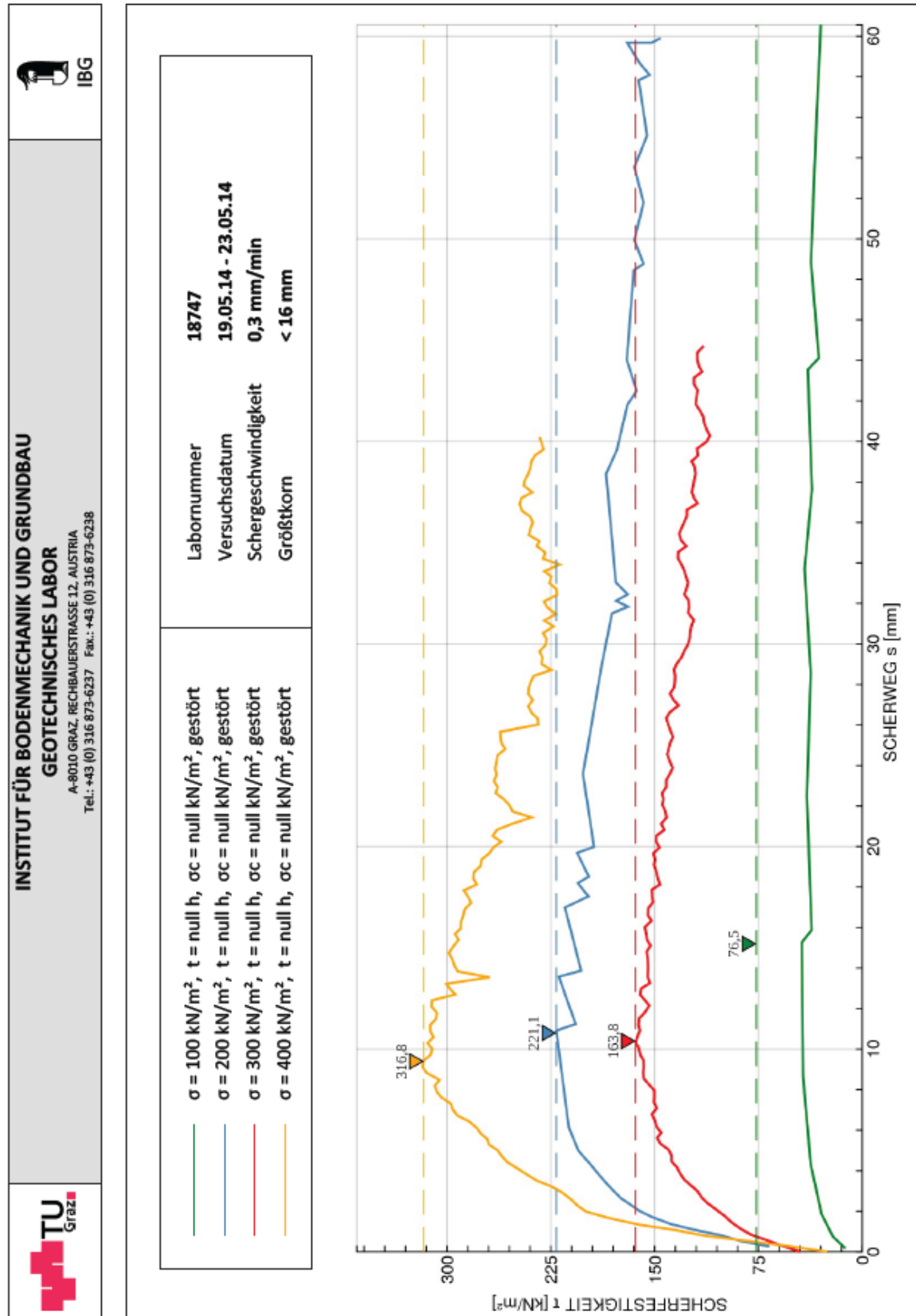
| | | | | | |
|---|--|--|--|---|--|
|  | | INSTITUT FÜR BODENMECHANIK UND GRUNDBAU GEOTECHNISCHES LABOR <small>A-8010 GRAZ, RECHBAUERSTRASSE 12, AUSTRIA Tel.: +43 (0) 316 873-6237 Fax.: +43 (0) 316 873-6238</small> | |  IBG | |
| AUFTRAGGEBER: Institut für Felsmechanik und Tunnelbau | | BODENART: | | LABORNUMMER: 18747 | |
| PROJEKT: Scherversuch | | TIEFE: | | AUFTRAGSNR: 2746 | |
| BEZEICHNUNG: Ankerfüllung | | BEARBEITER: Hen | | DATUM: 19.05.14 - 23.05.14 | |

RAHMENSCHERVERVERSUCH NACH ÖNORM B 4416

Büchsengröße: 225 x 225 x 200 mm

| GRÖSSTKORN: < 16 mm | | Versuch 1 | Versuch 2 | Versuch 3 | Versuch 4 |
|-------------------------------|------------------------------|--------------------------|-----------|------------|-----------|
| KONSOLIDIERUNGSDRUCK | α_c kN/m ² | | | | |
| KONSOLIDIERUNGSZEIT | t_c h | | | | |
| NORMALSPANNUNG | σ kN/m ² | 100 | 200 | 300 | 400 |
| SCHERFESTIGKEIT | τ_r kN/m ² | 76,5 | 163,8 | 221,1 | 316,8 |
| SCHERWEG | s_1 mm | 15,2 | 10,4 | 10,8 | 9,4 |
| RESTSCHERFESTIGKEIT | τ_r kN/m ² | | | | |
| RESTSCHERWEG | s_2 mm | | | | |
| WASSERGEHALT nach dem Versuch | w % | | | | |
| REIBUNGSWINKEL (ϕ') | 37,9 ° | PROBENZUSTAND | | gestört | |
| KOHÄSION (c') | kN/m ² | SCHERGESCHWINDIGKEIT | | 0,3 mm/min | |
| RESTSCHERWINKEL (ϕ_r) | ° | RESTSCHERGESCHWINDIGKEIT | | mm/min | |





Annex C

Results of the laboratory oedometer test

| GENERAL DESCRIPTION | |
|-------------------------------|--|
| Project | Oedometer Analysis on Pea Gravel |
| Applicant | MHR |
| Example Denotation | 001 |
| Soil Type | Pea Gravel |
| Date | 06.08.2014 - 07.08.2014 |
| Laboratory | Institute for Rock Mechanics and Tunnelling |
| Laboratory Number | TU Graz |
| Investigator | 001 Al Haddad |
| Description of Test Equipment | Floating Ring Configuration (RF) with determination of friction force; drained on both sides; greasing of rings; 2x filter plate with two layers of geotextile |
| Example Assembly | Disturbed |

| Information about the Sample Material | |
|--|----------------------------|
| Sampling Site | - [m] |
| Sampling Depth h_z | - [m] |
| Day of sampling | - |
| Start of Experiment | 06.08.2014 |
| End of Experiment | 07.08.2014 |
| Age of Sample | - [d] |
| Duration of Test | 00:17:54:14 |
| Grain Unit Weight γ_s | - [kN/m ³] |
| Bulk Gravity γ_0 | - [kN/m ³] |
| Dry-Unit Weight γ_d | - [kN/m ³] |
| Initial Water Content w_0 | - [-] |
| Initial Degree of Saturation $S_{r,0}$ | - [-] |
| Initial Void Ratio e_0 | - [-] |
| Initial Porosity n_0 | - [-] |
| Expansion/ Final Unit Weight γ_r | - [kN/m ³] |
| Dry Density Expansion γ_{dr} | - [kN/m ³] |
| Final Water Content w_r | - [-] |
| Final Degree of Saturation $S_{r,r}$ | - [-] |
| Final Void Ratio e_r | - [-] |
| Final Porosity n_r | - [-] |
| Laboratory Temperature θ | 20.0 [°C] |
| Water Density at Laboratory Temperature ρ_w | 998.2 [kg/m ³] |

| Information about the Specimen | |
|--------------------------------|----------------------------|
| Maximum Aggregate Size G_K | 10 [mm] |
| Initial Compacted Height h_0 | 64.00 [mm] |
| Final Height h_f | - [mm] |
| Diameter $d_{0.95}$ | 300 [mm] |
| Surface Area A_0 | 0.0707 [m ²] |
| Sample Mass m_0 | 7295.5 [g] |
| Initial Compacted Volume V_0 | 4523.89 [cm ³] |
| Final Volume V_f | - [cm ³] |

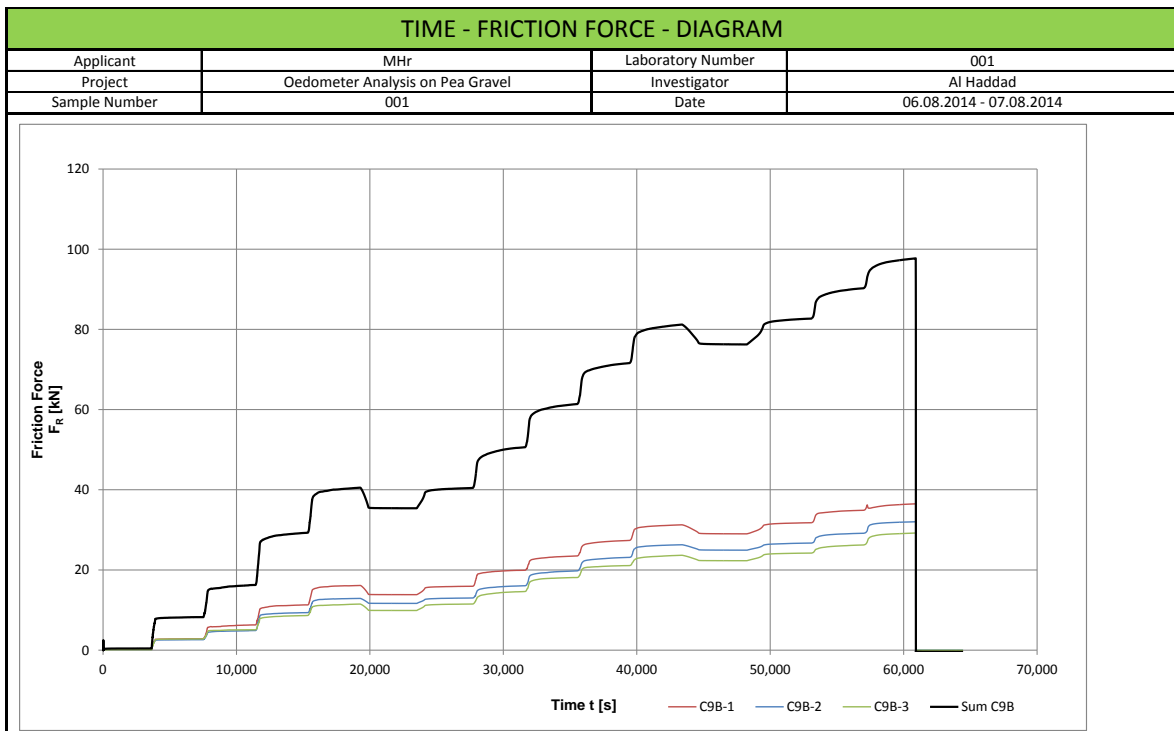
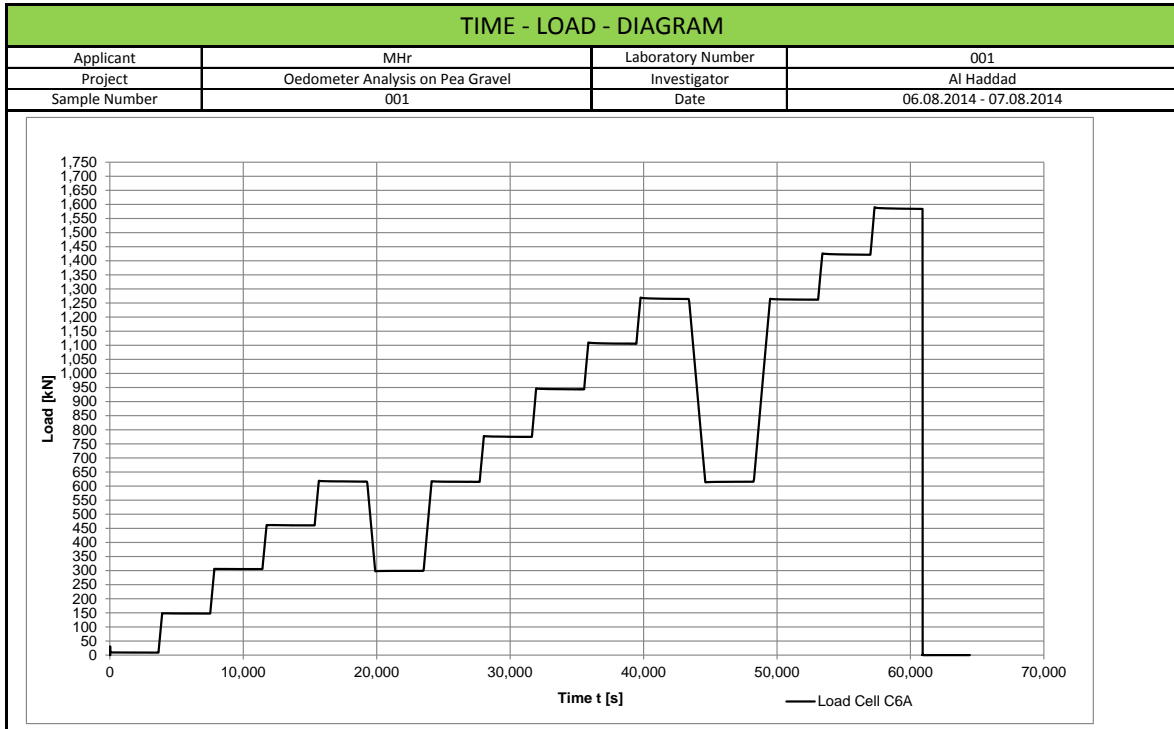
| Material Sieving | |
|------------------------------|-------------|
| Maximum Aggregate Size G_K | 10 [mm] |
| Mass > 10,0 mm m_{10} | 0.00 [g] |
| Mass < 10,0 mm m_{10} | 7295.50 [g] |
| Percentage > 10,0 mm | 0.00 [%] |
| Percentage < 10,0 mm | 100.00 [%] |

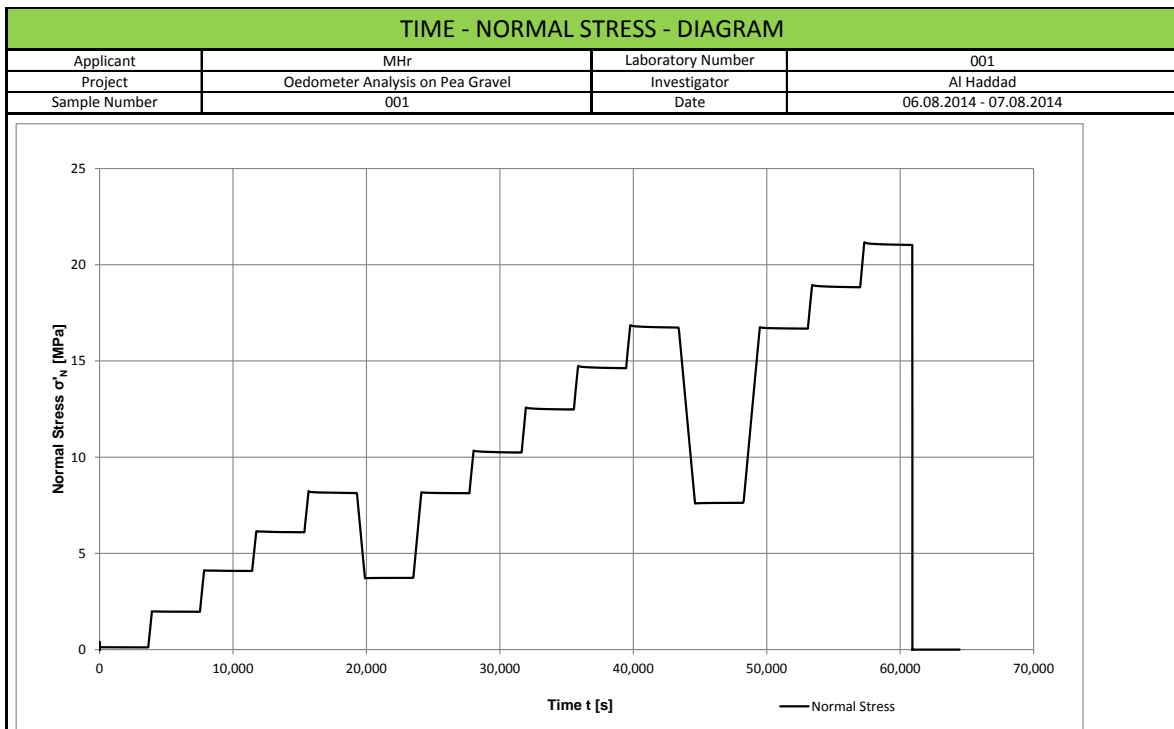
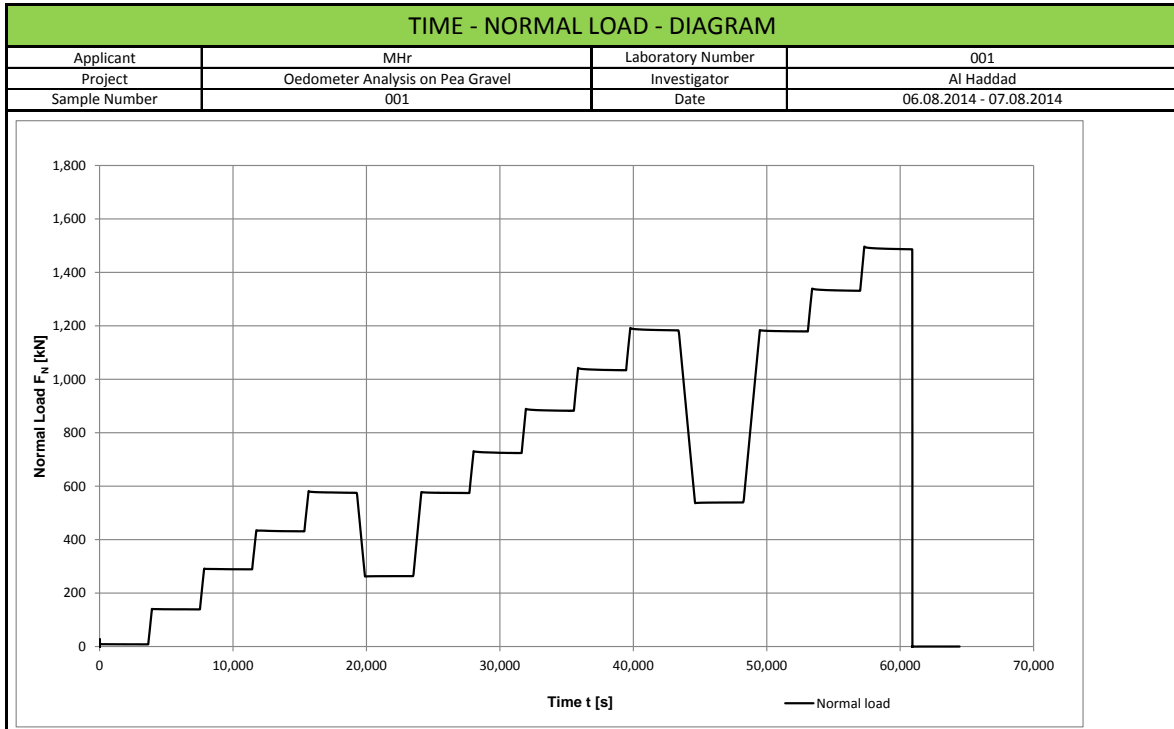
| Load Levels - Applied | | |
|-----------------------|---------|---------------------------------|
| Type of Load | Stage # | Normal Stress σ'_N [MPa] |
| loading 1 | 1 | 0.15 |
| loading 2 | 2 | 0.11 |
| loading 3 | 3 | 0.16 |
| loading 4 | 4 | 0.35 |
| unloading 1 | 5 | 0.16 |
| reloading 1 | 6 | 0.36 |
| loading 5 | 7 | 0.82 |
| loading 6 | 8 | 0.39 |
| loading 7 | 9 | 0.82 |
| loading 8 | 10 | 1.79 |
| unloading 2 | 11 | 0.86 |
| reloading 2 | 12 | 1.79 |
| loading 9 | 13 | 3.74 |
| loading 10 | 14 | 1.80 |
| unloading 3 | 15 | 2.84 |

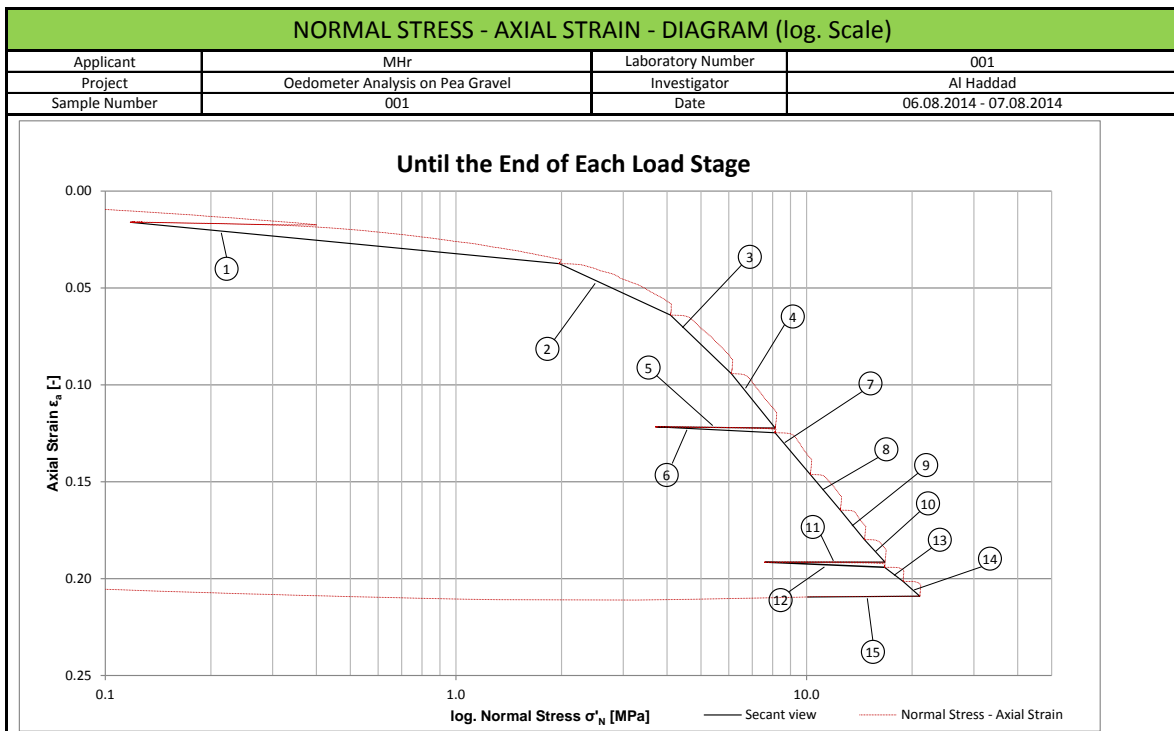
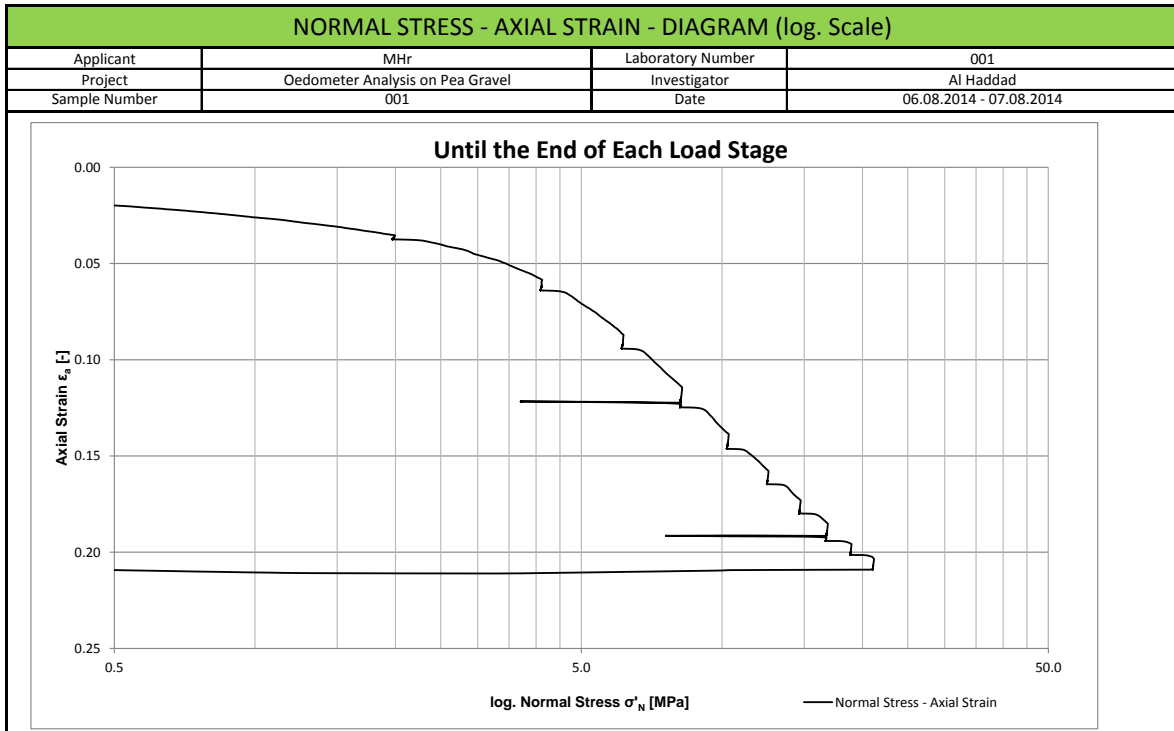
| YOUNGS MODULUS - TO THE END OF THE LOAD LEVEL | | | | | |
|---|----------------------------------|---------------------------------|-------------------------|-------------|------------------|
| Applicant | MHR | Laboratory Number | 001 | | |
| Project | Oedometer Analysis on Pea Gravel | Investigator | Al Haddad | | |
| Sample Number | 001 | Date | 06.08.2014 - 07.08.2014 | | |
| # | Situation | Normal Stress σ'_N [MPa] | Strain ϵ_s [-] | E_s [MPa] | Duration [hh:mm] |
| 1 | loading 1 | 0.12 | 0.0161 | 90 | 01:04 |
| | | 1.97 | 0.0374 | | |
| 2 | loading 2 | 1.97 | 0.0374 | 80 | 01:05 |
| | | 4.09 | 0.0640 | | |
| 3 | loading 3 | 4.09 | 0.0640 | 70 | 01:05 |
| | | 6.10 | 0.0942 | | |
| 4 | loading 4 | 6.10 | 0.0942 | 70 | 01:05 |
| | | 8.14 | 0.1223 | | |
| 5 | unloading 1 | 8.14 | 0.1223 | 6,860 | 01:10 |
| | | 3.73 | 0.1217 | | |
| 6 | reloading 1 | 3.73 | 0.1217 | 1,440 | 01:10 |
| | | 8.13 | 0.1247 | | |
| 7 | loading 5 | 8.13 | 0.1247 | 100 | 01:05 |
| | | 10.25 | 0.1463 | | |
| 8 | loading 6 | 10.25 | 0.1463 | 120 | 01:05 |
| | | 12.48 | 0.1647 | | |
| 9 | loading 7 | 12.48 | 0.1647 | 140 | 01:05 |
| | | 14.62 | 0.1799 | | |
| 10 | loading 8 | 14.62 | 0.1799 | 180 | 01:05 |
| | | 16.74 | 0.1915 | | |

| YOUNG'S MODULUS - TO THE END OF THE LOAD LEVEL | | | | | |
|--|----------------------------------|---------------------------------|-------------------------|-------------|------------------|
| Applicant | MHR | Laboratory Number | 001 | | |
| Project | Oedometer Analysis on Pea Gravel | Investigator | Al Haddad | | |
| Sample Number | 001 | Date | 06.08.2014 - 07.08.2014 | | |
| # | Situation | Normal Stress σ'_N [MPa] | Strain ϵ_s [-] | E_s [MPa] | Duration [hh:mm] |
| 11 | unloading 2 | 16.74 | 0.1915 | -* | 01:21 |
| | | 7.63 | 0.1915 | | |
| 12 | reloading 2 | 7.63 | 0.1915 | 3,450 | 01:20 |
| | | 16.68 | 0.1941 | | |
| 13 | loading 9 | 16.68 | 0.1941 | 300 | 01:05 |
| | | 18.83 | 0.2014 | | |
| 14 | loading 10 | 18.83 | 0.2014 | 290 | 01:05 |
| | | 21.03 | 0.2090 | | |
| 15 | unloading 3 | 21.03 | 0.2090 | 25,730 | 00:00 |
| | | 10.07 | 0.2095 | | |

comment
*) It is not possible to evaluate the young's modulus at load stage unloading 2 because the strains are identical. Due to this, the youngs modulus would be infinite at this stage.







Annex D

Input File of the numerical shear box calculation

```

1  **-----
2  **-----SHEAR BOX CALCULATION -----
3  **-----
4  ** Normal Pressure: 400kN/m2
5  **-----
6  **
7  ** Created by Christoph Sinkovec
8  ** Institute for Rock Mechanics and Tunnelling
9  ** Graz University of Technology
10 **
11 **-----
12 ** (1) Input of the Geometry
13 **-----
14 **
15 *Node
16     1,      -102.5,      -102.5,      17.
17     2,      -102.5,       97.5,      17.
18     3,      -102.5,       97.5,       7.
19     4,      -102.5,      -102.5,       7.
20     5,       97.5,       97.5,      17.
21     6,       97.5,       97.5,       7.
22     7,       97.5,      -102.5,       7.
23 ***** some lines deleted *****
24     17810,      92.5,      22.5,      29.
25     17811,      92.5,      32.5,      29.
26     17812,      92.5,      42.5,      29.
27     17813,      92.5,      52.5,      29.
28     17814,      92.5,      62.5,      29.
29     17815,      92.5,      72.5,      29.
30     17816,      92.5,      82.5,      29.
31     17817,      92.5,      92.5,      29.
32 *Element, type=PD3D, ELSET=dem1
33     1, 170
34     2, 1111
35     3, 1112
36     4, 1113
37     5, 1114
38     6, 1115
39     7, 1116
40     8, 1117
41     9, 1118
42 ***** some lines deleted *****
43     13190, 3000
44     13191, 3001
45     13192, 3002
46     13193, 3003
47     13194, 3004
48     13195, 3005
49     13196, 3006
50     13197, 3007
51     13198, 3008
52     13199, 3009
53     13200, 3010

```

```

54 *Element, type=S4R
55 13201, 17, 485, 4911, 536
56 13202, 485, 486, 4912, 4911
57 13203, 486, 487, 4913, 4912
58 13204, 487, 488, 4914, 4913
59 13205, 488, 489, 4915, 4914
60 13206, 489, 490, 4916, 4915
61 13207, 490, 491, 4917, 4916
62 13208, 491, 492, 4918, 4917
63 ##### some lines deleted #####
64 15321, 6619, 6620, 1104, 1105
65 15322, 6620, 6621, 1103, 1104
66 15323, 6621, 6622, 1102, 1103
67 15324, 6622, 6623, 1101, 1102
68 15325, 6623, 6624, 1100, 1101
69 15326, 6624, 6625, 1099, 1100
70 15327, 6625, 6626, 1098, 1099
71 15328, 6626, 1071, 56, 1098
72 *Nset, nset=BOX_U
73 31, 32, 33, 34, 35, 36, 37, 38, 39, 40, 700, 701, 702, 703, 704, 705
74 706, 707, 708, 709, 710, 711, 712, 713, 714, 715, 716, 717, 718, 719, 720, 721
75 722, 723, 724, 725, 726, 727, 728, 729, 730, 731, 732, 733, 734, 735, 736, 737
76 738, 739, 740, 741, 742, 743, 744, 745, 746, 747, 748, 749, 750, 751, 752, 753
77 ##### some lines deleted #####
78 6056, 6057, 6058, 6059, 6060, 6061, 6062, 6063, 6064, 6065, 6066, 6067, 6068, 6069, 6070, 6071
79 6072, 6073, 6074, 6075, 6076, 6077, 6078, 6079, 6080, 6081, 6082, 6083, 6084, 6085, 6086, 6087
80 6088, 6089, 6090, 6091, 6092, 6093, 6094, 6095, 6096, 6097, 6098, 6099, 6100, 6101, 6102, 6103
81 6104, 6105, 6106
82 *Elset, elset=BOX_U, generate
83 13929, 14656, 1
84 *Nset, nset=BOX_O1
85 21, 22, 23, 24, 25, 26, 27, 28, 29, 30, 537, 538, 539, 540, 541, 542
86 543, 544, 545, 546, 547, 548, 549, 550, 551, 552, 553, 554, 555, 556, 557, 558
87 559, 560, 561, 562, 563, 564, 565, 566, 567, 568, 569, 570, 571, 572, 573, 574
88 ##### some lines deleted #####
89 5451, 5452, 5453, 5454, 5455, 5456, 5457, 5458, 5459, 5460, 5461, 5462, 5463, 5464, 5465, 5466
90 5467, 5468, 5469, 5470, 5471, 5472, 5473, 5474, 5475, 5476, 5477, 5478, 5479, 5480, 5481, 5482
91 5483, 5484, 5485, 5486, 5487, 5488, 5489, 5490, 5491, 5492, 5493, 5494, 5495, 5496, 5497, 5498
92 5499, 5500, 5501, 5502, 5503, 5504, 5505, 5506, 5507, 5508
93 *Elset, elset=BOX_O1, generate
94 13397, 13928, 1
95 *Nset, nset=BOX_O2
96 41, 42, 43, 44, 45, 46, 47, 48, 49, 50, 51, 52, 53, 54, 55, 56
97 863, 864, 865, 866, 867, 868, 869, 870, 871, 872, 873, 874, 875, 876, 877, 878
98 879, 880, 881, 882, 883, 884, 885, 886, 887, 888, 889, 890, 891, 892, 893, 894
99 ##### some lines deleted #####
100 6579, 6580, 6581, 6582, 6583, 6584, 6585, 6586, 6587, 6588, 6589, 6590, 6591, 6592, 6593, 6594
101 6595, 6596, 6597, 6598, 6599, 6600, 6601, 6602, 6603, 6604, 6605, 6606, 6607, 6608, 6609, 6610
102 6611, 6612, 6613, 6614, 6615, 6616, 6617, 6618, 6619, 6620, 6621, 6622, 6623, 6624, 6625, 6626
103 *Elset, elset=BOX_O2, generate
104 14657, 15328, 1
105 *Nset, nset=TOPPLATE
106 17, 18, 19, 20, 485, 486, 487, 488, 489, 490, 491, 492, 493, 494, 495, 496
107 497, 498, 499, 500, 501, 502, 503, 504, 505, 506, 507, 508, 509, 510, 511, 512
108 513, 514, 515, 516, 517, 518, 519, 520, 521, 522, 523, 524, 525, 526, 527, 528
109 ##### some lines deleted #####
110 5031, 5032, 5033, 5034, 5035, 5036, 5037, 5038, 5039, 5040, 5041, 5042, 5043, 5044, 5045, 5046
111 5047, 5048, 5049, 5050, 5051, 5052, 5053, 5054, 5055, 5056, 5057, 5058, 5059, 5060, 5061, 5062
112 5063, 5064, 5065, 5066, 5067, 5068, 5069, 5070, 5071, 5072, 5073, 5074, 5075, 5076, 5077, 5078
113 5079,
114 *Elset, elset=TOPPLATE, generate
115 13201, 13396, 1
116 *Nset, nset=TENSION
117 22, 23, 27, 30, 41, 44, 47, 48, 550, 551, 552, 553, 554, 555, 556, 557
118 558, 559, 560, 561, 562, 620, 621, 622, 623, 624, 682, 683, 684, 685, 686, 687
119 688, 689, 690, 691, 692, 693, 694, 695, 696, 697, 698, 699, 894, 895, 896, 897
120 898, 956, 957, 958, 959, 960, 961, 962, 963, 964, 965, 966, 967, 968, 969, 970
121 ##### some lines deleted #####

```



```

122 6317, 6318, 6319, 6320, 6321, 6322, 6323, 6324, 6325, 6326, 6327, 6328, 6329, 6330, 6331, 6332
123 6333, 6334, 6335, 6336, 6337, 6338, 6339, 6340, 6341, 6342, 6343, 6344, 6345, 6346, 6347, 6348
124 6349, 6350, 6351, 6352, 6353, 6354, 6355, 6356, 6357, 6358, 6359, 6360, 6361, 6362, 6363, 6364
125 6365, 6366
126 *Elset, elset=TENSION
127 13845, 13846, 13847, 13848, 13849, 13850, 13851, 13852, 13853, 13854, 13855, 13856, 13857, 13858, 13859, 13860
128 13861, 13862, 13863, 13864, 13865, 13866, 13867, 13868, 13869, 13870, 13871, 13872, 13873, 13874, 13875, 13876
129 13877, 13878, 13879, 13880, 13881, 13882, 13883, 13884, 13885, 13886, 13887, 13888, 13889, 13890, 13891, 13892
130 ##### some lines deleted #####
131 14937, 14938, 14939, 14940, 14941, 14942, 14943, 14944, 14945, 14946, 14947, 14948, 14949, 14950, 14951, 14952
132 14953, 14954, 14955, 14956, 14957, 14958, 14959, 14960, 14961, 14962, 14963, 14964, 14965, 14966, 14967, 14968
133 14969, 14970, 14971, 14972, 14973, 14974, 14975, 14976, 14977, 14978, 14979, 14980, 14981, 14982, 14983, 14984
134 14985, 14986, 14987, 14988, 14989, 14990, 14991, 14992
135 **
136 **-----
137 ** (2) Material Parameters Discrete Elements
138 **-----
139 **
140 ** Radius = 5mm (0.005m)
141 ** Density = 2600 kg/m3 (2.6 10^-9kg/m3)
142 **
143 *discrete section,elset=dem1,shape=sphere,density=2.6e-09, alpha=7
144 5,
145 **
146 ** Make the sets rigid
147 **
148 *RIGID BODY, REF NODE =          31, ELSET = box_u
149 *RIGID BODY, REF NODE =          21, ELSET = box_o1
150 *RIGID BODY, REF NODE =          41, ELSET = box_o2
151 *RIGID BODY, REF NODE =          17, ELSET = topplate
152 **
153 **
154 ** Important: Change the node number if the geometry is changing!!
155 **
156 **-----
157 ** (3) Material Parameters of the box
158 **-----
159 **
160 *Material, name=STEEL
161 *density
162 7.85e-09
163 *elastic
164 2.08e+5,0.3
165 **
166 **
167 *SHELL SECTION, ELSET=box_o1, MATERIAL=STEEL,
168 2,
169 *SHELL SECTION, ELSET=box_o2, MATERIAL=STEEL,
170 2,
171 *SHELL SECTION, ELSET=topplate, MATERIAL=STEEL,
172 2,
173 *SHELL SECTION, ELSET=box_u, MATERIAL=STEEL,
174 2,
175 **
176 **-----
177 ** (4) Surface definition
178 **-----
179 **
180 *surface, type=element, name=dem1
181 dem1,
182 *surface, type=element, name=box_u
183 box_u,
184 *surface, type=element, name=box_o1
185 box_o1,
186 *surface, type=element, name=box_o2
187 box_o2,
188 *surface, type=element, name=tension
189 tension,
190 *Surface, type=ELEMENT, name=TOPPLATE
191 TOPPLATE, SNEG
192 **

```

```

193 **-----
194 ** (5) Boundary Conditions
195 **-----
196 **
197 ** Name: BC-1 Type: Velocity/Angular velocity
198 *Boundary, type=VELOCITY
199 BOX_U, 1, 1
200 BOX_U, 2, 2
201 BOX_U, 3, 3
202 BOX_U, 4, 4
203 BOX_U, 5, 5
204 BOX_U, 6, 6
205 ** Name: BC-2 Type: Velocity/Angular velocity
206 *Boundary, type=VELOCITY
207 BOX_O1, 1, 1
208 BOX_O1, 2, 2
209 BOX_O1, 3, 3
210 BOX_O1, 4, 4
211 BOX_O1, 5, 5
212 BOX_O1, 6, 6
213 ** Name: BC-3 Type: Velocity/Angular velocity
214 *Boundary, type=VELOCITY
215 BOX_O2, 1, 1
216 BOX_O2, 2, 2
217 BOX_O2, 3, 3
218 BOX_O2, 4, 4
219 BOX_O2, 5, 5
220 BOX_O2, 6, 6
221 ** Name: BC-3 Type: Velocity/Angular velocity
222 *Boundary, type=VELOCITY
223 TOPPLATE, 1, 1
224 TOPPLATE, 2, 2
225 TOPPLATE, 4, 4
226 TOPPLATE, 5, 5
227 TOPPLATE, 6, 6
228 **
229 **-----
230 ** (6) force-overclosure relationship based on Hertz contact formulation
231 ** (output data of the Excel file - transferred by the macro)
232 **-----
233 ** dem1: Radius = 5mm E= 200.000 N/mm2, poisson's ratio = 0.20
234 ** box: E= 208.000 N/mm2, poisson's ratio = 0.25
235 **
236 **
237 *surface interaction, name=P1f
238 *Contact Damping, definition=DAMPING COEFFICIENT
239 0.07
240 *surface behaviour, pressure-overclosure=tabular
241 0.0000000E+00 , 0.0000000E+00
242 1.2662346E+00 , 2.5000000E-04
243 3.5680302E+00 , 4.9875000E-04
244 6.5466775E+00 , 7.4750000E-04
245 ##### some lines deleted #####
246 3.4750795E+03 , 4.9005000E-02
247 3.5015724E+03 , 4.9253750E-02
248 3.5281322E+03 , 4.9502500E-02
249 3.5814522E+03 , 5.0000000E-02
250 **
251 *surface interaction, name=P11
252 *friction
253 0.70
254 *Contact Damping, definition=DAMPING COEFFICIENT
255 0.07
256 *surface behaviour, pressure-overclosure=tabular
257 0.0000000E+00 , 0.0000000E+00
258 8.6805556E-01 , 2.5000000E-04
259 2.4460305E+00 , 4.9875000E-04
260 ##### some lines deleted #####
261 2.4004710E+03 , 4.9253750E-02
262 2.4186788E+03 , 4.9502500E-02
263 2.4552319E+03 , 5.0000000E-02

```

```

264 **
265 **-----
266 ** (7) STEP 1 - settling of particles
267 **-----
268 **
269 *step
270 step 1 - settling of particles
271 **
272 *dynamic, explicit, direct
273 0.2e-6,0.50
274 **
275 *dload
276 dem1, grav, 9800.0,0.,0.,-1.0
277 topplate, grav, 9800.0,0.,0.,-1.0
278 *contact
279 *contact controls assignment, rotational terms=structural
280 **
281 *contact inclusions
282 dem1,box_u
283 dem1,box_o1
284 dem1,box_o2
285 dem1,topplate
286 dem1,dem1
287 *contact property assignment
288 dem1,box_u,P1f
289 dem1,box_o1,P1f
290 dem1,box_o2,P1f
291 dem1,topplate,P1f
292 dem1,dem1,P11
293 *output, history,frequency=1
294 CRM1,CRM2,CRM3,CVR1,CVR2,CVR3
295 *energy output, var=all
296 **
297 *output, field, number interval=60
298 *node output
299 U, V, RM, RT
300 **
301 **
302 *end step
303 **
304 **-----
305 ** (8) STEP 2 - pressure
306 **-----
307 **
308 *step
309 step 2 - pressure
310 **
311 *dynamic, explicit, direct
312 0.2e-6,0.20
313 **
314 ** LOADS
315 **
316 ** Name: Load-3   Type: Pressure
317 *Dsload
318 TOPPLATE, P, -0.38430
319 **
320 **
321 ** 100 kN/m2 => 0.08430 N/mm2 (0,10 - 0.0157)
322 ** 200 kN/m2 => 0.18430 N/mm2 (0,20 - 0.0157)
323 ** 300 kN/m2 => 0.28430 N/mm2 (0,30 - 0.0157)
324 *****
325 ** 400 kN/m2 => 0.38430 N/mm2 (0,40 - 0.0157) - own weight *****
326 *****
327 **
328 **
329 *output, history,frequency=1
330 CRM1,CRM2,CRM3,CVR1,CVR2,CVR3
331 *energy output, var=all
332 **

```

```
333 *output, field, number interval=12
334 *node output
335 U, V, RM, RT
336 **
337 **
338 *end step
339 **-----
340 ** (9) STEP 3 - shearing (shearing speed: 3mm/sec)
341 **-----
342 **
343 *step
344 step 3 - shearing
345 **
346 *dynamic, explicit, direct
347 0.2e-6,10
348 **
349 ** BOUNDARY CONDITIONS
350 **
351 ** Name: Vel-BC-4 Type: Velocity/Angular velocity
352 *Boundary, type=VELOCITY
353 BOX_O1, 1, 1, 3
354 BOX_O2, 1, 1, 3
355 TOPPLATE, 1, 1, 3
356 **
357 *output, history,frequency=1
358 CRM1,CRM2,CRM3,CVR1,CVR2,CVR3
359 *energy output, var=all
360 **
361 *output, field, number interval=1200
362 *node output
363 U, V, RM, RT
364 *Contact Output
365 CFORCE, CSTRESS, CTHICK, FSLIP, FSLIPR
366 **
367 **
368 *end step
```

Annex E

Python Code for the evaluation of the shear test

```

1  # -----
2  # Name:          shear diagram creator (without laboratory tests)
3  #
4  # Author:       sinko
5  #
6  # Created:      14.11.2014
7  # Copyright:    (c) sinkovec 2014
8  # -----
9
10 from pylab import *
11 import math
12 import matplotlib
13 import matplotlib.pyplot as plt
14 import numpy as np
15 from scipy import stats
16 import matplotlib.image as mpimg
17
18 # -----
19 # input number !!
20 # -----
21
22 number = '01_050'
23
24 # -----
25 # input data
26 # -----
27
28 d1,s1,d2,s2,d3,s3,d4,s4 = np.loadtxt(number+".txt", dtype=float, unpack=True)
29
30 dl1,s11,dl2,s12,dl3,s13,dl4,s14 = np.loadtxt("lab.txt", dtype=float, unpack=True)
31
32 # -----
33 # Plot 1 - shear stress / distance
34 # -----
35
36 fig = plt.figure(figsize=(9, 6))
37
38 name1='numerical  $\sigma_{n} = 1000 \text{ kN/m}^2$ '
39
40 # -----
41 # (a) without the laboratory results
42 # -----
43
44 # numerical results
45 line1, = plt.plot(d1,s1, 'b',label=' $\sigma_{n} = 1000 \text{ kN/m}^2$ ')
46 line2, = plt.plot(d2,s2, 'g',label=' $\sigma_{n} = 2000 \text{ kN/m}^2$ ')
47 line3, = plt.plot(d3,s3, 'm',label=' $\sigma_{n} = 3000 \text{ kN/m}^2$ ')
48 line4, = plt.plot(d4,s4, 'c',label=' $\sigma_{n} = 4000 \text{ kN/m}^2$ ')
49
50 # labeling
51 plt.ylabel('shear stress  $\tau$  [kN/m2]')
52 plt.xlabel('shear distance  $\tau$  [mm]')
53 plt.ticklabel_format(style='plain', axis='both', useOffset=False)
54
55 first_legend = plt.legend(handles=[line1,line2,line3,line4],bbox_to_anchor=[0.995, 0.995],
56 title="numerical results",prop={'size':9}, loc='upper right')
57
58 plt.grid(True)
59 plt.xlim(0,40)
60 plt.ylim(0,150)
61
62 plt.savefig('sd_'+number+'.png')
63 #plt.show()

```

```

64
65 plt.clf() # clean up the plot window
66
67 # -----
68 # (b) included the laboratory results
69 # -----
70
71 fig = plt.figure(figsize=(9, 6))
72
73 name1='numerical  $\sigma_{n}$  = 1000 kN/m2'
74
75 # numerical results
76 line1, = plt.plot(d1,s1, 'b',label=' $\sigma_{n}$  = 1000 kN/m2')
77 line2, = plt.plot(d2,s2, 'g',label=' $\sigma_{n}$  = 2000 kN/m2')
78 line3, = plt.plot(d3,s3, 'm',label=' $\sigma_{n}$  = 3000 kN/m2')
79 line4, = plt.plot(d4,s4, 'c',label=' $\sigma_{n}$  = 4000 kN/m2')
80
81 # laboratory results
82 line5, = plt.plot(dl1,sl1, 'b:',label=' $\sigma_{n}$  = 1000 kN/m2')
83 line6, = plt.plot(dl2,sl2, 'g:',label=' $\sigma_{n}$  = 2000 kN/m2')
84 line7, = plt.plot(dl3,sl3, 'm:',label=' $\sigma_{n}$  = 3000 kN/m2')
85 line8, = plt.plot(dl4,sl4, 'c:',label=' $\sigma_{n}$  = 4000 kN/m2')
86
87 # labeling
88 plt.ylabel('shear stress  $\tau$  [kN/m2']')
89 plt.xlabel('shear distance  $x$  [mm]')
90 plt.ticklabel_format(style='plain', axis='both', useOffset=False)
91 plt.title("Shear Diagram")
92
93
94 legend1 = plt.legend(handles=[line1,line2,line3,line4],bbox_to_anchor=[0.995, 0.995],
95 title="numerical results",prop={'size':9}, loc='upper right')
96 ax = plt.gca().add_artist(legend1)
97 plt.legend(handles=[line5,line6,line7,line8],bbox_to_anchor=[0.765, 0.995],
98 title="laboratory results",prop={'size':9}, loc='upper right')
99
100 plt.grid(True)
101 plt.xlim(0,40)
102 plt.ylim(0,420)
103
104 # Save to file
105 plt.savefig('sd_lab_'+number+'.png')
106 #plt.show()
107
108 plt.clf() # clean up the plot window
109
110 # -----
111 # Plot 2 - max shear stress / normal stress
112 # -----
113
114 # create max values
115 s1max=max(s1)
116 s2max=max(s2)
117 s3max=max(s3)
118 s4max=max(s4)
119
120 # create array
121 shear_max=array([0,s1max,s2max,s3max,s4max])
122
123 sigma_n=array([-5,100,200,300,400]) # adapt first value to avoid negative cohesion
124
125 # create compensation line
126 x0,x1,x2,x3,x4= stats.linregress(sigma_n,shear_max)
127 shear_est=x1+x0*array(sigma_n)

```

```

128
129 # Friction angle
130 phi = np.arctan(x0)*180/np.pi
131 shearline=('friction angle  $\phi$  = '+str(round(phi,2))+
132 '$^\circ$ \n cohesion          c = '+str(round(x1,2))+ '00 kN/m $^2$ ')
133
134 # -----
135 # (a) without the laboratory results
136 # -----
137
138 plt.figure(figsize=(6, 6))
139
140 dots1, = plt.plot(sigma_n,shear_max,'bd', label='single values')
141 line1, =plt.plot(sigma_n,shear_est,'b', label ='\n '+shearline)
142
143 # labelling
144
145 plt.ylabel('shear stress  $\tau$  [kN/m $^2$ ]')
146 plt.xlabel('normal stress  $\sigma_n$  [kN/m $^2$ ]')
147 plt.ticklabel_format(style='plain', axis='both', useOffset=False)
148
149 first_legend = plt.legend(handles=[dots1,line1],bbox_to_anchor=[0.01, 0.99],
150 title="numerical results \n",prop={'size':8}, loc=2,borderaxespad=0.)
151
152 plt.grid(True)
153 plt.xlim(0,420)
154 plt.ylim(0,420)
155
156 plt.savefig('sn_'+number+'.png')
157 #plt.show()
158
159 plt.clf() # clean up the plot window
160
161 # -----
162 # (b) included the laboratory results
163 # -----
164
165 s11max=max(s11)
166 s12max=max(s12)
167 s13max=max(s13)
168 s14max=max(s14)
169
170 # create array
171 shear_lab_max=array([5,s11max,s12max,s13max,s14max])
172
173 sigma_n_lab=array([-20,100,200,300,400])
174
175 # create compensation line
176
177 x10,x11,x12,x13,x14= stats.linregress(sigma_n_lab,shear_lab_max)
178 shear_lab_est=x11+x10*array(sigma_n_lab)
179
180 # Friction angle
181 phi_lab = np.arctan(x10)*180/np.pi
182 shearline_lab=('friction angle  $\phi$  = '+str(round(phi_lab,2))+
183 '$^\circ$ \n cohesion          c = '+str(round(x11,2))+ '00 kN/m $^2$ ')
184
185 # create plot figure
186 plt.figure(figsize=(6, 6))
187 dots1, = plt.plot(sigma_n,shear_max,'bd', label='single values')
188 line1, =plt.plot(sigma_n,shear_est,'b', label ='\n '+shearline)
189 dots2, = plt.plot(sigma_n_lab,shear_lab_max,'rd', label='single values')
190 line2, = plt.plot(sigma_n_lab,shear_lab_est,'r:', label='\n '+shearline_lab)
191

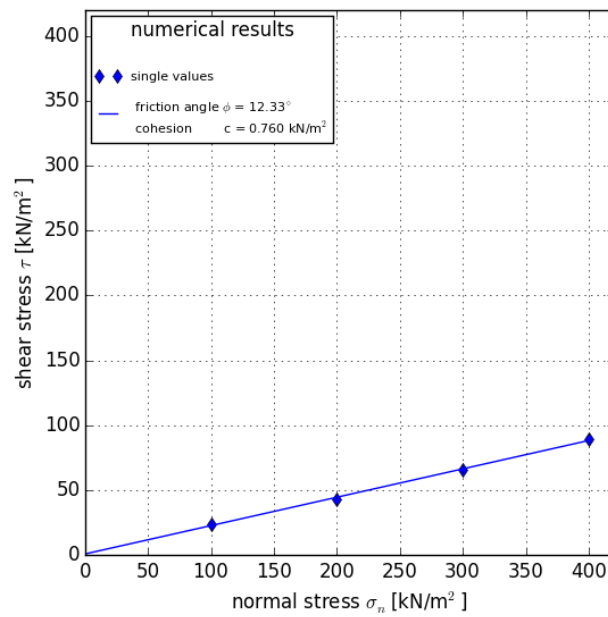
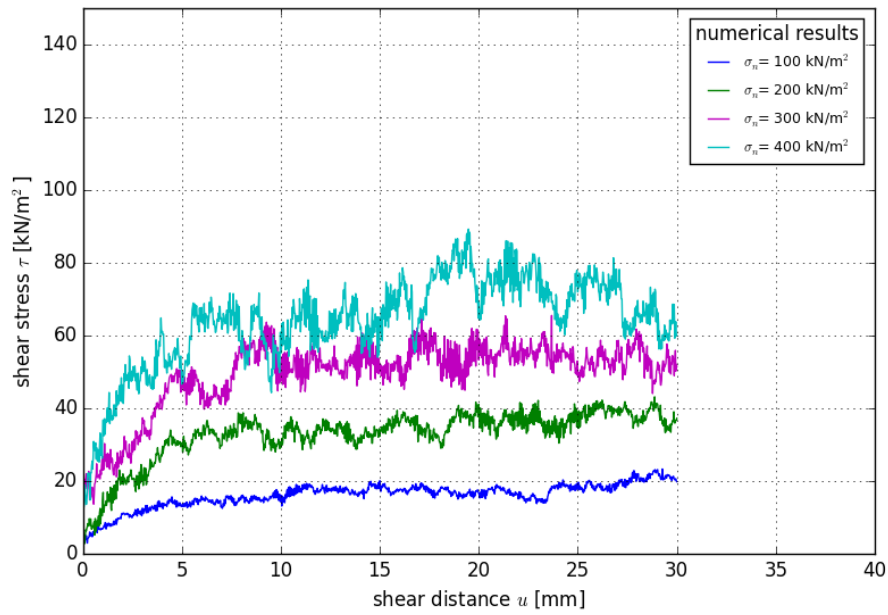
```

```
192 # labelling
193 plt.ylabel('shear stress  $\tau$  [kN/m2]')
194 plt.xlabel('normal stress  $\sigma_n$  [kN/m2]')
195 plt.ticklabel_format(style='plain', axis='both', useOffset=False)
196 #plt.title("Shear Diagram")
197 plt.grid(True)
198 plt.xlim(0,420)
199 plt.ylim(0,420)
200
201 # Legend
202 legend2 = plt.legend(handles=[dots1,line1],bbox_to_anchor=[0.01, 0.99],title="numerical results \n",prop={'size':8}, loc=2)
203 ax = plt.gca().add_artist(legend2)
204 plt.legend(handles=[dots2,line2],bbox_to_anchor=[0.01, 0.75],title="laboratory results \n",prop={'size':8}, loc=2)
205
206 plt.savefig('sn_lab_'+number+'.png')
207
208 #plt.show()
209
210
```

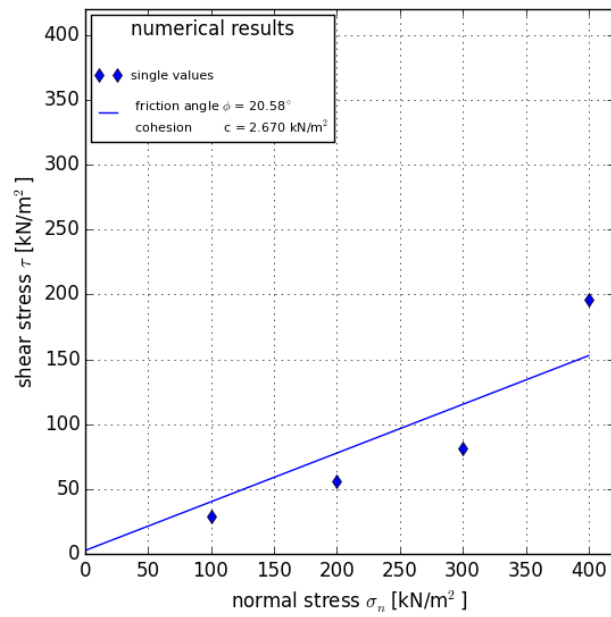
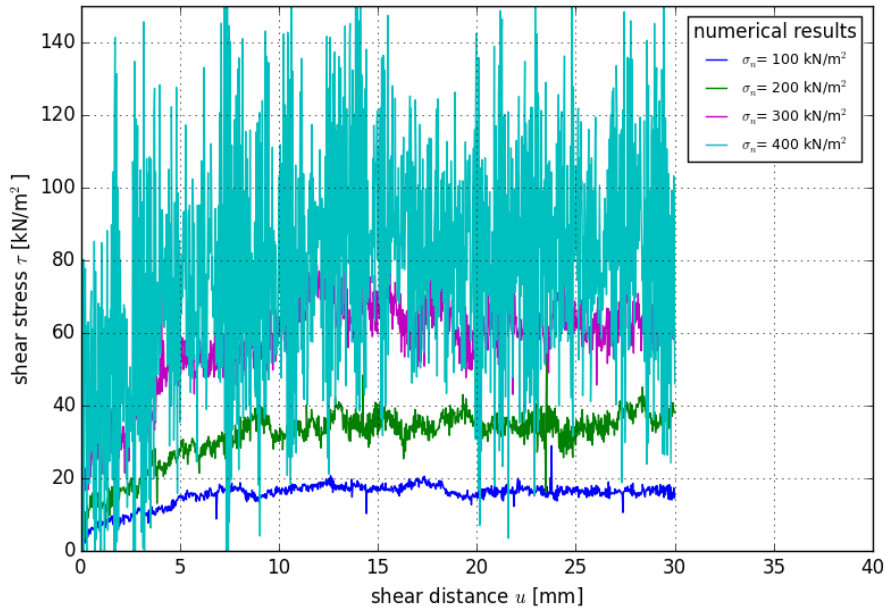

Annex F

Numerical shear test results

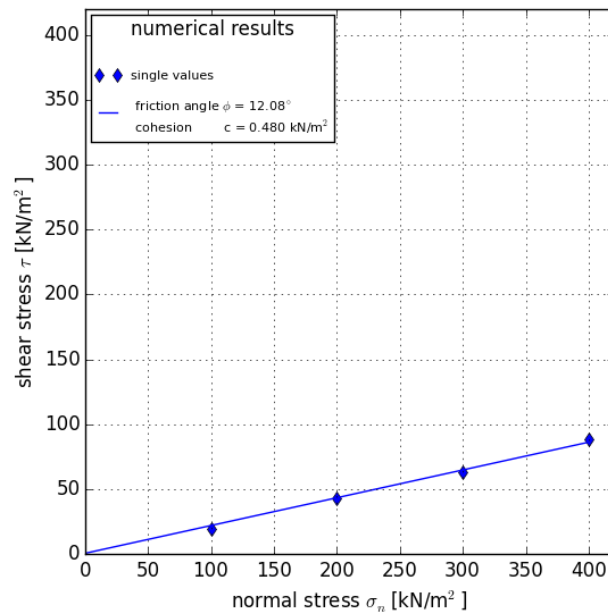
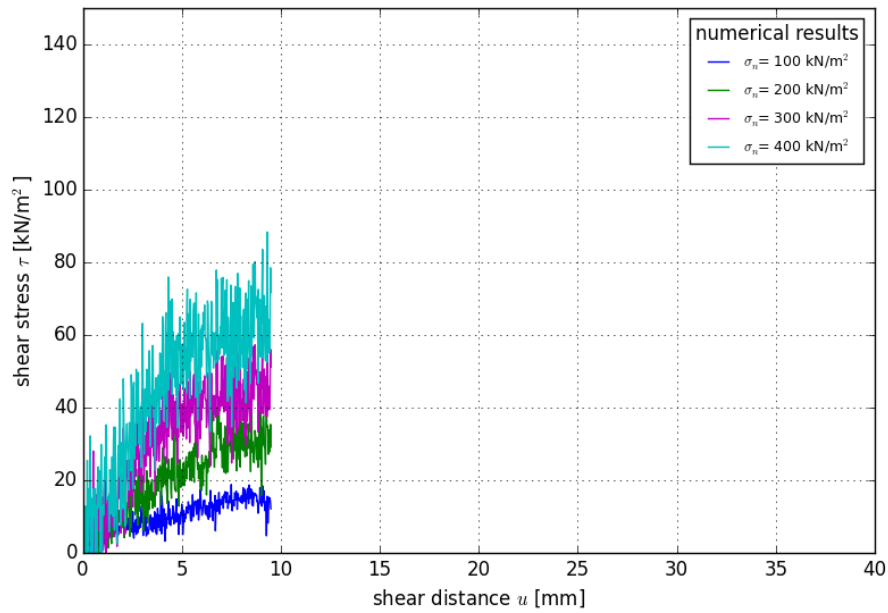
Variation 01a



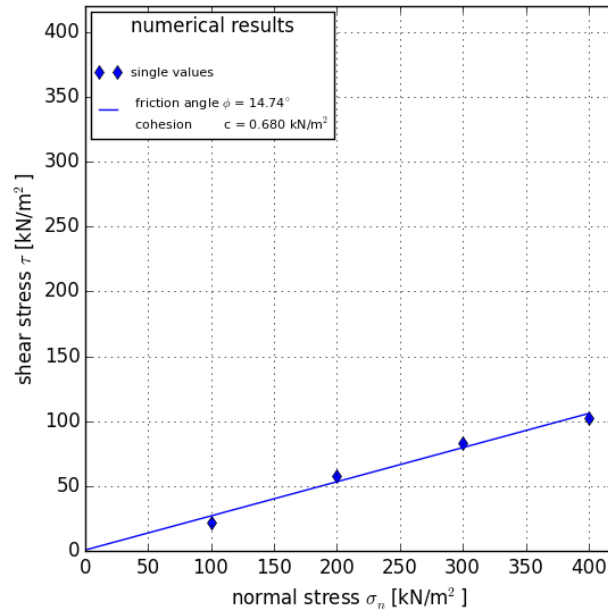
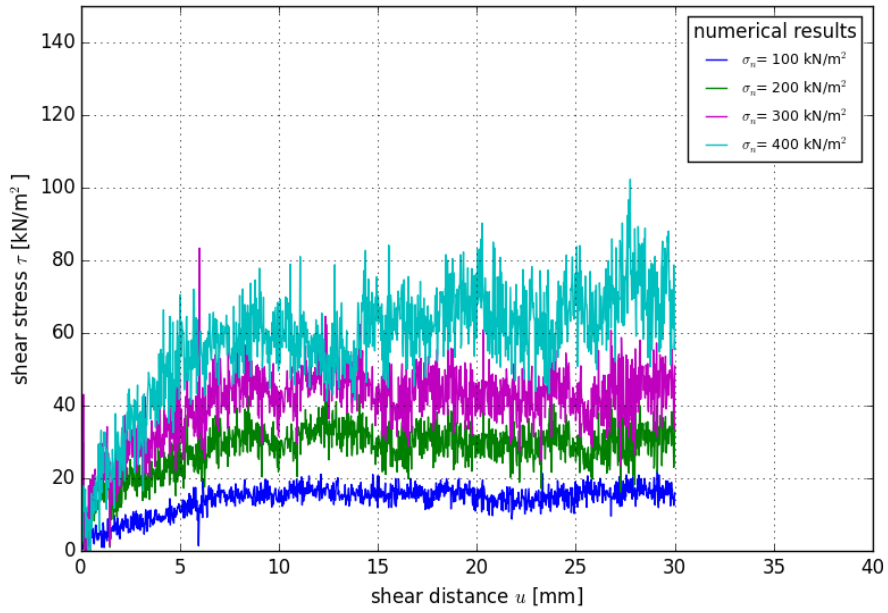
Variation 01b



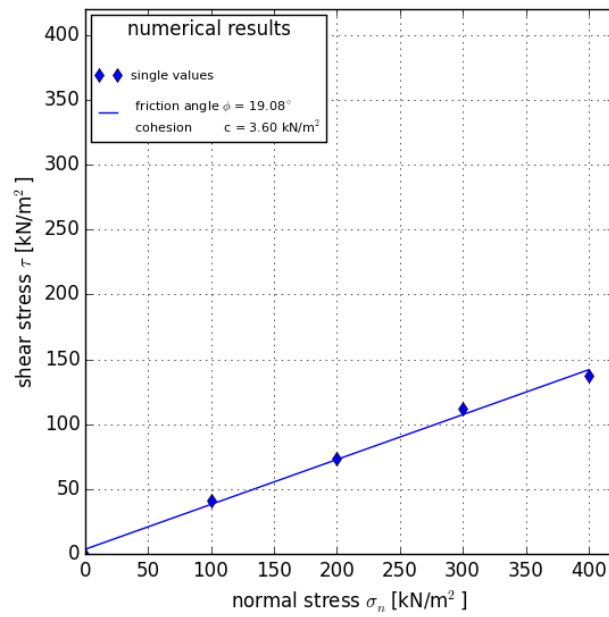
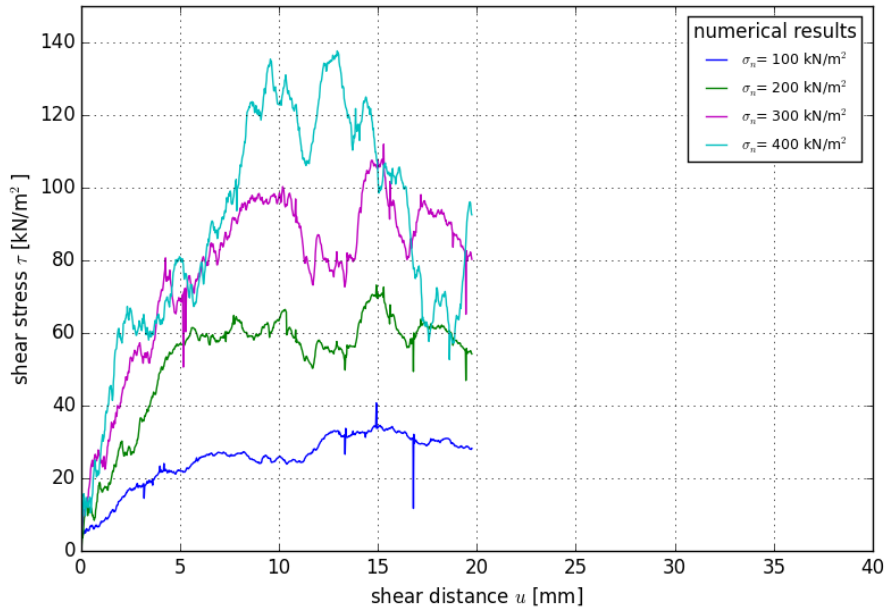
Variation 02a



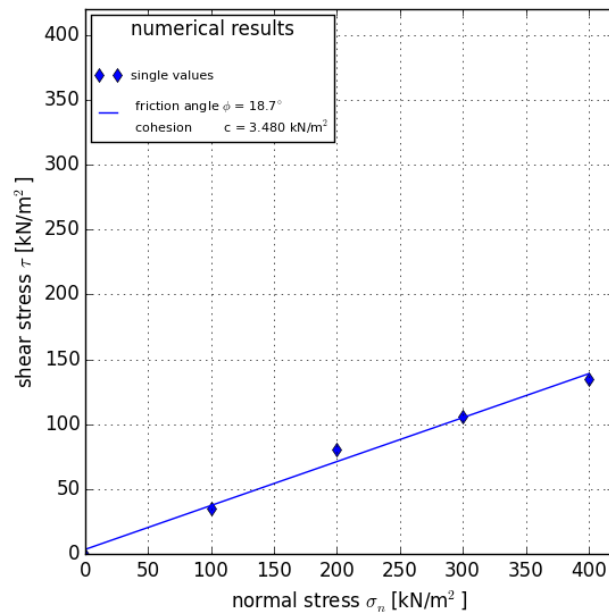
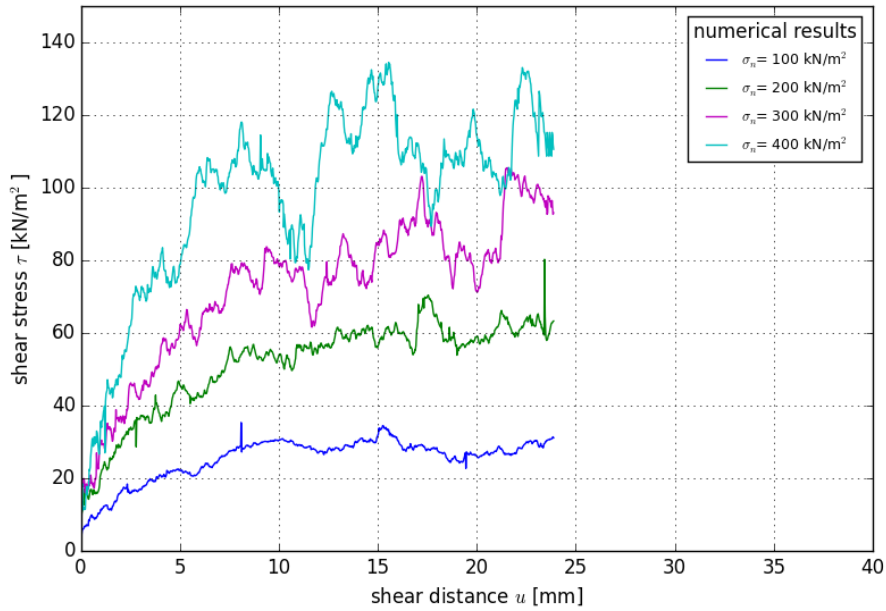
Variation 02b



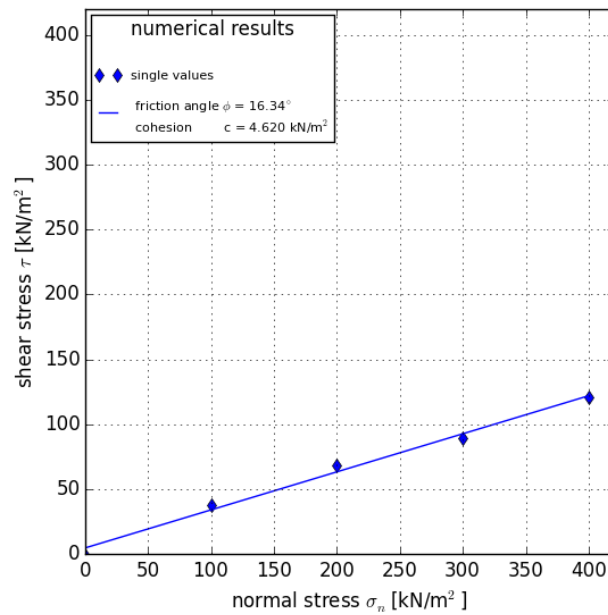
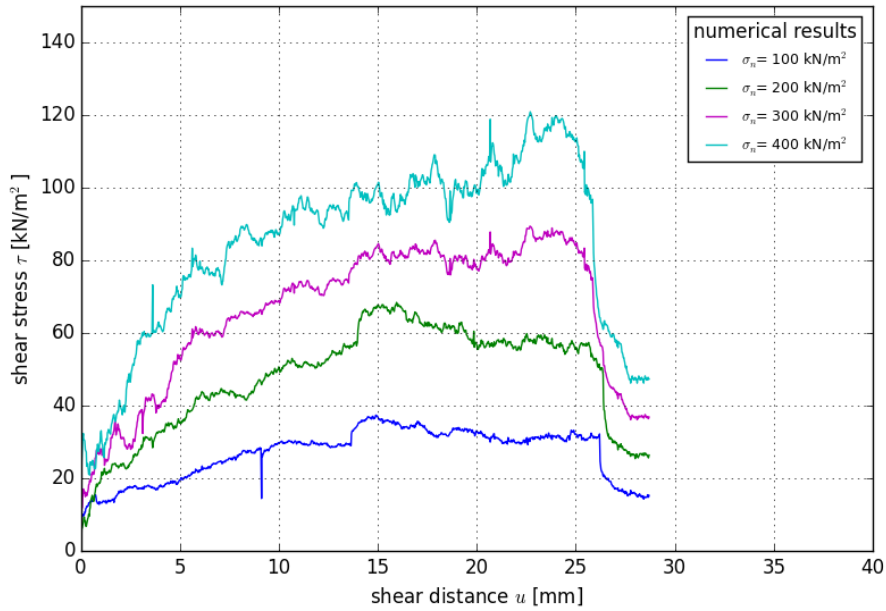
Variation 03



Variation 05



Variation 07



Annex G

Input file of the numerical oedometer test

```

1  **-----
2  **---- OEDOMETERTEST  CALCULATION  -----
3  **-----
4  **
5  ** Created by Christoph Sinkovec
6  ** Institute for Rock Mechanics and Tunnelling
7  ** Graz University of Technology
8  **
9  **-----
10 ** (1) Input of the Geometry
11 **-----
12 **
13 *Node
14     1,      -100.,    -100.,    182.5
15     2,      -100.,     100.,    182.5
16     3,      -100.,     100.,     22.5
17     4,      -100.,    -100.,     22.5
18 ##### some lines deleted #####
19     12850,     90.,     60.,     32.5
20     12851,     90.,     70.,     32.5
21     12852,     90.,     80.,     32.5
22     12853,     90.,     90.,     32.5
23 *Element, type=PD3D, ELSET=dem1
24     1, 198
25     2, 2273
26     3, 2274
27     4, 2275
28 ##### some lines deleted #####
29     6797, 278
30     6798, 277
31     6799, 276
32     6800, 275
33 *Element, type=S4R
34     6801, 17, 389, 3717, 3810
35     6802, 389, 390, 3718, 3717
36     6803, 390, 391, 3719, 3718
37     6804, 391, 392, 3720, 3719
38 ##### some lines deleted #####
39     10919, 7042, 6994, 7058, 7426
40     10920, 7428, 7301, 7287, 7294
41     10921, 7431, 7205, 7182, 7155
42     10922, 7254, 7206, 7236, 7437
43 *Element, type=S3
44     9057, 6458, 5752, 6081
45     9058, 6087, 6067, 6073
46     9059, 6113, 6528, 6076
47     9060, 6139, 6101, 6106
48 ##### some lines deleted #####
49     10013, 7197, 7213, 7168
50     10014, 7433, 7308, 7428
51     10015, 7435, 7190, 7232
52 *Nset, nset=BOTTOM
53     23, 947, 948, 949, 950, 951, 952, 953, 954, 955, 956, 957, 958, 959, 960, 961
54     962, 963, 964, 965, 966, 967, 968, 969, 970, 971, 972, 973, 974, 975, 976, 977
55     978, 979, 980, 981, 982, 983, 984, 985, 986, 987, 988, 989, 990, 991, 992, 993
56     994, 995, 996, 997, 998, 999, 1000, 1001, 1002, 1003, 1004, 1005, 1006, 1007, 1008, 1009
57 ##### some lines deleted #####
58     6509, 6510, 6511, 6512, 6513, 6514, 6515, 6516, 6517, 6518, 6519, 6520, 6521, 6522, 6523, 6524
59     6525, 6526, 6527, 6528, 6529, 6530, 6531, 6532, 6533, 6534, 6535, 6536, 6537, 6538, 6539, 6540
60     6541, 6542, 6543, 6544, 6545, 6546, 6547, 6548, 6549, 6550, 6551, 6552, 6553, 6554, 6555, 6556
61     6557, 6558, 6559, 6560, 6561, 6562, 6563, 6564
62 *Elset, elset=BOTTOM, generate
63     9057, 9989, 1

```



```

64 *Nset, nset=BOX_U
65     19, 20, 575, 576, 577, 578, 579, 580, 581, 582, 583, 584, 585, 586, 587, 588
66     589, 590, 591, 592, 593, 594, 595, 596, 597, 598, 599, 600, 601, 602, 603, 604
67     605, 606, 607, 608, 609, 610, 611, 612, 613, 614, 615, 616, 617, 618, 619, 620
68     621, 622, 623, 624, 625, 626, 627, 628, 629, 630, 631, 632, 633, 634, 635, 636
69 ##### some lines deleted #####
70     4971, 4972, 4973, 4974, 4975, 4976, 4977, 4978, 4979, 4980, 4981, 4982, 4983, 4984, 4985, 4986
71     4987, 4988, 4989, 4990, 4991, 4992, 4993, 4994, 4995, 4996, 4997, 4998, 4999, 5000, 5001, 5002
72     5003, 5004, 5005, 5006, 5007, 5008, 5009, 5010, 5011, 5012, 5013, 5014, 5015, 5016, 5017, 5018
73     5019, 5020, 5021, 5022, 5023, 5024, 5025, 5026, 5027, 5028, 5029, 5030, 5031, 5032
74 *Elset, elset=BOX_U, generate
75     7553, 8304, 1
76 *Nset, nset=BOX_O
77     17, 18, 21, 22, 389, 390, 391, 392, 393, 394, 395, 396, 397, 398, 399, 400
78     401, 402, 403, 404, 405, 406, 407, 408, 409, 410, 411, 412, 413, 414, 415, 416
79     417, 418, 419, 420, 421, 422, 423, 424, 425, 426, 427, 428, 429, 430, 431, 432
80     433, 434, 435, 436, 437, 438, 439, 440, 441, 442, 443, 444, 445, 446, 447, 448
81 ##### some lines deleted #####
82     5615, 5616, 5617, 5618, 5619, 5620, 5621, 5622, 5623, 5624, 5625, 5626, 5627, 5628, 5629, 5630
83     5631, 5632, 5633, 5634, 5635, 5636, 5637, 5638, 5639, 5640, 5641, 5642, 5643, 5644, 5645, 5646
84     5647, 5648, 5649, 5650, 5651, 5652, 5653, 5654, 5655, 5656, 5657, 5658, 5659, 5660, 5661, 5662
85     5663, 5664, 5665, 5666, 5667, 5668, 5669, 5670, 5671, 5672, 5673, 5674, 5675, 5676, 5677, 5678
86     5679, 5680, 5681, 5682, 5683, 5684, 5685, 5686, 5687, 5688, 5689, 5690
87 *Elset, elset=BOX_O
88     6801, 6802, 6803, 6804, 6805, 6806, 6807, 6808, 6809, 6810, 6811, 6812, 6813, 6814, 6815, 6816
89     6817, 6818, 6819, 6820, 6821, 6822, 6823, 6824, 6825, 6826, 6827, 6828, 6829, 6830, 6831, 6832
90     6833, 6834, 6835, 6836, 6837, 6838, 6839, 6840, 6841, 6842, 6843, 6844, 6845, 6846, 6847, 6848
91     6849, 6850, 6851, 6852, 6853, 6854, 6855, 6856, 6857, 6858, 6859, 6860, 6861, 6862, 6863, 6864
92 ##### some lines deleted #####
93     9009, 9010, 9011, 9012, 9013, 9014, 9015, 9016, 9017, 9018, 9019, 9020, 9021, 9022, 9023, 9024
94     9025, 9026, 9027, 9028, 9029, 9030, 9031, 9032, 9033, 9034, 9035, 9036, 9037, 9038, 9039, 9040
95     9041, 9042, 9043, 9044, 9045, 9046, 9047, 9048, 9049, 9050, 9051, 9052, 9053, 9054, 9055, 9056
96 *Nset, nset=TOPPLATE
97     24, 1040, 1041, 1042, 1043, 1044, 1045, 1046, 1047, 1048, 1049, 1050, 1051, 1052, 1053, 1054
98     1055, 1056, 1057, 1058, 1059, 1060, 1061, 1062, 1063, 1064, 1065, 1066, 1067, 1068, 1069, 1070
99     1071, 1072, 1073, 1074, 1075, 1076, 1077, 1078, 1079, 1080, 1081, 1082, 1083, 1084, 1085, 1086
100    1087, 1088, 1089, 1090, 1091, 1092, 1093, 1094, 1095, 1096, 1097, 1098, 1099, 1100, 1101, 1102
101 ##### some lines deleted #####
102    7383, 7384, 7385, 7386, 7387, 7388, 7389, 7390, 7391, 7392, 7393, 7394, 7395, 7396, 7397, 7398
103    7399, 7400, 7401, 7402, 7403, 7404, 7405, 7406, 7407, 7408, 7409, 7410, 7411, 7412, 7413, 7414
104    7415, 7416, 7417, 7418, 7419, 7420, 7421, 7422, 7423, 7424, 7425, 7426, 7427, 7428, 7429, 7430
105    7431, 7432, 7433, 7434, 7435, 7436, 7437, 7438
106 *Elset, elset=TOPPLATE, generate
107    9990, 10922, 1
108 **
109 -----
110 ** (2) Material Parameters Discrete Elements
111 -----
112 **
113 ** Radius = 5mm (0.005m)
114 ** Density = 2600 kg/m3 (2.6 10^-9kg/m3)
115 **
116 *discrete section,elset=dem1,shape=sphere,density=2.6e-09, alpha=7
117 S,
118 **
119 ** Make the sets rigid
120 **
121 *RIGID BODY, REF NODE =          17, ELSET = box_o
122 *RIGID BODY, REF NODE =          19, ELSET = box_u
123 *RIGID BODY, REF NODE =          23, ELSET = bottom
124 *RIGID BODY, REF NODE =          24, ELSET = topplate
125 **
126 ** Important: Change the node numbers if the geometry is changing!!
127 **

```

```
128 **-----
129 ** (3) Material Parameters of the box
130 **-----
131 **
132 *Material, name=STEEL
133 *density
134 7.85e-09
135 *elastic
136 2.08e+5,0.3
137 **
138 **
139 *SHELL SECTION, ELSET=box_u, MATERIAL=STEEL,
140 2,
141 *SHELL SECTION, ELSET=box_o, MATERIAL=STEEL,
142 2,
143 *SHELL SECTION, ELSET=topplate, MATERIAL=STEEL,
144 2,
145 *SHELL SECTION, ELSET=bottom, MATERIAL=STEEL,
146 2,
147 **
148 **-----
149 ** (4) Surface definition
150 **-----
151 **
152 *surface, type=element, name=dem1
153 dem1,
154 *surface, type=element, name=box_u
155 box_u,
156 *surface, type=element, name=box_o
157 box_o,
158 *Surface, type=ELEMENT, name=TOPPLATE
159 TOPPLATE, SNEG
160 *Surface, type=ELEMENT, name=bottom
161 bottom,
162 **
163 **-----
164 ** (5) Boundary Conditions
165 **-----
166 **
167 ** Name: BC-1 Type: Velocity/Angular velocity
168 *Boundary, type=VELOCITY
169 BOX_U, 1, 1
170 BOX_U, 2, 2
171 BOX_U, 3, 3
172 BOX_U, 4, 4
173 BOX_U, 5, 5
174 BOX_U, 6, 6
175 ** Name: BC-2 Type: Velocity/Angular velocity
176 *Boundary, type=VELOCITY
177 BOX_O, 1, 1
178 BOX_O, 2, 2
179 BOX_O, 3, 3
180 BOX_O, 4, 4
181 BOX_O, 5, 5
182 BOX_O, 6, 6
183 ** Name: BC-3 Type: Velocity/Angular velocity
184 *Boundary, type=VELOCITY
185 BOTTOM, 1, 1
186 BOTTOM, 2, 2
187 BOTTOM, 3, 3
188 BOTTOM, 4, 4
189 BOTTOM, 5, 5
190 BOTTOM, 6, 6
191 ** Name: BC-3 Type: Velocity/Angular velocity
192 *Boundary, type=VELOCITY
193 TOPPLATE, 1, 1
194 TOPPLATE, 2, 2
195 TOPPLATE, 4, 4
196 TOPPLATE, 5, 5
197 TOPPLATE, 6, 6
```

```

198 **
199 **-----
200 ** (6) force-overclosure relationship based on Hertz contact formulation
201 **-----
202 ** dem1: Radius = 5mm E= 200.000 N/mm2, poisson's ratio = 0.20
203 ** box: E= 208.000 N/mm2, poisson's ratio = 0.25
204 **
205 **
206 *surface interaction, name=P1f
207 *friction
208 0.50
209 *Contact Damping, definition=DAMPING COEFFICIENT
210 0.07
211 *surface behavior, pressure-overclosure=tabular
212 0.0000000E+00 , 0.0000000E+00
213 1.2662346E+00 , 2.5000000E-04
214 3.5680302E+00 , 4.9875000E-04
215 ##### some lines deleted #####
216 3.5015724E+03 , 4.9253750E-02
217 3.5281322E+03 , 4.9502500E-02
218 3.5814522E+03 , 5.0000000E-02
219 **
220 *surface interaction, name=P11
221 *friction
222 0.70
223 *Contact Damping, definition=DAMPING COEFFICIENT
224 0.07
225 *surface behavior, pressure-overclosure=tabular
226 0.0000000E+00 , 0.0000000E+00
227 8.6805556E-01 , 2.5000000E-04
228 2.4460305E+00 , 4.9875000E-04
229 ##### some lines deleted #####
230 2.4004710E+03 , 4.9253750E-02
231 2.4186788E+03 , 4.9502500E-02
232 2.4552319E+03 , 5.0000000E-02
233 **
234 **-----
235 ** (7) STEP 1 - settling of particles
236 **-----
237 **
238 *step
239 step 1 - settling of particles
240 **
241 *dynamic, explicit, direct
242 0.2e-6,1.00
243 **
244 *dload
245 dem1, grav, 9800.0,0.,0.,-1.0
246 topplate, grav, 9800.0,0.,0.,-1.0
247 *contact
248 *contact controls assignment, rotational terms=structural
249 **
250 *contact inclusions
251 dem1,box_u
252 dem1,box_o
253 dem1,topplate
254 dem1,bottom
255 dem1,dem1
256 *contact property assignment
257 dem1,box_u,p1f
258 dem1,box_o,p1f
259 dem1,topplate,p1f
260 dem1,bottom,p1f
261 dem1,dem1,P11
262 *output, history,frequency=1
263 CRM1,CRM2,CRM3,CVR1,CVR2,CVR3
264 *energy output, var=all
265 **
266 *output, field, number interval=60
267 *node output
268 U, V, RM, RT

```

```
269 **
270 **
271 *end step
272 **
273 -----
274 ** (8) STEP 2 - pressure (01)
275 -----
276 **
277 *step
278 step 2 - pressure
279 **
280 *dynamic, explicit, direct
281 0.2e-6,1.00
282 **
283 ** LOADS
284 **
285 ** Name: Load-3    Type: Pressure
286 *Dsload
287 TOPPLATE, P, -0.08430
288 **
289 **
290 **
291 ** (01) 0.0843 N/mm2   (0.10 - 0.0157) <<<<<<<<<<<<<<<<<<<<<<<<<<<<<<<<
292 ** (02) 1.9843 N/mm2   (2.00 - 0.0157)
293 ** (03) 3.9843 N/mm2   (4.00 - 0.0157)
294 ** (04) 5.9843 N/mm2   (6.00 - 0.0157)
295 ** (05) 7.9843 N/mm2   (8.00 - 0.0157)
296 ** (06) 3.9843 N/mm2   (4.00 - 0.0157)
297 ** (07) 7.9843 N/mm2   (8.00 - 0.0157)
298 ** (08) 9.9843 N/mm2   (10.00 - 0.0157)
299 ** (09) 11.9843 N/mm2  (12.00 - 0.0157)
300 **
301 **
302 *output, history,frequency=1
303 CRM1,CRM2,CRM3,CVR1,CVR2,CVR3
304 *energy output, var=all
305 **
306 **
307 *output, field, number interval=400
308 *node output
309 U, V, RM, RT
310 *Contact Output
311 CFORCE, CSTRESS
312 **
313 **
314 *end step
315 -----
316 ** (8) STEP 3 - pressure (02)
317 -----
318 **
319 **
320 ** #####
321 ** until load stage 09 (step 10)
322 ** change of the pressure on the topplate
323 ** everything else is the same!!
324 ** #####
```

Annex H

Input file of the annular gap model

```

1  **-----
2  **----- ANNULAR GAP CALCULATION -----
3  **-----
4  **
5  ** Created by Christoph Sinkovec
6  ** Institute for Rock Mechanics and Tunnelling
7  ** Graz University of Technology
8  **
9  **-----
10 ** (1) Input of the Geometry
11 **-----
12 **
13 *Node
14     1,          910.,        1000.,        4950.
15     2,          910.,        -1000.,        4950.
16     3,          110.,        -1000.,        4950.
17     4,          110.,         1000.,        4950.
18     5,          910.,        -1000.,        7950.
19 ##### some rows deleted #####
20     7542,        210.,        -500.,        7850.
21     7543,        210.,        -600.,        7850.
22     7544,        210.,        -700.,        7850.
23     7545,        210.,        -800.,        7850.
24     7546,        210.,        -900.,        7850.
25 *Element, type=PD3D, ELSET=dem1
26     1, 185
27     2, 1347
28     3, 1348
29     4, 1349
30 ##### some rows deleted #####
31     4796, 936
32     4797, 937
33     4798, 938
34     4799, 939
35     4800, 940
36 *Element, type=S4R
37     4801, 9, 244, 2449, 2508
38     4802, 244, 245, 2450, 2449
39     4803, 245, 246, 2451, 2450
40     4804, 246, 247, 2452, 2451
41 ##### some rows deleted #####
42     6345, 3685, 3687, 3679, 3666
43     6346, 3668, 3671, 3680, 3681
44     6347, 3652, 3679, 3687, 3684
45     6348, 3689, 3658, 3688, 3670
46 *Element, type=S3
47     6131, 595, 594, 21
48     6132, 624, 566, 623
49     6133, 566, 624, 567
50 ##### some rows deleted #####
51     6241, 514, 13, 359
52     6242, 3681, 3673, 3677
53     6243, 3669, 3682, 3672
54 *Nset, nset=ANNULAR_GAP
55     9, 10, 11, 12, 13, 14, 15, 16, 17, 18, 244, 245, 246, 247, 248, 249
56     250, 251, 252, 253, 254, 255, 256, 257, 258, 259, 260, 261, 262, 263, 264, 265
57     266, 267, 268, 269, 270, 271, 272, 273, 274, 275, 276, 277, 278, 279, 280, 281
58     282, 283, 284, 285, 286, 287, 288, 289, 290, 291, 292, 293, 294, 295, 296, 297
59 ##### some rows deleted #####
60     3597, 3598, 3599, 3600, 3601, 3602, 3603, 3604, 3605, 3606, 3607, 3608, 3609, 3610, 3611, 3612
61     3613, 3614, 3615, 3616, 3617, 3618, 3651, 3652, 3653, 3654, 3655, 3656, 3657, 3658, 3659, 3660
62     3661, 3662, 3663, 3664, 3665, 3666, 3667, 3668, 3669, 3670, 3671, 3672, 3673, 3674, 3675, 3676
63     3677, 3678, 3679, 3680, 3681, 3682, 3683, 3684, 3685, 3686, 3687, 3688, 3689

```

```

64 *Elset, elset=ANNULAR_GAP
65 4801, 4802, 4803, 4804, 4805, 4806, 4807, 4808, 4809, 4810, 4811, 4812, 4813, 4814, 4815, 4816
66 4817, 4818, 4819, 4820, 4821, 4822, 4823, 4824, 4825, 4826, 4827, 4828, 4830, 4831, 4832
67 4833, 4834, 4835, 4836, 4837, 4838, 4839, 4840, 4841, 4842, 4843, 4844, 4845, 4846, 4847, 4848
68 4849, 4850, 4851, 4852, 4853, 4854, 4855, 4856, 4857, 4858, 4859, 4860, 4861, 4862, 4863, 4864
69 ##### some rows deleted #####
70 6284, 6285, 6286, 6287, 6288, 6289, 6290, 6291, 6292, 6293, 6294, 6295, 6296, 6297, 6298, 6299
71 6300, 6301, 6302, 6303, 6304, 6305, 6306, 6307, 6308, 6309, 6310, 6311, 6312, 6313, 6314, 6315
72 6316, 6317, 6318, 6319, 6320, 6321, 6322, 6323, 6324, 6325, 6326, 6327, 6328, 6329, 6330, 6331
73 6332, 6333, 6334, 6335, 6336, 6337, 6338, 6339, 6340, 6341, 6342, 6343, 6344, 6345, 6346, 6347
74 6348,
75 *Nset, nset=FRONT
76 19, 20, 21, 22, 23, 538, 539, 540, 541, 542, 543, 544, 545, 546, 547, 548
77 549, 550, 551, 552, 553, 554, 555, 556, 557, 558, 559, 560, 561, 562, 563, 564
78 565, 566, 567, 568, 569, 570, 571, 572, 573, 574, 575, 576, 577, 578, 579, 580
79 ##### some rows deleted #####
80 661, 662, 663, 664, 665, 666, 667, 668, 669, 670, 3619, 3620, 3621, 3622, 3623, 3624
81 3625, 3626, 3627, 3628, 3629, 3630, 3631, 3632, 3633, 3634, 3635, 3636, 3637, 3638, 3639, 3640
82 3641, 3642, 3643, 3644, 3645, 3646, 3647, 3648, 3649, 3650
83 *Elset, elset=FRONT, generate
84 6131, 6237, 1
85 **
86 -----
87 ** (2) Material Parameters Discrete Elements
88 -----
89 **
90 ** Radius = 5.0mm (0.005m)
91 ** Density = 2600 kg/m3 (2.6 10^-9kg/m3)
92 **
93 *discrete section,elset=dem1,shape=sphere,density=2.6e-09, alpha=10.0
94 50,
95 **
96 -----
97 ** (3) Material Parameters of the box
98 -----
99 **
100 ** Density = 7850 kg/m3 (7.85e-09 10^-9kg/m3)
101 ** Youngs Modulus = 210.000 N/mm2
102 ** Poisson's Ratio = 0,30 -
103 **
104 **
105 *Material, name=STEEL
106 *density
107 7.85e-09
108 *elastic
109 2.10e+05,0.3
110 **
111 **
112 *SHELL SECTION, ELSET=front, MATERIAL=STEEL
113 10,
114 *SHELL SECTION, ELSET=annular_gap, MATERIAL=STEEL
115 10,
116 **
117 -----
118 ** (4) Surface definition
119 -----
120 **
121 *surface, type=element, name=dem1
122 dem1,
123 *surface, type=element, name=front
124 front,
125 *surface, type=element, name=annular_gap
126 annular_gap,
127 **

```

```

128 **-----
129 ** (5) Boundary Conditions
130 **-----
131 **
132 ** Name: BC-1 Type: Velocity/Angular velocity
133 *Boundary, type=VELOCITY
134 FRONT, 1, 1
135 FRONT, 2, 2
136 FRONT, 3, 3
137 ** Name: BC-2 Type: Velocity/Angular velocity
138 *Boundary, type=VELOCITY
139 ANNULAR_GAP, 1, 1
140 ANNULAR_GAP, 2, 2
141 ANNULAR_GAP, 3, 3
142 **
143 **-----
144 ** (6) force-overclosure relationship based on Hertz contact formulation
145 **-----
146 ** dem1: Radius = 5mm E= 20.000, poisson's ratio = 0.20 density = 0.0026
147 **
148 **
149 *surface interaction, name=P1f
150 *Contact Damping, definition=DAMPING COEFFICIENT
151 0.07
152 *surface behavior, pressure-overclosure=tabular
153 0.0000000E+00 , 0.0000000E+00
154 3.6634889E-04 , 4.9950004E-06
155 1.0361911E-03 , 9.9900008E-06
156 1.9036046E-03 , 1.4985001E-05
157 2.9307911E-03 , 1.9980002E-05
158 ##### some rows deleted #####
159 1.012961 , 9.8401273E-04
160 1.020684 , 9.8900776E-04
161 1.028426 , 9.9400280E-04
162 1.036188 , 9.9899783E-04
163 **
164 *surface interaction, name=P11
165 *friction
166 0.35
167 *Contact Damping, definition=DAMPING COEFFICIENT
168 0.05
169 *surface behavior, pressure-overclosure=tabular
170 0.0000000E+00 , 0.0000000E+00
171 8.8888897E-05 , 2.4999999E-06
172 2.5141580E-04 , 4.9999999E-06
173 ##### some rows deleted #####
174 0.2457796 , 4.9249921E-04
175 0.2476534 , 4.9499923E-04
176 0.2495320 , 4.9749925E-04
177 0.2514152 , 4.9999927E-04
178 **
179 **-----
180 ** (7) STEP 1 - Movement back
181 **-----
182 **
183 *step
184 step 1 - movement back
185 **
186 *dynamic, explicit, direct
187 0.5e-5,0.10
188 **
189 ** BOUNDARY CONDITIONS
190 **
191 ** Name: Vel-BC-3 Type: Velocity/Angular velocity
192 *Boundary, type=VELOCITY
193 FRONT, 1, 1, -45000
194 **
195 *contact
196 *contact controls assignment, rotational terms=structural
197 **

```

```
198 dem1,front
199 dem1,annular_gap
200 dem1,dem1
201 *contact property assignment
202 dem1,front,P1f
203 dem1,annular_gap,P1f
204 dem1,dem1,P11
205 *output, history,frequency=1
206 CRM1,CRM2,CRM3,CVR1,CVR2,CVR3
207 *energy output, var=all
208 **
209 *output, field, number interval=200
210 *node output
211 U, V, RM, RT
212 **
213 *end step
214 **
215 **-----
216 ** (8) STEP 2 - settlement of the Particles
217 **-----
218 **
219 *step
220 step 2 - settlement
221 **
222 *dynamic, explicit, direct
223 0.5e-5,50
224 **
225 *dload
226 dem1, grav, 9800.0,0.,0.,-1.0
227 **
228 ** BOUNDARY CONDITIONS
229 *Boundary, type=VELOCITY
230 FRONT, 1, 1, 0
231 **
232 *output, history,frequency=1
233 CRM1,CRM2,CRM3,CVR1,CVR2,CVR3
234 *energy output, var=all
235 **
236 *output, field, number interval=500
237 *node output
238 U, V, RM, RT
239 *Contact Output
240 CFORCE, CSTRESS, CTHICK, FSLIP, FSLIPR
241 **
242 *end step
243 **-----
244 ** (9) STEP 3 - movement forward
245 **-----
246 **
247 *step
248 step 3 - movement forward
249 **
250 *dynamic, explicit, direct
251 0.5e-5,20
252 **
253 ** BOUNDARY CONDITIONS
254 *Boundary, type=VELOCITY
255 FRONT, 1, 1, 200
256 **
257 *output, history,frequency=1
258 CRM1,CRM2,CRM3,CVR1,CVR2,CVR3
259 *energy output, var=all
260 **
261 *output, field, number interval=100
262 *node output
263 U, V, RM, RT
264 *Contact Output
265 CFORCE, CSTRESS, CTHICK, FSLIP, FSLIPR
266 **
267 *end step
```